

JANUARY 2018

M.Sc. in Civil Engineering

KHABAT STAR MOHAMMED

**UNIVERSITY OF GAZIANTEP
GRADUATE SCHOOL OF
NATURAL & APPLIED SCIENCES**

**SIMULATION OF LOCAL SCOUR AROUND A GROUP OF BRIDGE
PIER USING FLOW-3D SOFTWARE**

**M. SC. THESIS
IN
CIVIL ENGINEERING**

**BY
KHABAT STAR MOHAMMED
JANUARY 2018**

**Simulation of Local Scour Around a Group of Bridge Pier Using
FLOW-3D Software**

M.Sc. Thesis

in

Civil Engineering

University of Gaziantep

Supervisor

Prof. Dr. Mustafa GÜNAL

By

Khabat Star MOHAMMED

January 2018



© 2018 [Khabat Star MOHAMMED]

REPUBLIC OF TURKEY
UNIVERSITY OF GAZİANTEP
GRADUATE SCHOOL OF NATURAL & APPLIED SCIENCES
CIVIL ENGINEERING DEPARTMENT

Name of the thesis: Simulation of local scour around a group of bridge pier using
FLOW-3D software

Name of the student: Khabat Star Mohammed

Exam date: 04.01.2018

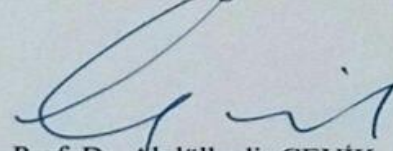
Approval of the graduate school of natural and applied science.



Prof. Dr. Ahmet Necmeddin YAZICI

Director

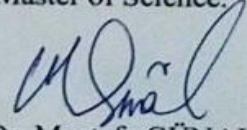
I certify that this thesis satisfies all the requirements as a thesis for the degree of
Master of Science.



Prof. Dr. Abdülkadir ÇEVİK

Head of Department

This is to certify that we have read this thesis and that in our consensus opinion it is
fully adequate, in scope and quality, as a thesis for the degree of Master of Science.



Prof. Dr. Mustafa GÜNAL

Supervisor

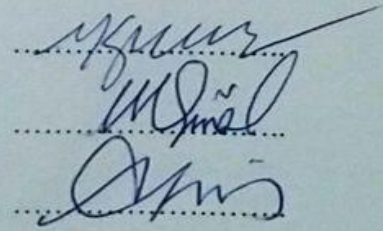
Examining Committee Members:

Prof. Dr. Mehmet KARPUZCU

Prof. Dr. Mustafa GÜNAL

Prof. Dr. Aytaç GÜVEN

Signature





I hereby declare that all information in this document has obtained and presented in accordance with academic rules and ethical conducts. I also declare that, as required by these rules and conducts, I have fully cited and referenced all the materials and results that are not authentic to this work.

Khabat Star MOHAMMED

ABSTRACT

SIMULATION OF LOCAL SCOUR AROUND A GROUP OF BRIDGE PIER USING FLOW-3D SOFTWARE

MOHAMMED, KHABAT STAR MOHAMMED

M.Sc. in Civil Engineering

Supervisor Prof. Dr. Mustafa GÜNAL

January 2018

73 pages

Computational Fluid Dynamics is one of the effective methods to study various hydraulic problems as it saves cost, turnaround time and procures reliable results. It is applied for resolving different fluid flow related problems like flow velocity, density, temperature, and chemical concentrations for any area where flow is present. Today it's a numerical method applied in various industries by combining computational tools and the theory of fluid dynamics in order to achieve flawless product designing. The reduction of local scour downstream of bridge piers got a considerable attention by numerous studies. The purpose of this study was to calculate and quantify the influence of hydraulic structural measures on reducing the scour around a group of bridge piers. In the simulation, the downstream semicircle diameter was fixed by a 10 cm, while the upstream diameter was changed to 4 and 10 cm. Discharges with $Q=0.057 \text{ m}^3/\text{s}$ and $0.038 \text{ m}^3/\text{s}$ the piers were tested under clear-water conditions for the duration of 6 hours. Then the results have been compared with laboratory measurements. The agreement between calculated scour depths and laboratory measurements is found reasonable.

Keywords: Local scour, scour reduction, bridge pier, group bridge pier.

ÖZET

GRUP KÖPRÜ AYAKLARI ETRAFINDA OLUŞAN YEREL OYULMANIN FLOW-3D PROGRAMI İLE SİMÜLASYONU

KHABAT STAR MOMAMMED

Yüksek Lisans Tezi, İnşaat Mühendisliği Bölümü

Danışman: Prof. Dr. Mustafa GÜNAL

Ocak 2018

73 sayfa

Hesaplamalı Akışkanlar Dinamiği, çeşitli hidrolik problemleri, maliyetten tasarruf sağlama süresini ve güvenilir sonuçlar elde etmeyi sağlayan etkili yöntemlerden biridir. Hesaplamalı Akışkanlar Dinamiği akış hızı, yoğunluk, sıcaklık ve akışın bulunduğu herhangi bir alan için kimyasal konsantrasyonlar gibi farklı akışkan akışıyla ilgili sorunları çözmek için uygulanır. Günümüzde, Hesaplamalı Akışkanlar Dinamiği, kusursuz ürün tasarımı gerçekleştirilmek için hesaplama araçlarını ve akışkan dinamikleri teorisini birleştirerek çeşitli endüstrilerde uygulanan sayısal bir yöntemdir. Köprü ayaklarının mansabında oluşan yerel oyulmanın azaltılması sayısız araştırmacının dikkatini çekmiştir. Bu çalışmanın amacı, grup köprü ayakları etrafında oluşan yerel oyulmanın azaltılması üzerine hidrolik yapısal önlemlerin etkisini hesaplamak ve ölçmektir. Bu çalışmada, köprü ayağı mansap tarafı çapı 10 cm olan yarım daire olarak, memba tarafı ise 4 cm ve 10 cm çapında yarım daire olarak tasarlanmıştır. Deneyler 6 saat süre ile temiz su oyulması şartlarında ve $Q=0.057 \text{ m}^3/\text{s}$ ve $0.038 \text{ m}^3/\text{s}$ debi kullanılarak yapılmıştır. Daha sonra sonuçlar laboratuvar ölçümleri ile karşılaştırılmıştır. Hesaplanan yerel oyulma derinlikleri ile laboratuvar ölçümleri arasındaki benzerlik arasında bir uyum bulunmuştur.

Anahtar Kelimeler: Yerel oyulma, oyulmanın azaltılması, köprü ayağı, grup köprü ayağı.



To

my parents

My wife and my children

Thank you for being there for me

ACKNOWLEDGEMENT

I would like to express my special appreciation and gratitude to my supervisor **Prof. Dr. Mustafa GÜNAL**, for all her help, patience, valuable advice, always providing and guiding me to the right direction. I'm very grateful and proudest to work under her academic guidance.

I would like to express heartfelt appreciation to The Republic of Turkey and their people for hospitality and generosity throughout my study which cannot be denied.

Special thanks to my family. Words cannot express how grateful I am to my father that his words led me to get certificates and my mother for all of the sacrifices that she made for me. Also to all my siblings, for the many years of encouragement and support they gave me and which enabled me to complete this thesis.

The assistance and support of all the members and professor of the Gaziantep University, Civil Engineering Department throughout the conduction of the study, is highly acknowledged

TABLE OF CONTENTS

ABSTRACT.....	v
ÖZET.....	vi
ACKNOWLEDGEMENT	viii
TABLE OF CONTENTS.....	ix
LIST OF TABLES	xiii
LIST OF FIGURES	xiv
LIST OF SYMBOLS/ABBREVIATIONS	xviii
CHAPTER ONE	1
INTRODUCTION	1
1.1 Introduction	1
1.2 Scour Types	4
1.2.1 General Scouring of River bed.....	5
1.2.2 Localized Scour.....	5
1.3 Objectives of This Study	6
CHAPTER TWO	7
LITERATURE REVIEW.....	7
2.1 Introduction	7

2.2	Local Scour Mechanisms	7
2.3	Sediment Transport and Motion Around Bridge Piers.....	9
2.3.1	Down-Flow at the Pier Face.....	9
2.3.2	Horseshoe Vortex.....	9
2.3.3	Wake Vortices.....	9
2.3.4	Bow Wave.....	10
2.4	Parameters Influence to Scour Depth.....	10
2.4.1	Approaching Flow Velocity.....	10
2.4.2	Approaching Flow Depth.....	11
2.4.3	Size And Gradation of Sediments	11
2.4.4	Channel Geometry	12
2.4.5	Time-Variation of Scour	12
2.4.6	Bridge Pier Shape and Attack Angle of Flow	14
2.4.7	CFD Numerical Simulation	16
2.5	Field Observation of Local Scour around Bridge Piers.....	18
CHAPTER THREE.....		21
CASE-STUDY		21
3.1	Introduction	21
3.2	Physical Set-up and Experimental Procedure.....	21
3.2.1	Inflow Pipe	21
3.2.2	The Flume	22

3.2.3	Outflow Pipe and Storage Tank	24
3.3	Bed Material	24
3.4	Brief Introduction to Flow 3D	25
3.5	Numerical Model Set-Up	26
3.5.1	Physics	27
3.5.2	Geometry	29
3.5.3	Meshing	29
3.5.4	Data Sharing	30
3.5.5	Specifying Boundary Conditions and Initial Conditions	31
CHAPTER FOUR		34
RESULTS AND DISCUSSION		34
4.1	Introduction	34
4.2	Comparing between Experimental and CFD (Flow-3D) Software	35
4.2.1	Comparison of Scour	35
4.2.2	Longitudinal Bed Profile of Sand	40
4.3	Velocity Field	43
4.4	Rate of Scouring	44
CHAPTER FIVE		47
CONCLUSIONS AND RECOMMENDATIONS		47
5.1	Conclusions	47
5.2	Recommendation	48

6	REFERENCES.....	50
7	APPENDICES	57
8	APPENDIX A	58
	Scour Hole.....	58
10	APPINDIX B	64
	Water Surface and Vectors.....	64
11	APPENDIX C	66
	Velocity magnitude at different shapes.....	66
12	APPINDIX D	68
	2D Pressure contours at different shape.....	68
13	RESULTS APPENDIX E	70
	The data for the Scour hole contour.....	70

LIST OF TABLES

Table 3.1 The test conditions	27
Table 4.1 Max. scour depths corresponding to pier shape and discharge	35



LIST OF FIGURES

Figure 1.1 Bridge failure in South Africa, United States and New Zealand (Annandale, 1993)	2
Figure 1.2 Scour Types in the stream (Robert et al, 2006).....	5
Figure 1.3 Kinds of scour at bridge opening (Robert et al., 2006).....	6
Figure 2.1 Illustration of the flow and scour pattern at a circular pier (Melville & Coleman 2000)	8
Figure 2.2 Time development of clearwater and live-bed scour (after Chabert & Engeldinger 1956)	13
Figure 2.3 Tested pier shape (Chabert and Engeldinger, 1956)	15
Figure 2.4 Effect of Angle of flow attack corresponding to Scour depth at different pier shape (Chabert and Engeldinger, 1956)	15
Figure 2.5 Comparative temporal variation of the local scour around the side-by- side and triangular arrangement of the piles.....	18
Figure 2.6 Pier shapes which used in experiments. (Al-Shukur and Obeid,2016).....	19
Figure 2.7 Descriptions of shapes and results of study (Al-Shukur and Obeid,2016)	20
Figure 3.1 Laboratory layout	22
Figure 3.2 Hydraulic flume test, Gaziantep University	22
Figure 3.3 Piers and flume geometry in Flow 3D model (4-10)	23
Figure 3.4 Piers position and flume geometry in Flow 3D model (10-10)	23

Figure 3.5 Shapes and dimensions of tested bridge piers.....	24
Figure 3.6 The grain size distribution curve of the bed material.....	25
Figure 3.7 Sediment definition in Flow-3D.....	27
Figure 3.8 Computational domain and mesh setup around the bridge piers model (10-10)	30
Figure 3.9 2D Computational domain model (10-10)	31
Figure 3.10 Computational domain and mesh setup around the bridge piers model (4-10)	31
Figure 3.11 2D computational domain model (4-10).....	31
Figure 3.12 Inlet boundary condition for $Q=0.038 \text{ m}^3/\text{s}$, velocity=0.5 m/s and fluid elevation =0.295m.....	32
Figure 3.13 Inlet boundary condition for $Q=0.057 \text{ m}^3/\text{s}$ velocity=0.593 m/s and fluid elevation =0.325m.....	33
Figure 3.14 Boundary conditions for the model (4-10).....	33
Figure 3.15 Boundary conditions for the model (10-10).....	33
Figure 4.1 Comparison between Experimental and Flow-3D results of scour development with time in pier number (1) at a flow rate (0.057) m^3/sec . and pier shape (4-10)	36
Figure 4.2 Comparison between Experimental and Flow-3D results of scour development with time in pier number (2) at a flow rate (0.057) m^3/sec . and pier shape (4-10)	36
Figure 4.3 Comparison between Experimental and Flow-3D results of scour development with time in pier number (3) at a flow rate (0.057) m^3/sec . and pier shape (4-10)	36

Figure 4.4 Comparison between Experimental and Flow-3D results of scour development with time in pier number (1) at a flow rate (0.057) m ³ /sec. and pier shape (10-10)	37
Figure 4.5 Comparison between Experimental and Flow-3D results of scour development with time in pier number (2) at a flow rate (0.057) m ³ /sec. and pier shape (10-10)	37
Figure 4.6 Comparison between Experimental and Flow-3D results of scour development with time in pier number (3) at a flow rate (0.057) m ³ /sec. and pier shape (10-10)	37
Figure 4.7 Comparison between Experimental and Flow-3D results of scour development with time in pier number (1) at a flow rate (0.038) m ³ /sec. and pier shape (4-10)	38
Figure 4.8 Comparison between Experimental and Flow-3D results of scour development with time in pier number (2) at a flow rate (0.038) m ³ /sec. and pier shape (4-10)	38
Figure 4.9 Comparison between Experimental and Flow-3D results of scour development with time in pier number (3) at a flow rate (0.038) m ³ /sec. and pier shape (4-10)	38
Figure 4.10 Comparison between Experimental and Flow-3D results of scour development with time in pier number (1) at a flow rate (0.038) m ³ /sec. and pier shape (10-10)	39
Figure 4.11 Comparison between Experimental and Flow-3D results of scour development with time in pier number (2) at a flow rate (0.038) m ³ /sec. and pier shape (10-10)	39
Figure 4.12 Comparison between Experimental and Flow-3D results of scour development with time in pier number (3) at a flow rate (0.038) m ³ /sec. and pier shape (10-10)	39

Figure 4.13 Comparison of the longitudinal profile of bed for bridge piers (10-10) and (4-10) for experimental and Flow-3D at flow rate 0.057 m ³ /s.	40
Figure 4.14 Comparison of the longitudinal profile of bed for bridge piers (10-10) and (4-10) for experimental and Flow-3D at flow rate 0.038 m ³ /s.	40
Figure 4.15 scour development at time = 5 min and discharge 0.057 m ³ /sec	41
Figure 4.16 scour development at time = 15 min and discharge 0.057 m ³ /sec	42
Figure 4.17 scour development at time = 60 min and discharge 0.057 m ³ /sec	42
Figure 4.18 scour development at time = 360 min and discharge 0.057 m ³ /sec	42
Figure 4.19 The velocity vectors in vertical plan for shape (4-10) at discharge 0.038 m ³ /sec and time 180 min	43
Figure 4.20 The velocity vectors in vertical plan for shape (10-10) at discharge 0.038 m ³ /sec and time 180 min	43
Figure 4.21 The velocity vectors in vertical plan for shape (4-10) at discharge 0.057 m ³ /sec and time 180 min	44
Figure 4.22 The velocity vectors in vertical plan for shape (10-10) at discharge 0.057 m ³ /sec and time 180 min	44
Figure 4.23 Flow around the shape (4-10) at Q=0.038 m ³ /s. and 180 min.	45
Figure 4.24 Flow around the shape (10-10) at Q=0.038 m ³ /s. and 180 min.	45
Figure 4.25 Flow around the shape (4-10) at Q=0.057 m ³ /s. and 180 min.	46
Figure 4.26 Flow around the shape (10-10) at Q=0.057 m ³ /s. and 180 min.	46

LIST OF SYMBOLS/ABBREVIATIONS

h	Depth of water flow (m)
Q	Approach discharge (m^3/s)
d	Pier width (cm)
ds	Local scour depth (m)
u	Stream velocity (m^2/s)
Uc	Critical velocity (m^2/s)
d ₅₀	Median size of the sediment particle (mm)
d ₈₄	Grain size for which 84% by weight of the sediment is finer (mm)
d ₁₆	Grain size for which 16% by weight of the sediment is finer (mm)
Fr	Froude number
Re	Reynolds number
σ_g	Geometric standard deviation of the sand size
t	Time (min)
u*	Shear velocity (m/s)
u*c	Critical Shear velocity (m/s)
Gs	Specific Gravity of sand
CFD	Computational Fluid Dynamic
D/s	downstream side
U/S	upstream side
TKE	Turbulent Kinetic Energy

RMS	Root Mean Square
FAVOM	Fractional Area Volume of Method
VOF	Volume of Fluid
US-FRNP	Upstream facing round nosed pier (4-10)
RNG	Renormalized group.



CHAPTER ONE

INTRODUCTION

1.1 Introduction

Every stable river in the world naturally consists of a complex hydrodynamic system, and the establishment of any hydraulic structure on the path flow field such as a dam, weir, barrage, bridge, regulator ... etc. this obstruction which immersed in the flow field leads to decrease the area of flow with constant of discharge, and according to continuity equation the velocity of water increase also the current capacity to carry sediment will increase. Subsequently, the stability of bed river disturbance as a result of change in bed shear stress, on the other hand, the water resists the trouble as a reaction of nature to human intervention, which causes instability of the hydraulic structure. The most important factor which causes hydraulic failure is called scour. Scour is described as removal of bed material and surround wet parameter of river as a result of increasing shear stress therefore the soil particle of bed river starts to move which stability of hydraulic structure will be under risk then more prone to catastrophic failures, also scour can be defined as a decrease in river bed level due to water erosion and tends to reveal the foundation of the bridge. (Melville and Coleman, 2000). Scour is an erosion of river bed sediment around abstraction in the flow field. (Chang 1988). Suddenly increase in shear stress can occur by changing the flow regime (Wu, S., & Rajaratnam, 1996) or by geometry (Pitt et al, 2007). Study of scour bridge piers is extremely important for the safe design of the piers and other hydraulic structures. If hydraulic and structural interactions are not accurately assessed, scouring can cause structure destruction, loss of life and properties, during high levels of the flood.

Formation of scour that damages and undermines the bridge piers and abutment foundation during the time of flood emerge is one of the main causes of the failure of

the bridge (Tulimilli et al, 2003) which happens as erosion. It has been evaluated that processes involving stream hydraulic lead to bridges failures about 60% like bridge piers (Melville and Coleman, 2000) see Figure1.1.

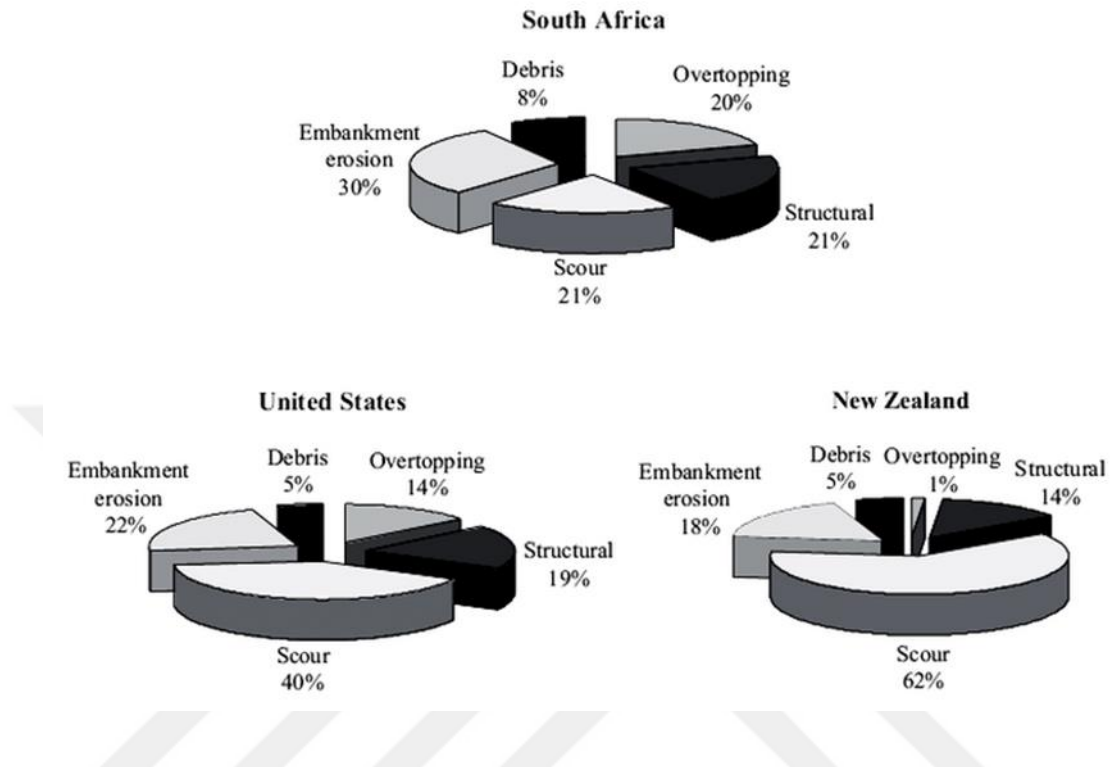


Figure 1.1 Bridge failure in South Africa, United States and New Zealand (Annandale, 1993)

Aggradation or degradation, overall scour, local scour, and side migration are blamed for 62% of all U.S. bridge failures (Alabi,2006). Scour around bridge piers and foundations, as a result of flood flows, is measured to be the major cause of bridge failure (Hoffmans. and Verheij.,1997). Scour was found to be the chief cause of the 1987 Scholarie Creek Bridge failure in New York in which ten people were killed in this incident (Ting et al. 2001; Wardhana and Hadipriono 2003). The 1989 catastrophic failure of a U.S. 51 bridge over the Hatchie River in Tennessee caused the death of 8 people (Lagasse and Richardson 2001). Also in California collapsed during a large flood; four vehicles plunged into the creek, resulting in seven deaths (Lagasse and Richardson,2001), In another two reports which released by Chiew and Lim (2003) and Chiew (2004) the case of the August 2000 failure of Kaoping Bridge in Southern islands Taiwan, and the Republic of Turkey has a good portion of these bridge failures in few years ago, several river bridges have failed or collapsed due to the flooding occurrences in Turkey. Some of them occurred in 1990, Trabzon, 1991,

Malatya; 1998, Bartin; 2001, Hatay (Yanmaz, 2002). On the other hand, New Zealand is one of those countries which have a good share of these failures. In the USA, the condition of the river bridges has been noted since 1991. It is determined that 66,000 of them are sensitive and 17,000 of them are critical to the scour. These bridges are monitored and repair work is on continuously (Lagasse et al., 2009). Many studies have been conducted in New Zealand since the 1970s, and monitoring instruments are installed in many bridges in parallel with these studies (Melville and Coleman, 2000).

In addition to a loss of human toll and property, the damage of bridges loses their functions, therefore, leads to interrupt the transportation and adds extra costs in direct expenditure for ensuring replacement and renovation. (Lagasse and Richardson 2001) In a study about bridge failure conducted by Cheremisinoff et al. (1987) in the United States, described that the Federal Highways Administration (FHWA) in 1978 claimed that loss or disruption to bridges and highways from major floods in 1964 and 1972 estimated about \$100,000,000 per event. In another survey by Macky (1990), Melville and Coleman (2000) indicated that, in New Zealand, scour caused by rivers results in the spending of NZ\$36,000,000 per year. In fact, failure of bridges by scouring is a common event, and a large amount of money is spent every year to repair bridges where the bridge pier was destroyed or damaged by scour (Dey 1997).

In an attempt to predict the scour process and sediment transportation, in 1914 Gilber proposed first equation to estimate sediment transport. After that, several equations for estimating sediment transport were proposed for single and multi- grain sediment size in uniform flow and steady state in open channel. These equations are used in different sediment transport modes such as those intended for total sediment loading without separating bed load or suspending loads, Also, for some target only the suspended load or load bed, Engineers most commonly use the equation of total load. Although massive investigations have been carried out to description sediment transport equation in the best way, there are no equations obtainable that have been approved commonly to measure the real rate of sediment transport. In addition, researchers have worked widely to understand a mechanism of sediment and scour. Raudkivi and Ettema (1983), Ahmed and Rajaratnam (1998), Chiew and Melville

(1987) and Breusers et al. (1977), among others, many of the researchers that have worked on pier scour. Local scour around bridge piers was studied by Shen and Schneider (1969) while Breusers et al. (1977) gave a state of the art. review on local scour around circular piers.

The physical model is commonly used for designing great hydraulic structure before the existence of computer technology, such as designing of dams, canals, regulars and so on. With the development of the technological state by the time in the world and the great openness in the world of technology and software, particularly, when the personal computer appears in the home or in work base, computational models in present time are becoming dependable and it is considered as a perfect economic tool for the purpose of engineering design. A computational fluid dynamic model which is used for hydraulic engineering purpose is initially developed for mechanical engineering and is improved version of CFD. Software models are able to be used for simulation of a different flow field modeling, for instance, flow around a group of bridge piers. Also, the accurateness and reliability of software hydro-dynamical should be check by the comparison of laboratory and numerical results.

1.2 Scour Types

The scour has been classified from many researchers; the total scour consists of three components in general, can add them together, and Richardson and Davies (1995). The scour includes general scour, local scour and contraction scour, Cheremisinoff et al. 1987, Melville and Coleman, 2000. Robert et al., 2006. Simons and Senturk, 1976. Figure 1.2 shows the scour types as Robert et al., 2006 classified.

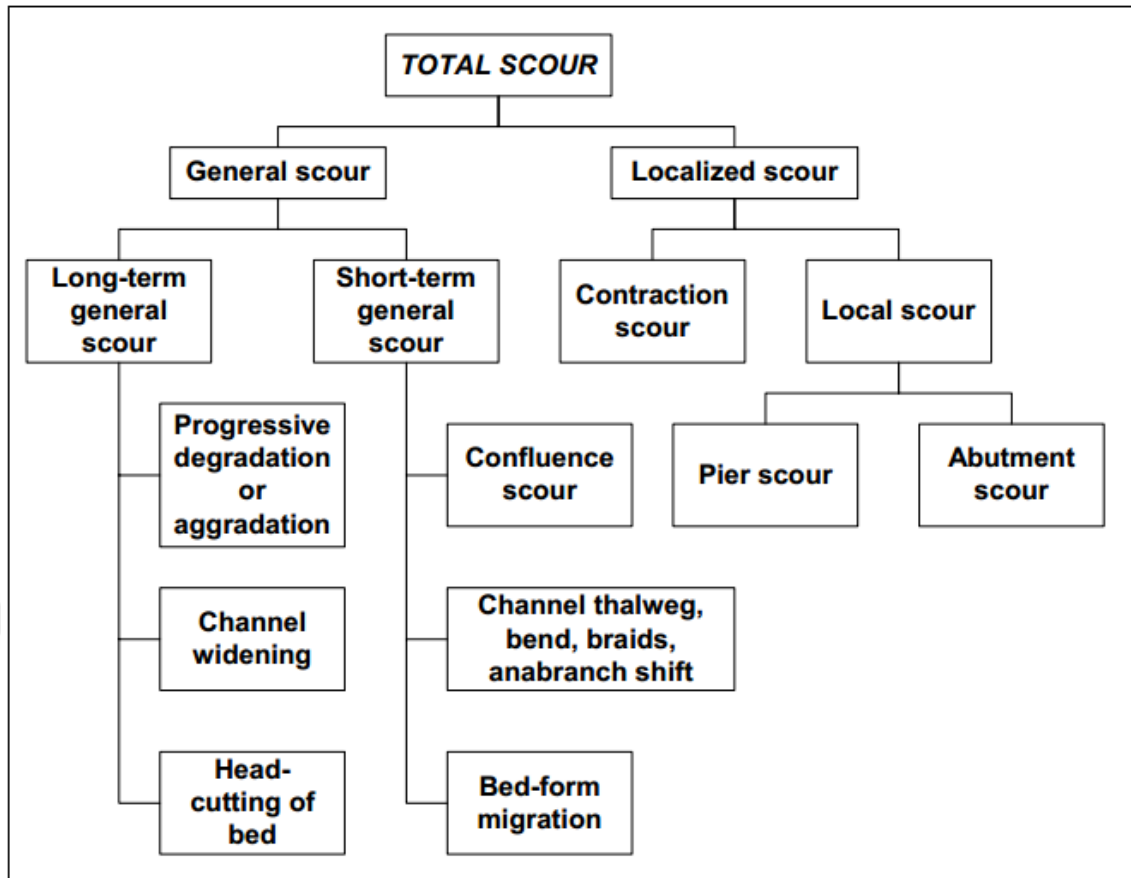


Figure 1.2 Scour Types in the stream (Robert et al, 2006)

1.2.1 General Scouring of River bed

General Scour appears as a result of natural processes, whether there is a bridge or not on the cross-section. It can be mentioned too as bed aggradation/degradation and classified as short-term scour and long-term scour after the time it takes to reach the scour. Short-term general happens for single or sequence flooding (daily, weekly, monthly or seasonal). Scour on channel conflicts, on curves, traces from a shift in the channel Thalweg and bed-form migration are included in short-term general scour (Coleman and Melville, 2001).

1.2.2 Localized Scour

This type of scour occurs due to the existence of a bridge or a river training structure like spur dike or groin. Local scour and Contraction scour, these two terms are named as localized scour. (Cheremisnoff et al. 1987). Contraction scour this type of scouring which appears as a result of constructing the waterway, and the local scour

is occurs as a result of the removal of sediment around and immediate of bridge piers. See Figure 1.3

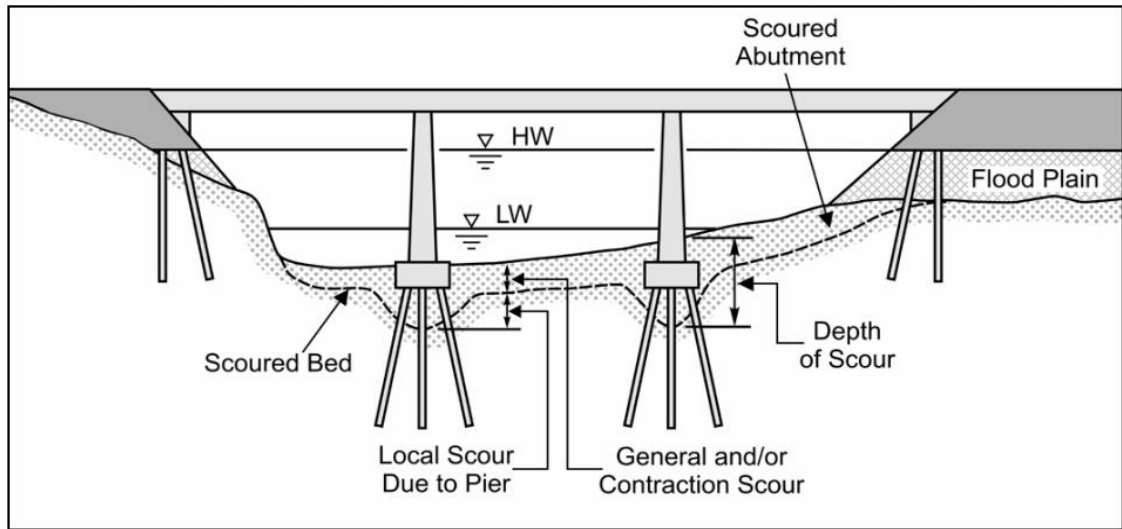


Figure 1.3 Kinds of scour at bridge opening (Robert et al., 2006)

1.3 Objectives of This Study

1. To study the main explanations of scouring phenomenon.
2. To understand the mechanism of scour around a group of bridge piers.
3. Assessment of the accuracy of Flow-3D software simulation through the comparison of the observed results.

CHAPTER TWO

LITERATURE REVIEW

2.1 Introduction

This chapter, presents the most important factors affecting on local scour and displays a brief review of the previous results of researchers as well as presents the investigations, theoretical methods, experimental studies about local scour, then focuses on the use of computer software such as simulation program and Numerical modeling also Artificial intelligence techniques which have been applied to describe the local scour around a group of pier and hydraulic structures.

2.2 Local Scour Mechanisms

It has long been evidenced that the fundamental mechanism that causes local scour at the bridge pier is the formation of vortices at the front face of the pier and down to the base river (Heidarpour et al., 2003; Muzzammil et al., 2004). The flow slows down as it approaches the bridge pier coming to rest at the front of the pier. Therefore, the approach flow velocity at the stagnation points on the nose of the pier decreases to zero, and the pressure will increase at the face of the pier. The stagnation pressure is high very extent near the surface, where the deceleration is greatest and decreases downward (Melville and Raudkivi 1977). In other words, this means, as the velocity decreases from the surface towards the bed, the stagnation pressure at the bridge pier face decreases too accordingly, that is, a downward pressure gradient. As a result of down-flow impinges on the river bed the holes are formed in the vicinity of the bridge pier base. The intensity of down-flow reaches the peak just in the bed level. (Melville and Raudkivi, 1977).

As shown in Figure 2.1, in addition to the horseshoe vortex near the base of the pier, there is a vertical vortex downstream of the pier called wake vortices (Dargahi 1990). When the flow separates at the side of the pier creates a so-called wake vortex. These wake vortices are not stable and shed alternately from one side of the pier and then the other. However, it should be known, that both of Horseshoe and Wake vortex lead to erosion of bed material around the pier. The strength of the wake vortex decreases greatly with downstream distance. (Richardson and Davies 1995).

Figure 2.1 shows the scour pattern at a circular bridge pier. The strong vortex motion resulted by the presence of the pier accompanies the bed sediment near the pier foundation (Lauchlan and Melville 2001). Down-flow rolls up as it continues to make scour holes and develops into a complex vortex system by interaction with the oncoming flows. The vortex stretches downstream along the side of the bridge piers. Because this vortex is very similar to a horseshoe, it is often called a horseshoe vortex (Breusers et al. 1977). Thus, the horseshoe vortex occurred caused by the separation of the flow at u/s face of the scour hole excavated by the downward flow. “The horseshoe vortex itself is a Lee vortex resembling a vortex or subsurface roller downstream of a sand dune vortex”. (Breusers and Raudkivi 1991). The hose show vortex has a good effect to carrying the particles around the bridge pier. The horseshoe vortex is considered as one of scour cause, but it is not the main cause of scour (Breusers and Raudkivi, 1991).

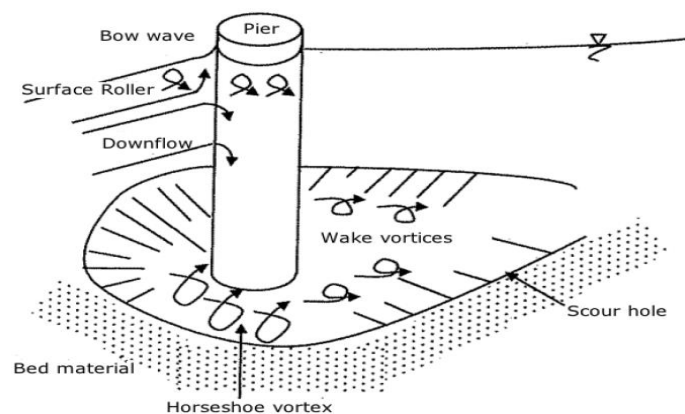


Figure 2.1 Illustration of the flow and scour pattern at a circular pier (Melville & Coleman 2000)

2.3 Sediment Transport and Motion Around Bridge Piers

When the flow field faces obstruction the flow direction separates into four different motions: down-flow, the horseshoe vortex, the bow waves and wake vortices, as it is explained below:

2.3.1 Down-Flow at the Pier Face

When the flow field hits the bridge pier face, the depth of flow increases and in front of bridge pier the stagnation point is formed. Thus, a pressure difference arises between the upstream side and the stagnation side. Yanmaz (2002). The depth of flow depends on the shape and flow velocity. When the velocity of flow decreases in front of the pier the pressure also decreases as it depends on approach velocity.

2.3.2 Horseshoe Vortex

In literature, the flow around bridge pier which is formed as a result of contact approach flow with down-flow known as horseshoe vortex(Ozalp et. Al., 2013).For this purpose, the pressure field must be high enough. Basically, a blunt nose pier induces a pressure gradient large enough to start the process as described above. (Breusers, Nicollet & Shen, 1977) if the bridge pier is parallel to the flow direction and the upstream side of the pier is sharp nosed this vortex will create, with a note that the vortex changing according to the pier.

2.3.3 Wake Vortices

As showing in Figure 2.1 Wake vortex is different from horseshoe vortex in the mechanism of creating, this type of vortex is generating by the bridge pier itself. Instability of shear stresses when the flow is passing the pier, considering the main cause to form this type of vortex at the side surface of the bridge pier. It is responsible to transport the sediment that is happened by down-flow (Melville and coleman, 2000). The effect of this vortex on erosion reduces whenever it moves away from upstream of the pier, in other words, it's strength is decreasing with downstream distance and the suspended particles will be deposited. (Richardson, and davies,1995).

2.3.4 Bow Wave

The waves which occur at water surface when it gets close to the face of the pier nosed then rotates counter direction to the horseshoe vortex and starts with an increase in depth water as a result of hitting a bridge pier face by the flow, defined as (Bow Wave) Figure 2.1. (Richardson and Davis, 2001). found that for shallow water, the bow wave has a positive action to some extent on local scour because it makes the horseshoe vortex is weak and that reduce the scour.

2.4 Parameters Influence to Scour Depth

Some researchers have reported such as (Barbhuiya& Dey,2004) that there are a lot of factors effect on depth of scour, the following shows some of these factors:

2.4.1 Approaching Flow Velocity

The velocity is considered as one of a more important factors which has a significant impact on scour depth, then both of Froude number (Fr) and velocity shear (u_*), (Garde. et. al., 1983) concluded that Froude number is sufficient to represent the effect of velocity on max. Depth scour in the natural channel, therefore and basing of this principle, (Mccrquodale,1975), Rajaratnam&Nwachwu,1983), (Zaghloul,1983), (Froehlich,1989), taking Froude number into consideration in their researches, and for shear velocity, represent the ability of current to scouring. It appears from previous researches and literature in case of using clear-water, the max. depth of scour takes place when ($U=U_c$) which means that the velocity flow equal to critical velocity and this depth is called (threshold peak), (Baker, 1986) and (Chien, 1984). Singh & Maiti. (2012).

In attempts experimentally to find relationship between depth of scour and Froude number, then concluded that the scour around circular bridge pier depends on (a) soil properties of the channel bed (b) shape and size of the pier (c) Froude number of flow (d) the scouring also depends on the vortex formation around the piers and its nature.

2.4.2 Approaching Flow Depth.

(Laursen., 1952) is considered the flow depth one of effectiveness factors to find the scour depth. (Gill,1972), (Wong, 1982), (Tey, 1984) & (Kandasamy, 1989), concluded that, with constant ration of shear velocity to critical velocity (U^*/U_c), the maximum scour depth decreases with drop of flow depth, as well as, they explain that depth of scour directly proportional with flow depth in shallow water.

2.4.3 Size And Gradation of Sediments

The sieve analyses decide the specification and gradation of bed material and the grain size soil (d_{50}), standard deviation (σ_g) which expresses the regularity river bed material ($\sigma_g = d_{84} / d_{16}$)^{0.5} are frequently used in more researches and the previous investigations, (Laursen & Toch 1956), (Ahmad 1953), (Lzzard & Bradley 1958) reached that maximum scour depth does not affect by grain size bed river, whereas, (Garde et. al., 1961) (Gill 1972), (Blench 1957), illustrated that the size of grain has a clear effect on scour depth and the depth scour ration increases with delicate of bed material, then (Laursen, 1960) reported that, maximum scour depth effect in case of using (clear-water) while does not affect in case of using (live-bed scour). (Gill.1972),(Wong, 1982), both of them conclude the scour depth increases if the granular diameter exceeds (2 mm). For gradation, (Ramu, 1964) observed different equilibrium scour depth at different standard deviation for same river bed grain size, (Ahmed, 1953) insisted that the equilibrium scour depth depends on the standard deviation of grain bed-river. (σ_g), (Ettema, 1980),(Raudkivi & Ettema,1983) confirmed Ahmed and by means of clear water they reached the following equation for describing the depth of scour:

$$D_s(\sigma_g)/D = K\sigma D_s/D$$

Where:

D_s = Equilibrium scour depth, σ_g = standard deviation, $K\sigma$ = coeffecian depend on (σ_g)

D = diameter of Pier

2.4.4 Channel Geometry

Cross section of channel is formed according to the geographical location of channel, for example, in hilly areas the shape of channel will be nearby to Hyperbola with a steep slope of the sides channel, while in the coastal areas, the shape of channel consists of main channel and Floodplain, (Richardson 1998) discussed his experimental results, he said that: scour in the rectangular flume does not represent the real scour at abutment. (Froehlich, 1989) inserts the effect of geometry in Froude number, then (Melville & Ettema, 1993), (Melville, 1995) conducted experiments which have been reported to quantify the effect of geometry on local scour depth at abutment of bridge traversing complex rivers.

This data is applied to the main channel in the case of an abutment. Channel geometry effects are represented by the multiplying factors. K_G has the effect of decreasing the scour depth from that in the rectangular channel, which is realized as the channel that has the similar overall width exactly like a compound channel and the equal depth such as the main channel Three times decrease of depth scour was observed from that of the corresponding rectangular channel. K_G is shown to be consistent with the experimental data, as determined by a simple equation including the main cross section and the cross-sectional shape and roughness of the flood channel. Expression of equivalent-length abutments in compound channels has also been proposed.

2.4.5 Time-Variation of Scour

Figure 2.3 shows a chart diagram of the time-variation of scour depth around a cylindrical bridge pier (after Chabert & Engeldinger 1956). Time to reach equilibrium scour depth differs approximately it is about a day to two weeks long.

By feature of the logarithmic character of the development of the scour area with time, a practical equilibrium is reached after a comparatively short time, after which the developing in the scour depth becomes virtually unnoticeable. (Rouse, 1965), however, States that there is no real equilibrium and the scour phenomenon is ever increasing.

(Bresuers,1963, 1967), (Kohli & Hager, 2001) have the same view. However, (Laursen, 1952), (Carstens, 1966), (Gill, 1972) and (Zaghloul, 1983). they have a different opinion, where they believe in the existence of real equilibrium scour. Rouse (1965), (Gill, 1972), (Rajaratnam & Nwachukwu, 1983), (Dargahi, 1990), (Ettema,1980), (Kohli & Hager ,2001), (Oliveto & Hager 2002) and (Coleman et al, 2003) think that the variation of scour depth with time is logarithmic.

(Ahmad ,1953), (Franzetti et. al.,1982), (Kandasamy .1989), (Whitehouse, 1998), (Cardoso & Bettess, 1999) and (Ballio & Orsi 2000) propose an Exponential Time-Variation of scour; while (Bresuers,1967) and (Cunha, 1975) propose a power law distribution. (Debnathand Chaudhuri, 2012) after carrying out an investigation for local scour about three shape pier-round-nosed, square and rectangular piers on clay-sand mixed cohesive bed reported.

The values of maximum equilibrium scour depth, for round-nosed were lower, but it was higher for the square and the rectangular piers. Broadly, the consensus is that the equilibrium scour depth at the hydraulic structure is asymptotically achieved.

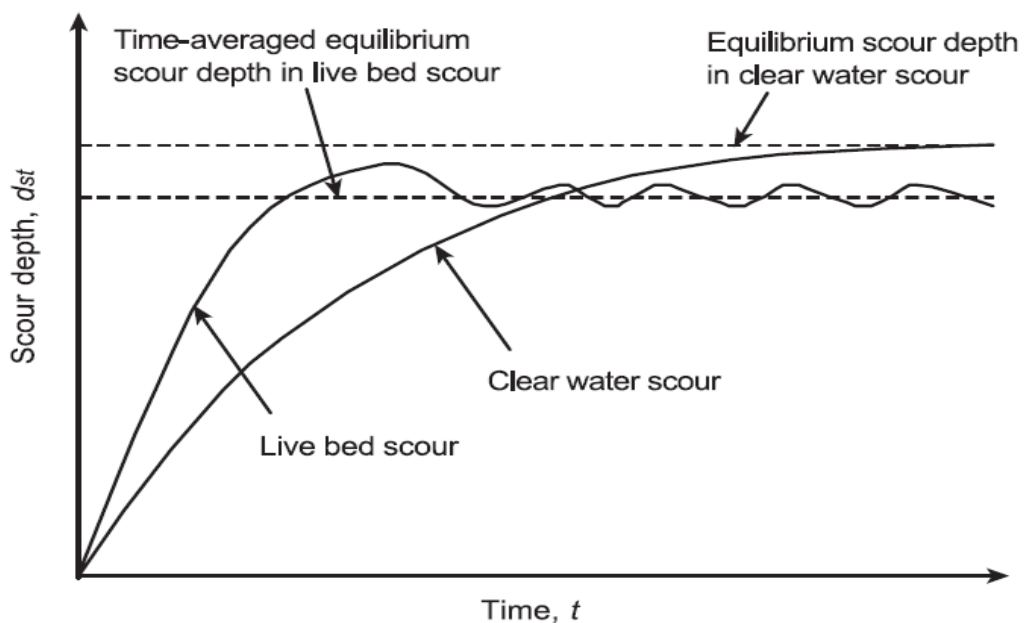


Figure 2.2 Time development of clearwater and live-bed scour (after Chabert & Engeldinger 1956)

2.4.6 Bridge Pier Shape and Attack Angle of Flow

Tison(1961), discovered that the velocity of water in the rivers does not the only reason for occur scour, but also by the curvature of the streamline. Shen et.al. (1969), has categorized the bridge pier into two types: Blunt nosed pier the system of this type creates a strong horseshoe vortex at pier upstream face which leads to significant the maximum scour in front of the bridge pier. Besides that, the shape of the pier and pier length must have the least influence when placed toward the flow using blunt nosed pier. The second type of pier is Sharp-nosed pier the system of type is contrary of first one in horseshoe vortex and in the approach of the work.

Study the effect of the bridge pier shape on scour is important to find the best shape which reduces scour as it possible. Several advanced investigations carried out by Rehbock (1921), Yarnell and Nagler(1931), Schneible (1951), Laursen and Toch(1956), Chabert and Engeldinger(1956), Romita(1960), Knezivic(1960), Varzeliotis (1960), Larras(1962), Paintal and Garde (1965) and Shen &Schneider (1970). In 1956 Chabert and Engeldinger they took six different types of bridge pier shape to study the scour around them, , and they concluded the following points:

- The shape of the pier of Group 1, which comprises the shape of all piers numbers,1 to 6 all have the same value in scour depth which almost the same for similar flow streams.
- According to the shape number 3 the highest depth of scour was about 33 to 86 percentage comparing to the same equivalent velocities from group number 1.

Figure 2.4 and 2.5 illustrates the shape of the piers and angle of attack impact. As shown in Figures below, the depth of scour is reduced as a result of streamlining of the pier with 0 angle of attack, this effect will be faded of the angle of attack of exceed than 10 degrees. When positioning two circular piers on a pier with three diameters, an exception is formed, and the angle of attack has just a small impact on scouring.

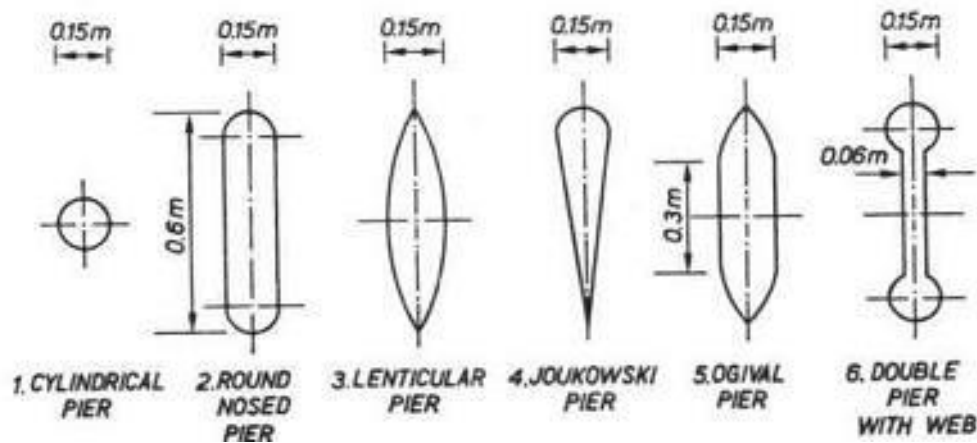


Figure 2.3 Tested pier shape (Chabert and Engelnlnger, 1956)

Paintal & Garde (1965) agree with this view and observed that pier tail side has no effect, but the upstream nose has the main influence on scour phenomenon.

In all indication, one can conclude that if the round nosed pier shape or the circular pier shape is taken as a reference, scour depth decreases about 25% can be obtained by streamlining the pier, even though for angles of attack more than 10 degrees to 15 degrees this perfect influence disappears. When comparing the rectangular bridge pier with the reference pier gives twenty to forty percent larger scour.as

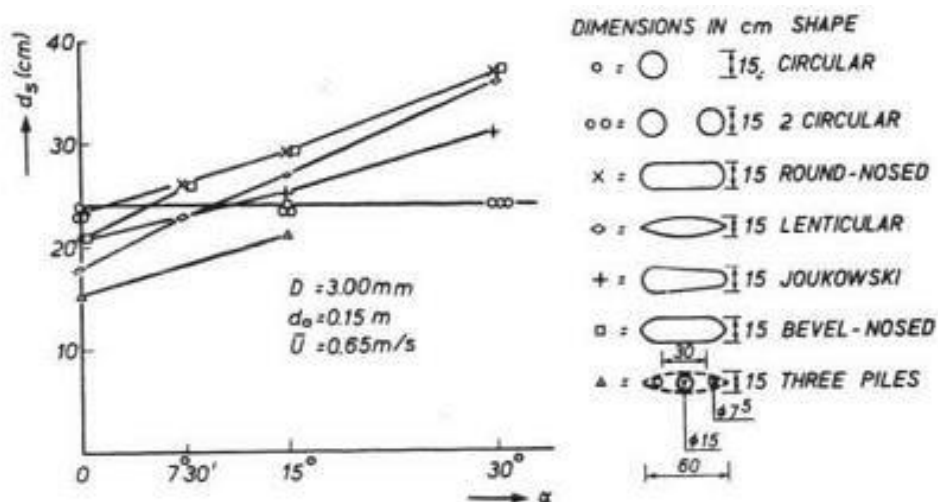


Figure 2.4 Effect of Angle of flow attack corresponding to Scour depth at different pier shape (Chabert and Engelnlnger, 1956)

2.4.7 CFD Numerical Simulation

In a few years ago massive researches have been done numerically to determine flow pattern in industrial and environmental applications by using of Computational Fluid Dynamic (CFD). First numerically simulations were reported about flow around a cylinder in the field of aerodynamics. Because the flow is Three-Dimensional, it formed a very complicated scour picture that can hardly be modeled numerically. Breusers (1975) used Reichardt inductive method to solve the velocity profile in scour holes numerically, and this attempt was only valid for two-dimensional flows while the sediment transport rate was not determined.

Briley & McDonald (1981) studied the mechanism of flow specifically the laminar horseshoe vortex flow at the junction between a level plate and a circular cylinder. The large-capability and high quality of computer since 1990's rapidly developed the area of the numerical modeling. Deng & Piquet (1992) studied the horseshoe vortex using the algebraic Baldwin-Lomax turbulence model.

Despite researching efforts in the past 20 years, numerical models have not been developed sufficiently for practical engineering purposes due to complicated three-dimensional flow. Therefore, the numerical flow model is required to solve complicated Three-Dimensional flow.

Olsen and Melaaen (1993) carried out a research under steady flow to study local scour around pier using the numerical model by means of three dimensional flow, finite-volume method, The $k-\omega$ turbulence model were used to solve non-transient (Navier-Stokes) equations and the Reynolds-stress respectively.

This sequence was repeated to physical model study. Sediment concentration and a new flow field were calculated. There was an agreement with observations from the experimental study. Next study same alike was held by Olsen, & Kjellesvig (1998). In the same approach with addition: The models contain time-dependency with transient terms, and calculation of the free surface is also carried out. The obtained results have the maximum depth which is compared with the empirical formula of local scour.

Roulund et al. (2005), 3D Model studied numerically and experimentally the flow around circular pile which exposed to steady flow. The horseshoe vortex influence, lee-wake vortex studied, also the Reynolds number and the bed roughness, was investigated. In the latter investigation, the steady solution of the model was selected.

A study of the influence of the unsteady solution on the previously mentioned flow processes was also carried out. Then (i) 2-D bed load sediment-transport explanation, and (ii) an explanation of surface-layer sand slides for bed slopes exceeding the angle of repose. The outcomes show that the Numerical Simulation captures all the chief features of the scour process. Equilibrium scour depth found from the simulation has a good agreement with the experiments for the upstream. With respect to that experienced at the initial stage where the bed is a plane.

(Salaheldin& Chaudhry,2004) conducted study to understanding the complicated flow field and the scour starting procedure around piers of multi size, shapes, and dimensions in this numerical study separation of flow around pier has been simulated. FLUENT software was used and satisfactorily results have found after compared with experimental study.

Liu, X., & Garcia, (2008). By Eulerian approach (VOF) system local scour with Free Water Surface (FWS) has been numerically studied and the findings are compared with observed results. Promising results achieved from the model.

Sumer & Fredsoe (2001), by combined irregular waves and current and subjected to the pile for study local scour around a pile and to simulation the scour with a free surface.Ahmad (2015), the 3D computational fluid dynamic REEF3D modeled under wave conditions to study to physics of local scour then compared with experimental results as shown in Figure 2.6 good agreement obtained.

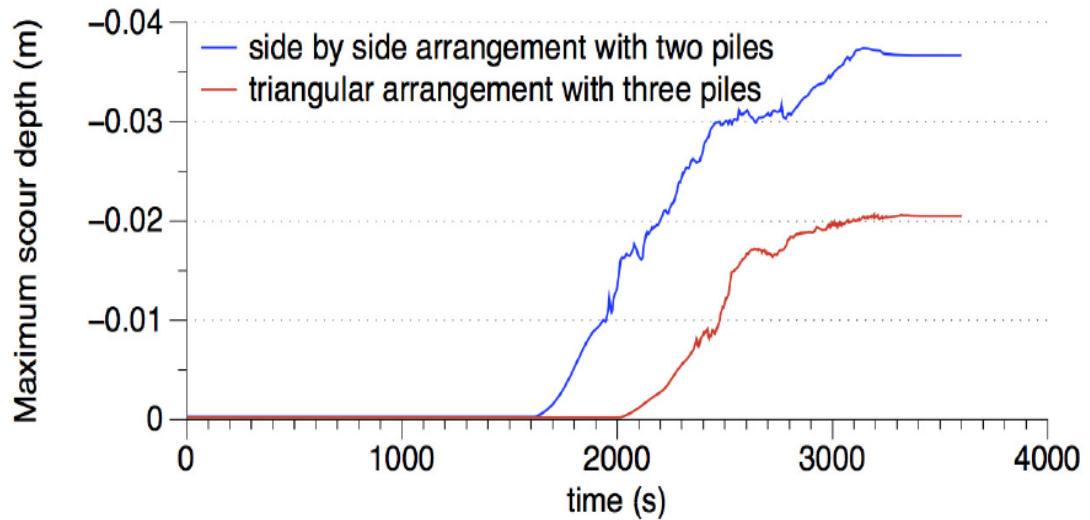


Figure 2.5 Comparative temporal variation of the local scour around the side-by-side and triangular arrangement of the piles

2.5 Field Observation of Local Scour around Bridge Piers

Froehlich (1988) based on field measurements to propose an equation for calculating the scour around cylinder bridge pier in uniform sediment under live bed conditions. Gao & Nordin (1993) they carried out about Two hundred and fifty laboratory and field cases in China to introduce an equation for prediction the scour around bridge pier which have two different formulae depending on the scour conditions if live bed scour or clear water scour, this equation has been used in China for a long time to calculate the scour around highway and railway bridge pier.

Ansari & Qadar (1994) provided by basing on envelopes derived from over one hundred field measurements from various sources and different countries to estimating the local scour depth around a bridge pier.

However, an availability of perfect documents is difficult and it is limited, most of the field data are of inferior quality. Besides that, the using of data is hampered because of the inaccuracy of mensuration precision, a complex of bridge pier shape, difference, and change of bed material around same the pier bed. It is obvious that field observation method only determinant the formulation of local scour depth and the creating of the mechanism of local scour is ignored.

In an attempt by Al-Shukur and Obeid, (2016), to find the optimal bridge pier shape that gives lowest scour among ten different shapes Figure 2.7, three different velocities (0.18, 0.25, and 0.3) m/sec are used. The experimental include this type of shape (circular, rectangular, octagonal, chamfered, hexagonal, elliptical, sharp, joukowski, oblong, streamline) and it found that the streamline shape gives minimum depth scour and the rectangular maximum Figure 2.8. Also, the results showed that there is a good agreement with theoretical equations (Colorado & Breusers et al,1977).

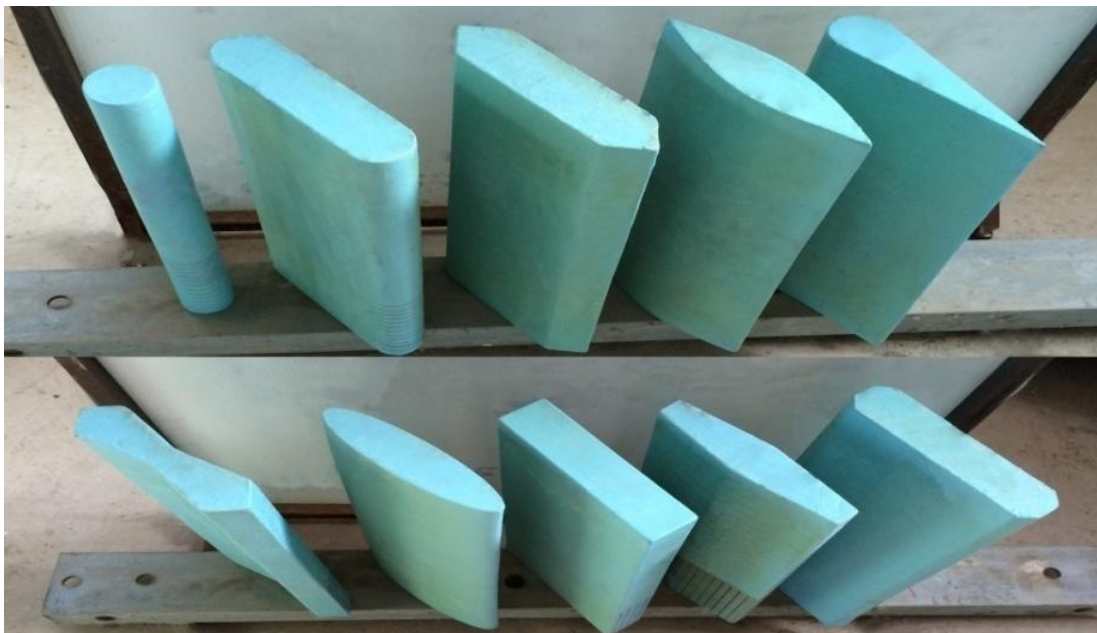


Figure 2.6 Pier shapes which used in experiments. (Al-Shukur and Obeid,2016)








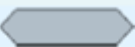


Pier Shape		V=0.18 m/s	V=0.25m/s	V=0.3 m/s
		Measured scour depth (cm)	Measured scour depth (cm)	Measured scour depth (cm)
Circular		3.9	6.1	6.9
Rectangular		4.3	6.8	7.6
Octagonal		4.2	5.2	5.9
Joukowsky		4.7	5.5	6.1
Chamfered		4.1	5.9	6.7
Oblong		4.1	4.6	5.8
Elliptical		3.6	4.9	5.6
Sharp nose		3	4.5	4.9
Hexagonal		2.8	3.6	4.1
Streamline		1.9	2.6	3

Figure 2.7 Descriptions of shapes and results of study (Al-Shukur and Obeid,2016)

CHAPTER THREE

CASE-STUDY

3.1 Introduction

In this section, a 3D numerical model of local scour around a group of bridge pier is simulated depended on an experimental study by (Tahssen, 2016). The experimental works were conducted in hydraulic laboratory in the civil engineering department at Gaziantep University, and the numerical models were carried out and simulated using Flow-3D software. The following part consists of complete detail of implemented work.

3.2 Physical Set-up and Experimental Procedure

Entire the experiments of local scour around a group of pier were done in the hydraulic laboratory of the civil engineering department at Gaziantep University, located in the Republic of Turkey. The laboratory flume which used in the experimental study is shown in Figure 3.1. The test channel consists of the following parts: (inflow pipe, flume, outflow pipe, storage tank)

3.2.1 Inflow Pipe

As depicted in Figure 3.1 the water supplied to flume by a centrifugal pump which was located beneath the laboratory floor. The valve was installed on supply pipe in order to control the flow rate during the run test.

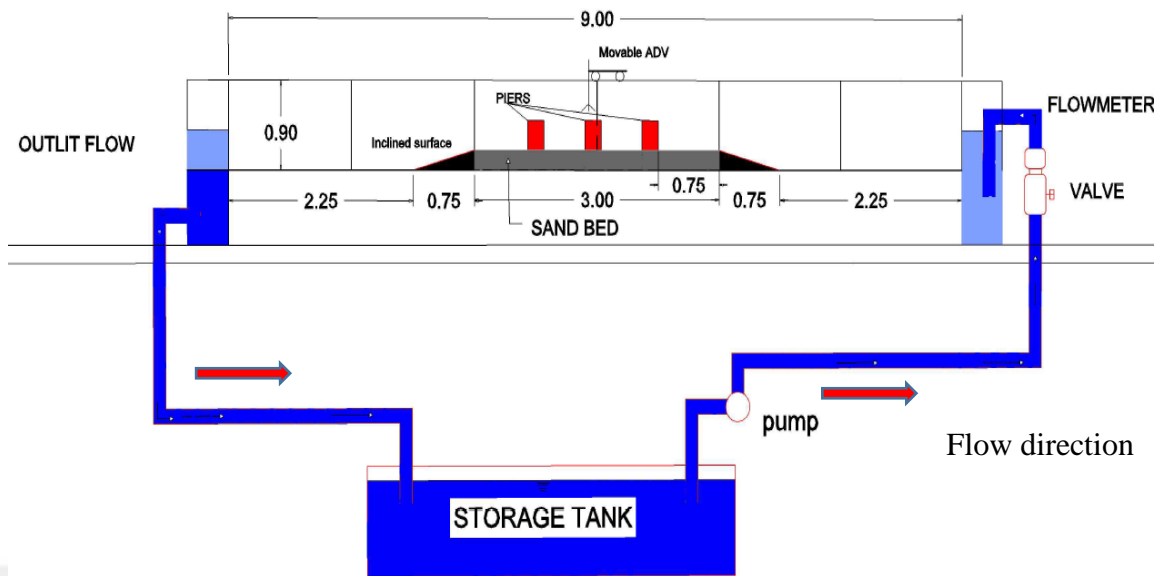


Figure 3.1 Laboratory layout



Figure 3.2 Hydraulic flume test, Gaziantep University

3.2.2 The Flume

The experiments were conducted in a recirculating flume, 9 m long, 0.80 m wide and 0.90 m in depth. Only the middle part of the flume which is filled with sand to a uniform thickness of 0.20 m. The sand bed recess was 3 m long and located at 3 m downstream of the inlet section of the flume. As seen in Figures 3.3 and 3.4 the piers were located on the center line of the channel test in all experiments, and the space between each pier was 0.50 m, also the coordinates of the piers centerline were

maintained to be constant for all cases, in order to ensure the inter-comparison of measured outline profiles. Figure 3.5 illustrates shapes and dimensions of tested piers. The working section of the flume is made up of a transparent glass sidewall along each side of the flume for entire of its length to simplify visual observations. The magnetic flow meter was installed on the water pipe before the inlet of the channel to measure the discharge. Steel mesh installed at beginning of front flume to avoid the turbulence of water spilling from inlet pipe.

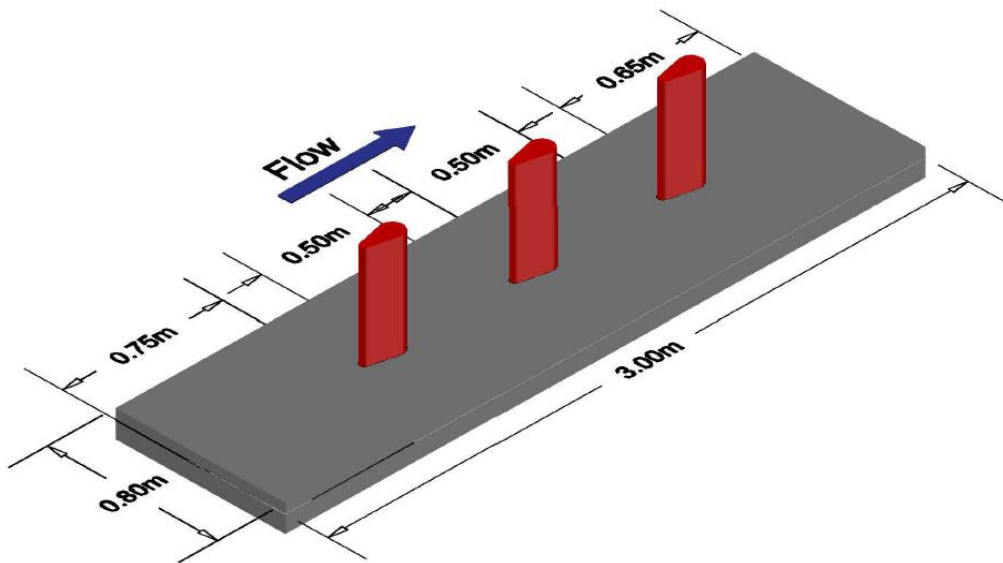


Figure 3.3 Piers and flume geometry in Flow 3D model (4-10)

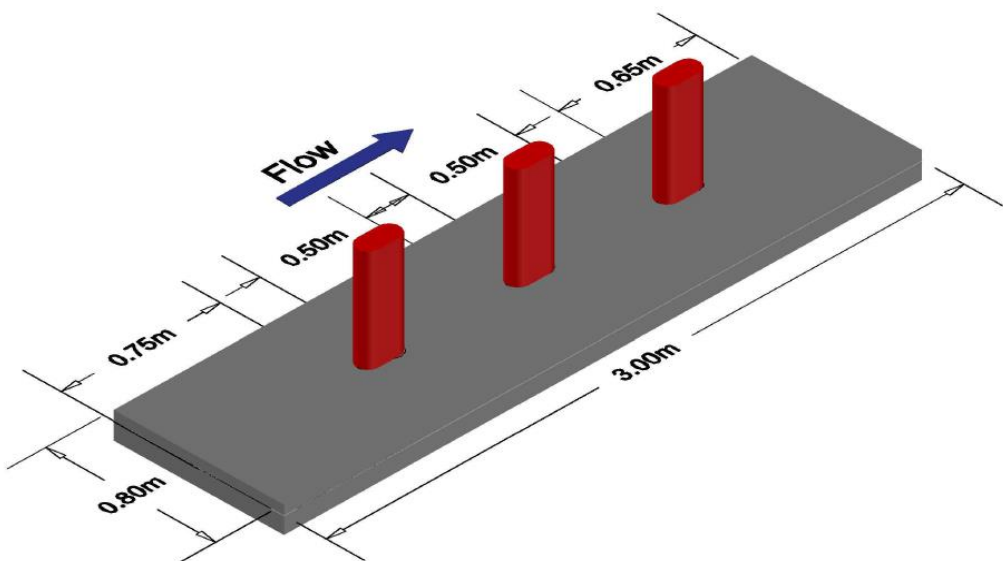


Figure 3.4 Piers position and flume geometry in Flow 3D model (10-10)

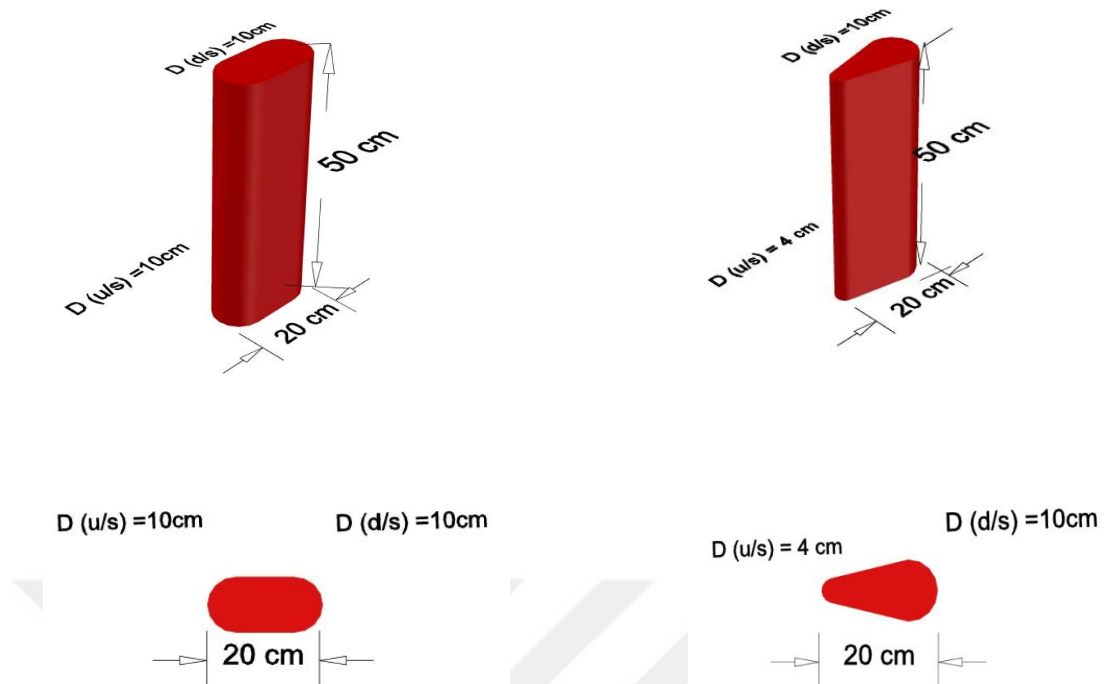


Figure 3.5 Shapes and dimensions of tested bridge piers

3.2.3 Outflow Pipe and Storage Tank

After the flow passing through the flume, it will divert through the outflow pipe to a storage tank which located underground of the laboratory.

3.3 Bed Material

The soil material which has been used in the tests were categorized according to the results obtained from two experiments soil sample (mechanical sieve analysis and a specific gravity). The results of tests showed that the bed material consists of Cohesion-less sand with a median particle size (d_{50}) = 1.60 mm and the specific gravity (σ_g) = 2.65 (g/cm^3), and the standard deviation of the sand was (σ_g) = 3.65

$$(\sigma_g) = \left(\frac{d_{84}}{d_{16}}\right)^{0.5}$$

That means the sand is having uniform size of the distribution. As illustrated in Figure 3.6:

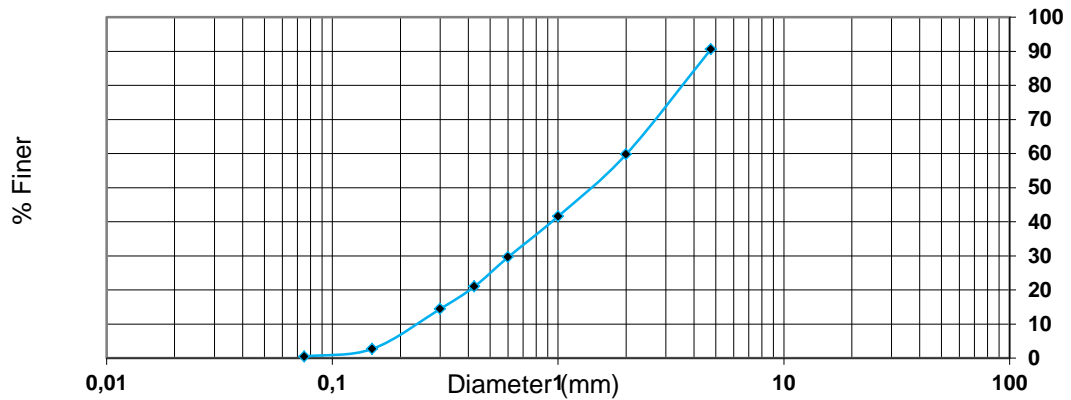


Figure 3.6 The grain size distribution curve of the bed material

3.4 Brief Introduction to Flow 3D

Numerical (CFD) is a technique of simulating the flow process in which flow equations such as (Navier-Stokes, continuity equation) are discretized and solved for every computational cell (Flow Science, 2008).

Computational fluid dynamics software is similar in several ways to the practical experiment procedure. If the experiment does not proceed correctly to simulate a real-life condition, then the results will not give the real-life situation. If the numerical model does not enter into the CFD software as accurately same as the practical ambient conditions, then the results cannot be used to make such a comparison. It means that the user must have an appropriate idea of how represent the problem and what important factors should included within.

For instance, the scale, the meshing, kinds of boundary conditions, kinds and properties of fluids, physical phenomena, initial fluid state, what system of units should be used? All those questions should be known before starting to modeling. It is very important to represent the actual observed conditions as possible as it be.

The FLOW-3D software package contains three main unit parts to solving and hydraulic engineering problems: the first one is a preprocessor (PREP3D) in this portion data inserting and mesh grid will arrange according to descrip of the problem which includes: sets up the geometry, grid, data inserting, boundary conditions and initial conditions. The second part is analyzer (HYDR3D) which is going to calculate flow solution at any time step, the final part is (FLSCON) this portion known as

postprocessor in this phases the outcome can see in many forms such as (data, image, graph, plot....etc..).

This software is a commercial CFD package with excellent modules suggested for hydraulic engineering researches. Flow-3D software uses an organized orthogonal grid and also by the features fractional area volume of method (FAVOR) can modeling and meshing of Complex shapes geometry.

Volume-of-fluid (VOF) method is used to model free surface flow, open channel for example (Hirt and Nichols, 1981) tracking air and fluid with fluid boundaries. Also, it is a perfect for modeling local scour (Brethour., 2001).

The software capable to solve the three-dimensional (Navier-Stokes equations) on grid domain with the continuity equations composed of the fluid flow equations for the turbulence quantities. Also, Flow 3D has many excellent facilities features such as facility of the select time step size automatically, graphical in short time, and additional features will be displayed in following sections.

Computational domain will be subdivided into cells , The finite-difference mesh utilized for numerically solving the main equations consists of rectangular cells of (dx_i, dy_j, dz_k) width, depth and height respectively.

The active mesh region identified in x-direction index i (IBAR), y-direction j (JBAR), and z-direction k (KBAR),(Flow science. 2008), The regions are surrounded by layers of fictitious or boundary cells used to set mesh boundary conditions. The region is surrounded by a layer of imaginary cells or boundary cells that are used to set the mesh boundary condition.

3.5 Numerical Model Set-Up

This study is a simulation of local scour around a group of pier by using Flow-3D software. To discretize the computational domain, the solver uses finite volume. For all run tests, one incompressible fluid with a free surface and clear water at 20 degrees Celsius were used for simulating.

Bed material is consisting of 20 cm of sand bed level which has a median grain size of sand (d_{50}) equal to 1.6 mm and (the density of mass = 2650kg/cm^3) and critical

shield parameter, entrainment coefficient, and bedload coefficient equal to (0.035,0.018,8.0) respectively. Also, the critical package fraction =0.64 as depicted in Figure3.9.

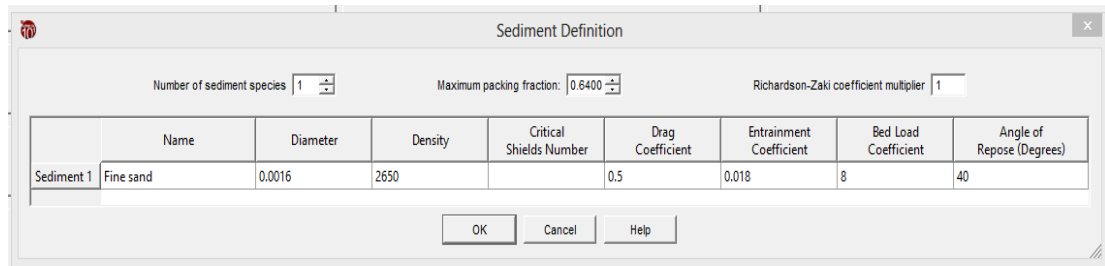


Figure 3.7 Sediment definition in Flow-3D.

The general model Arrangement of all the piers, were carried out very similar to the laboratory models. The depths of scour around a group of pier have been calculated for two models of piers with two different flow rates for each model. The flow rate, water depths, length span and velocity of water in upstream of the flume in Table 3.1 illustrated.

Table 3.1 The test conditions

#	Cases	Q (m ³ /s.)	Water depth (cm)	Velocity (m/s)	Span length (m)
1	(4-10)	0.038	9.50	0.50	0.50
2	(10-10)	0.057	12.50	0.593	0.50
3	(4-10)	0.038	9.50	0.50	0.50
4	(10-10)	0.057	12.50	0.593	0.50

3.5.1 Physics

In Flow-3D software to calibrate physical problems perfectly, there are various physical options should be arranged, for scouring it is necessary to take two specific parameters to obtain an accurate simulation of the data required in this study. The gravity was activated and should be negative 9.81 m/s², non-inertial with turbulence also viscosity were considered in this study, additionally ($k-\epsilon$) model and (RNG) and large eddy simulation model were activated. (Anu& Jennifer.,2011) according to the experiments that they are carried out, proved that (RNG) Model is the proper choice to predictions the mean flow field.

Each physical option includes many divergence options, there are five different choices in turbulence option, two equations (k - ε) model has been selected for this study.

(k - ε) model flow was to provide a reasonable approximation for many kinds of flow, additional transport equations for turbulent diffusion are solved, ε_T in Equation 3.1.

$$\frac{\partial \varepsilon_T}{\partial t} + \frac{1}{V_F} \left(u A_x \frac{\partial \varepsilon_T}{\partial x} + v A_y R \frac{\partial \varepsilon_T}{\partial y} + w A_z \frac{\partial \varepsilon_T}{\partial z} \right) = \frac{CDIS1 \cdot \varepsilon_T}{k_T} (P_T + CDIS3 \cdot G_T) + Diff \varepsilon - CDIS2 \frac{\varepsilon_T^2}{k_T} \quad (3.1)$$

Here CDIS1, CDIS2, and CDIS3 are all dimensionless user-adjustable parameters and have defaults of 1.44, 1.92 and 0.2, respectively for the (k - ε) model.

The diffusion of dissipation, Diff ε is showed in Equation 3.2.

$$Diff \varepsilon = \frac{1}{V_F} \left\{ \frac{\partial}{\partial x} \left(v \varepsilon A_x \frac{\partial \varepsilon_T}{\partial x} \right) + R \frac{\partial}{\partial y} \left(v \varepsilon A_y R \frac{\partial \varepsilon_T}{\partial y} \right) + \frac{\partial}{\partial z} \left(v \varepsilon A_z \frac{\partial \varepsilon_T}{\partial z} \right) + \xi \frac{v \varepsilon A_x \varepsilon_T}{x} \right\} \quad (3.2)$$

The rate of turbulent energy dissipation, ε_T , the one-equation model is related to the turbulent kinetic energy k_T as illustrated in Equation 3.3.

$$\varepsilon_T = CNU \sqrt{\frac{3}{2}} \frac{k_T^{3/2}}{TLEN} \quad (3.3)$$

CNU is a parameter (0.09 by default), k_T is the turbulent kinetic energy and TLEN is the turbulent length scale.

for bed shear stress this equation was used

$$u = u_\tau \left[\frac{1}{\kappa} \ln \left(\frac{Y}{\frac{v}{u_\tau} + k_s} \right) \right] \quad (3.4)$$

for critical shields parameter this equation was used

$$\theta'_{cr,n} = \theta_{cr,n} \frac{\cos \psi \sin \beta + \sqrt{\cos^2 \beta \tan^2 \phi_n - \sin^2 \psi \sin^2 \beta}}{\tan \phi_n} \quad (3.5)$$

where β is the slope angle of the packed bed, ϕ_n is the angle of repose

for bed load transportation velocity:

$$\mathbf{u}_{b,n} = \frac{\mathbf{q}_{b,n}}{h_n c_{b,n} f_b} \quad (3.6)$$

where f_b is the total packing fraction of sediments. Both \mathbf{u}_b , and \mathbf{q}_b , are in direction of the fluid flow adjacent to the bed interface.

$$\frac{\partial C_{s,n}}{\partial t} + \nabla \cdot (C_{s,n} \mathbf{u}_{s,n}) = \nabla \cdot \nabla (DC_{s,n}) \quad (3.7)$$

$C_{s,n}$ is the suspended sediment mass concentration

3.5.2 Geometry

Although there are several shapes available in Flow-3D software to create simple objects, complex objects should be drawn by any software able to draw a stereolithography and have (.*stl*) format in saving-(most CAD) package- to create the shape required to the investigation. All geometry of piers for each model was drawn in Auto-Cad software and exported as (.*stl*) file which able in Flow 3D bar. The (.*stl*) file directly import into the Flow-3D, and to more accuracy, the coordinates (x,y,z) should be known in Auto-Cad to layout at the correct location in Flow 3D.

3.5.3 Meshing

FLOW-3D uses orthogonal meshes defined in either Cartesian or cylindrical coordinate systems. Selection of a mesh (cylinder or Cartesian) influences some of the geometric definitions. Complex geometrical shapes are modeled using the FAVOR method, where obstacles and baffles are fixed in the orthogonal mesh by partially blocking cell volumes and appearance areas.

This permits completely independent descriptions of the mesh and geometry. That is, the geometry may be adapted without redefining the mesh, making this method much simpler and faster than mesh generation with frame fitted coordinates. It can be defined independently for all orthogonal coordinates.

We can also describe multiple mesh blocks (multi-block gridding) to make meshes more efficient when modeling composite flow domains. Additional mesh blocks can also be defined to be completely contained within other mesh blocks (Including Aligned with the containing Block Boundaries, this is called a nested block), at the boundary of another mesh block (called a linked block) (Flow 3D Manual, 2008). The size of mesh block is very important because it effects both of the running time

and the accuracy of results. In this study, the computational domain was distributed to the mesh sizes in (x,y, and z) directions are (0.025 m).

3.5.4 Data Sharing

In FLOW-3D there are many options for data output such as numerical data depictions, and animations for input in presentations and inserting in reports. For instance, (plot data output, Restart data, History data, sampling volume, flux surface, history probes, selected data) are available options for data output.

Figure 3.10 and 3.11 show the 3D and 2D computational domain model (10-10) content of 3.0 m long, 0.40 m width and 0.50 m high, and the mesh sizes in (x,y, and z) directions are (0.025 m).

And Figure 3.12 and 3.13 showing the 3D and 2D model of the computational domain model (4-10) that is 3.0m long, 0.40 m width and 0.50 m high.

(10-10): No of both active and passive cells equal to 67071, no of active cells equal to 52887, including real cells (used for solving flow equations) were 42132, open cells =42132 fully blocked real cells equal to zero, external boundary cells were 8663, inter-block boundary cells = 0 (Flow-3D report).

(4-10): No of both active and passive cells equal to 53463, no of active cells equal to 42035, including real cells (used for solving flow equations) were 33372, open cells =33372 fully blocked real cells equal to zero, external boundary cells were 8663, inter-block boundary cells = 0 (Flow-3D report).

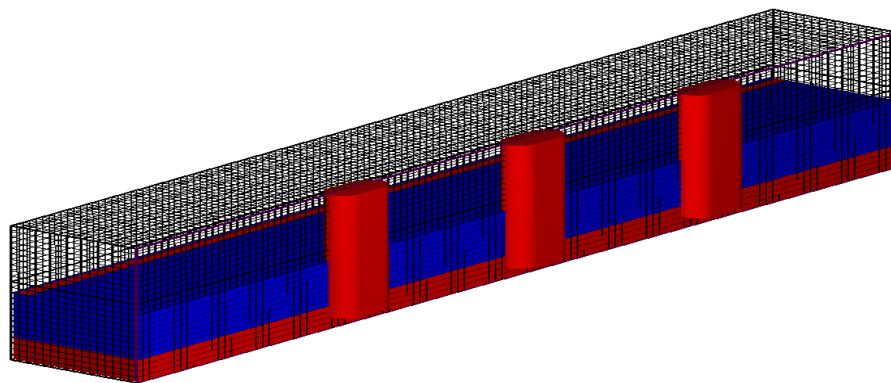


Figure 3.8 Computational domain and mesh setup around the bridge piers model (10-10)

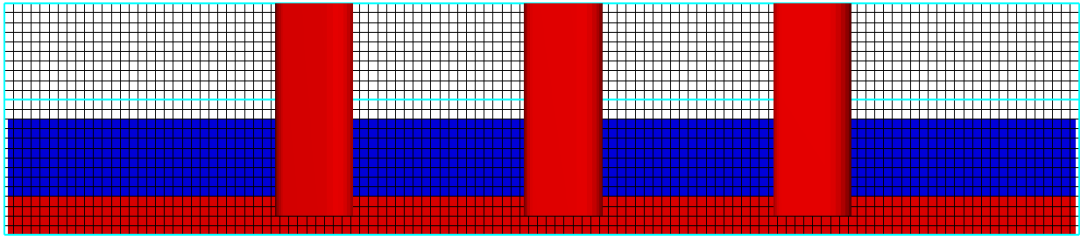


Figure 3.9 2D Computational domain model (10-10)

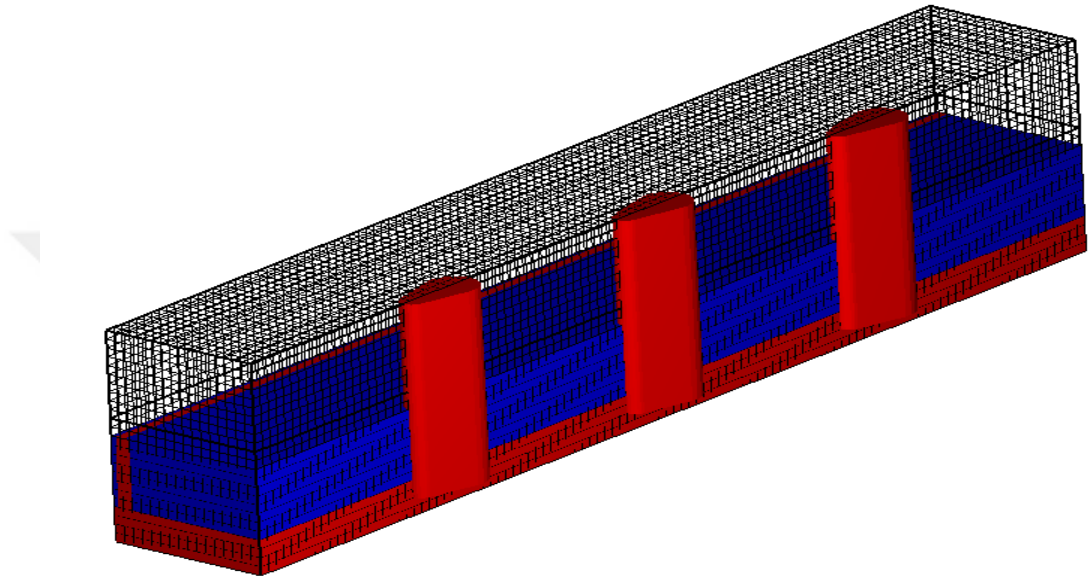


Figure 3.10 Computational domain and mesh setup around the bridge piers model (4-10)

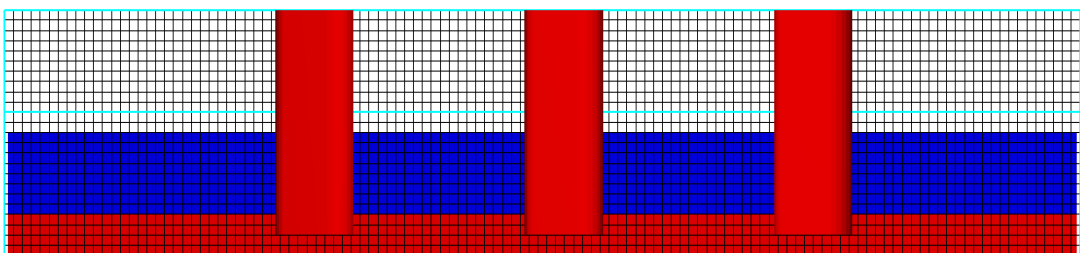


Figure 3.11 2D computational domain model (4-10)

3.5.5 Specifying Boundary Conditions and Initial Conditions

In the Flow-3D software there are two options to input limited flow rate whether for inlet discharge to the system or for outlet of the domain (Volume Flow rate and Specified velocity), for the X min boundary condition of this work, specified velocity

has been selected because this property generate a steady pressure change in the calculation domain which is difficult to calculate by any available iteration ways. At the end of the flume, there is nothing to be calculated, therefore, for Outlet, X max. Boundary condition Outflow chose like a more suitable select for this work. As shown in Figures 3.12 and 3.13 the velocity and the elevation of surface water have been set for flow rate 0.038 and 0.057 m³/s respectively

Flow-3D software needs a good and strong computer to calculate running process, the size of the domain and the shape of the model has a main effect on running time to calculate. Y min. boundary condition selected as symmetry to gain a time and minimize the size of the model, so half of the model is placed in the domain to calculate then by the feature of the Flow-3D the remaining part of the model it can be shown. The Y max is defined as a wall Boundary condition.

The Z min. (Bottom of the flume) is prepared as a wall boundary condition, but the top is counted as Pressure boundary condition.

Flow-3D has many types of boundary condition; each type uses for the specific condition of the models. The boundary conditions in Flow-3D are symmetry, continuative, specific pressure, grid overlay, wave, wall, periodic, specific velocity, outflow, and volume flow rate. As evidence in Figures 3.14 and 3.15 the boundary condition for the simulated models are presented by one capital word.

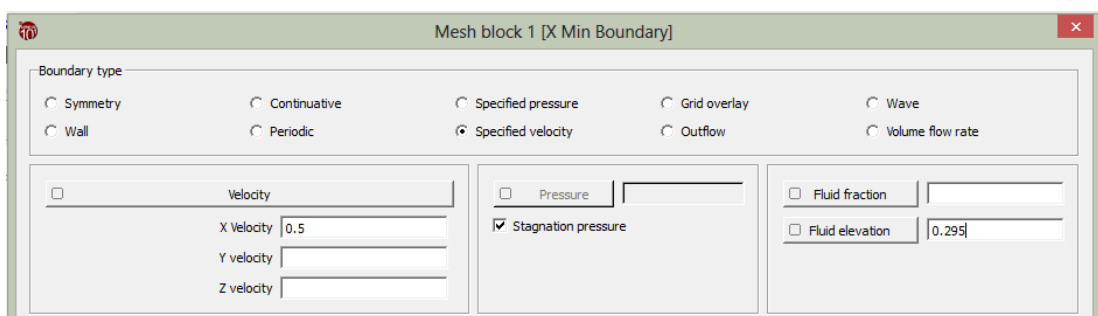


Figure 3.12 Inlet boundary condition for $Q=0.038 \text{ m}^3/\text{s}$, velocity=0.5 m/s and fluid elevation =0.295m.

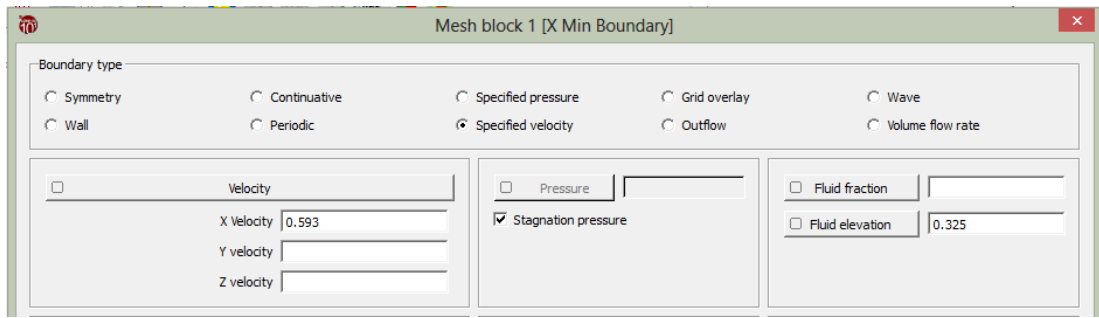


Figure 3.13 Inlet boundary condition for $Q=0.057 \text{ m}^3/\text{s}$ velocity= 0.593 m/s and fluid elevation = 0.325m .

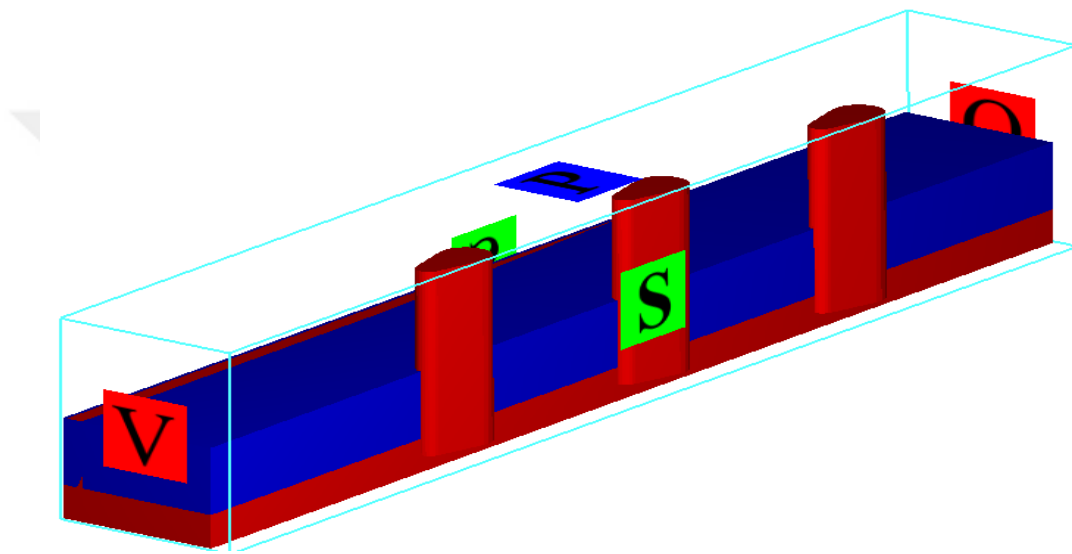


Figure 3.14 Boundary conditions for the model (4-10)

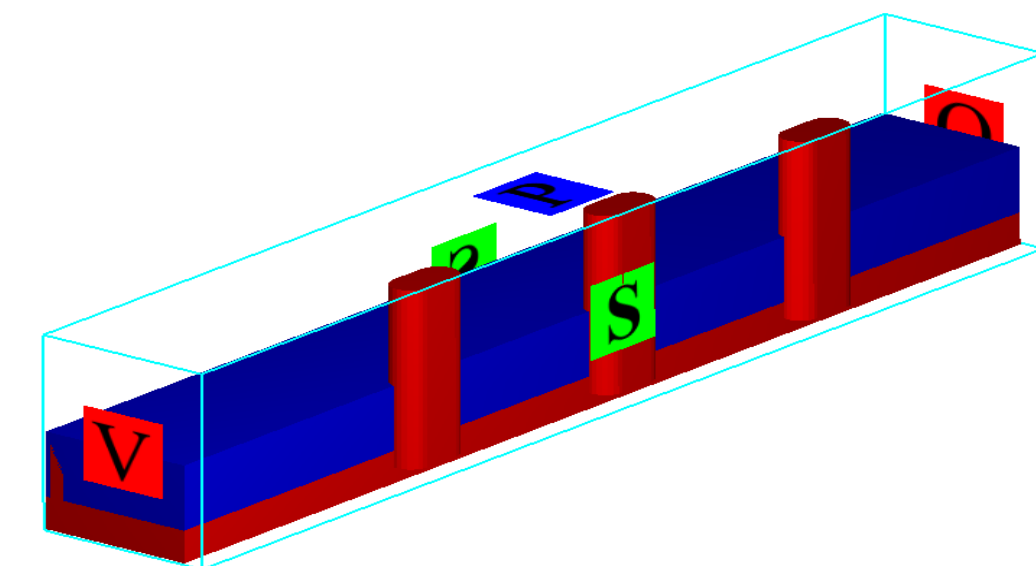


Figure 3.15 Boundary conditions for the model (10-10)

CHAPTER FOUR

RESULTS AND DISCUSSION

4.1 Introduction

In this study, simulated results by the Flow-3D software of two different bridge pier models with different discharges are compared with laboratory results for estimating the precision of CFD software, and to estimate the maximum depth of scouring around a group of bridge piers.

It is clear that the estimating of highest scour is an important step in the design of bridge piers foundation. In this part, results are presented the comparison between CFD and experimental findings for depth of scour in front of bridge pier in different discharges. The depth of scour is calculated by Flow-3D software on the bed of the used channel and compared with observed results, and then the effect of discharges with different shapes of pier and effect of the same pier on different discharges are presented. Besides that, the effect of shapes on the depth of scour in a group of bridge piers also showed.

Longitudinal profiles for different discharges and different shapes of piers are also noticed with the influence of velocity. To judge the sediment motion in scour, the shear stress is regarded as a key parameter, and after comparing all the results it is concluded that Flow-3D software is a good and reliable tool to discuss and predict the scour around a group of bridge pier and development of scouring process.

4.2 Comparing between Experimental and CFD (Flow-3D) Software

4.2.1 Comparison of Scour

The scour around piers in all models of group bridge pier showed that the results of both experimental and CFD are identical in terms of increase in depth of scouring corresponding to time. In order to compare the CFD and experimental results, to better understanding the comparisons, both centerline of the models, and physical channel are combined in one chart. As shown in Table 4.1 and Figure 4.1 to Figure 4.6 the scour around pier at discharge $0.057 \text{ m}^3/\text{sec}$ in centerline of flume and model for pier geometry (4-10) cm, (10-10) cm, respectively, the scour rapidly developed then it is going to reduce and to slow down to relative stability but not to reach equilibrium. Figure 4.7 to Figure 4.12 show the scour around the pier at discharge $0.038 \text{ m}^3/\text{s}$ in the centerline of flume and model for pier geometry (4-10) cm, (10-10) cm, respectively.

Table 4.1 Max. scour depths corresponding to pier shape and discharge

Run No.	Pier type	Piers	Q (m^3/s)	Experimental ds (cm)	Flow 3D ds (cm)
1	(10- 10)	pier1	0.057	12.50	6.20
	(10- 10)	pier 2	0.057	11.80	5.40
	(10- 10)	pier3	0.057	12.00	7.50
2	(4- 10)	pier1	0.057	9.20	2.20
	(4- 10)	pier 2	0.057	8.00	5.30
	(4- 10)	pier3	0.057	4.30	5.60
3	(10- 10)	pier1	0.038	11.50	5.40
	(10- 10)	pier 2	0.038	10.50	7.50
	(10- 10)	pier3	0.038	8.40	5.80
4	(4- 10)	pier1	0.038	7.70	2.1
	(4- 10)	pier 2	0.038	4.00	3.50
	(4- 10)	pier3	0.038	5.00	5.00

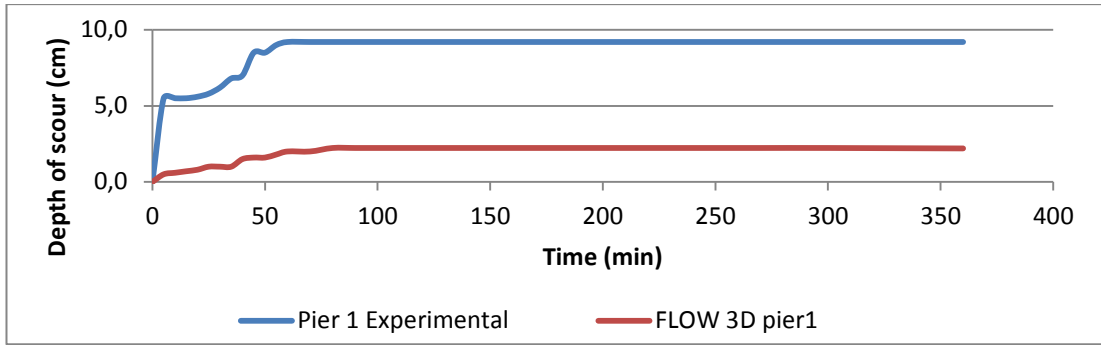


Figure 4.1 Comparison between Experimental and Flow-3D results of scour development with time in pier number (1) at a flow rate (0.057) m³/sec. and pier shape (4-10)

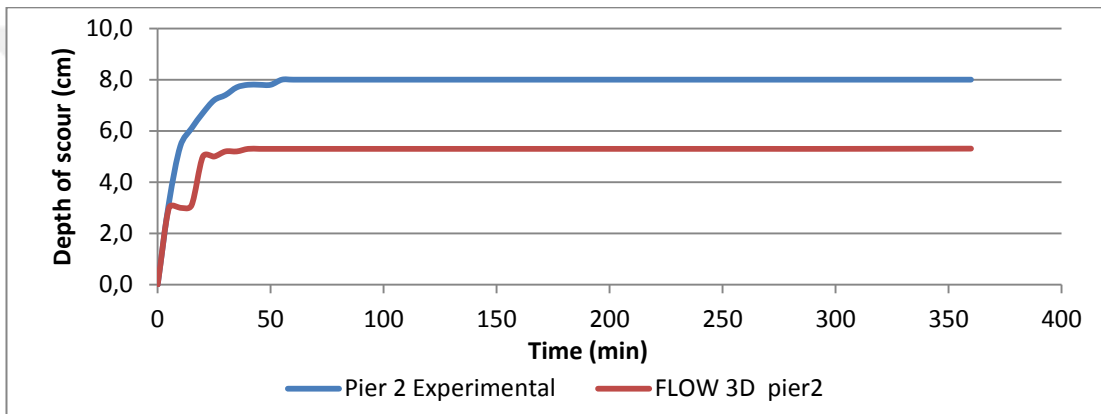


Figure 4.2 Comparison between Experimental and Flow-3D results of scour development with time in pier number (2) at a flow rate (0.057) m³/sec. and pier shape (4-10)

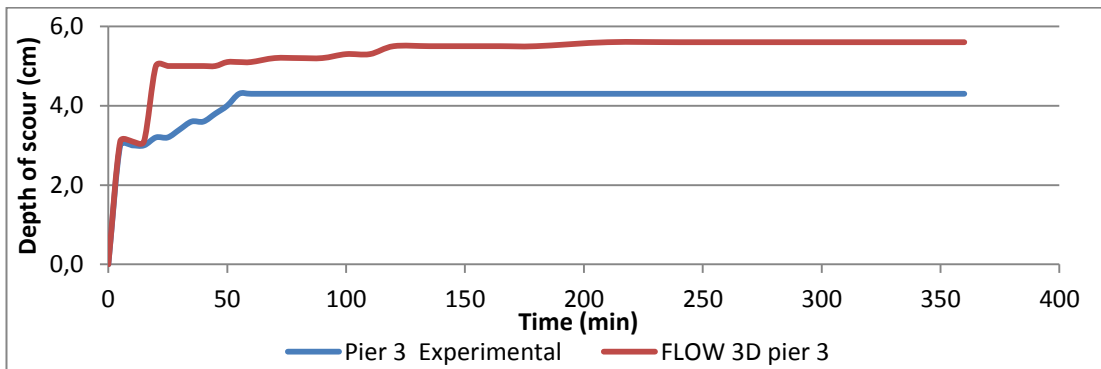


Figure 4.3 Comparison between Experimental and Flow-3D results of scour development with time in pier number (3) at a flow rate (0.057) m³/sec. and pier shape (4-10)

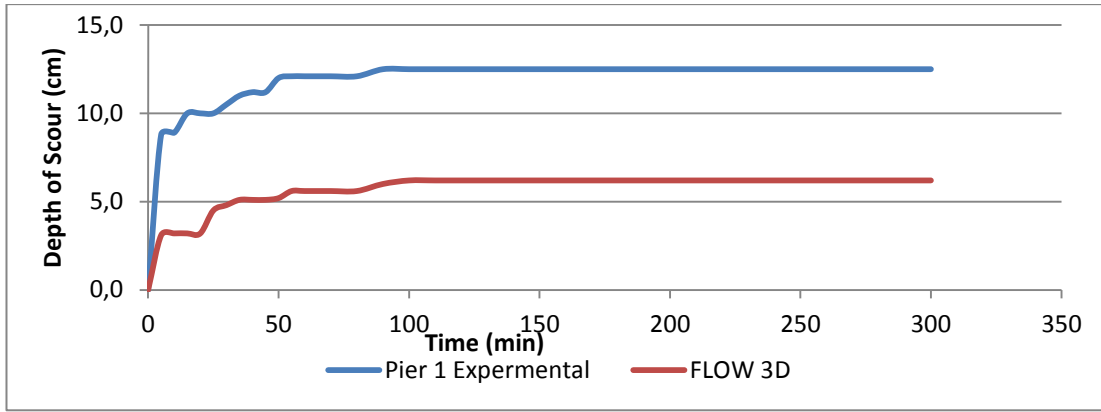


Figure 4.4 Comparison between Experimental and Flow-3D results of scour development with time in pier number (1) at a flow rate (0.057) m³/sec. and pier shape (10-10)

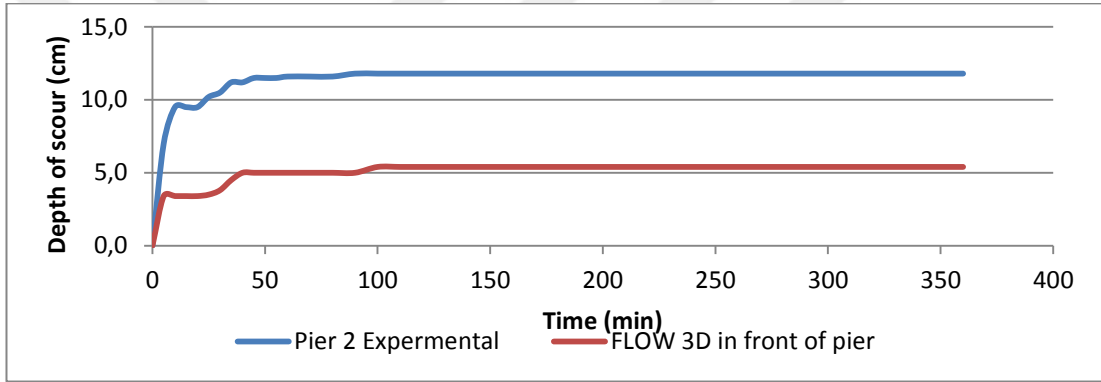


Figure 4.5 Comparison between Experimental and Flow-3D results of scour development with time in pier number (2) at a flow rate (0.057) m³/sec. and pier shape (10-10)

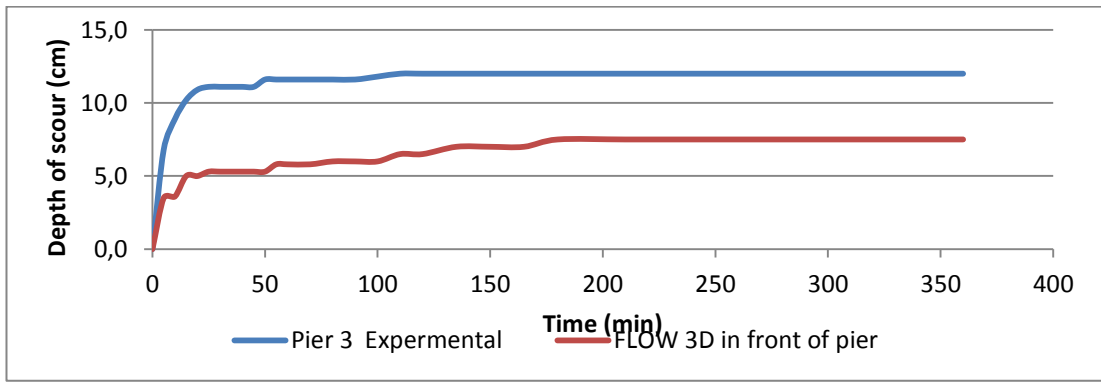


Figure 4.6 Comparison between Experimental and Flow-3D results of scour development with time in pier number (3) at a flow rate (0.057) m³/sec. and pier shape (10-10)

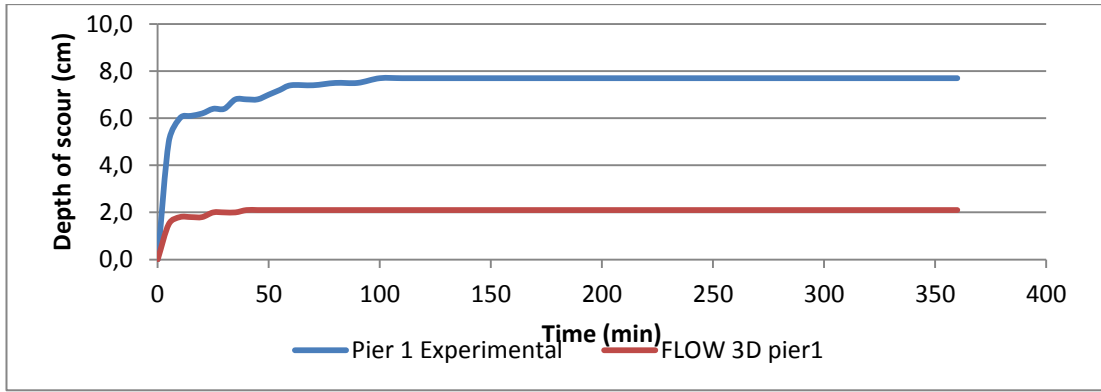


Figure 4.7 Comparison between Experimental and Flow-3D results of scour development with time in pier number (1) at a flow rate (0.038) m³/sec. and pier shape (4-10)

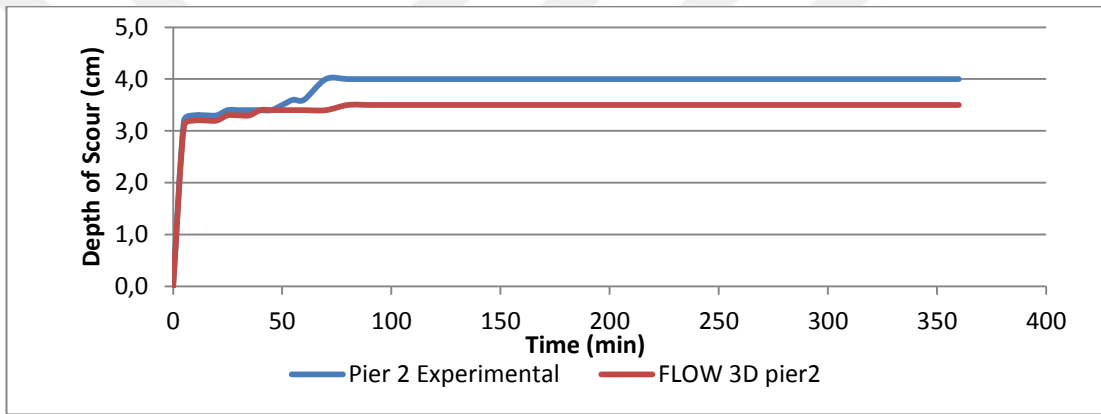


Figure 4.8 Comparison between Experimental and Flow-3D results of scour development with time in pier number (2) at a flow rate (0.038) m³/sec. and pier shape (4-10)

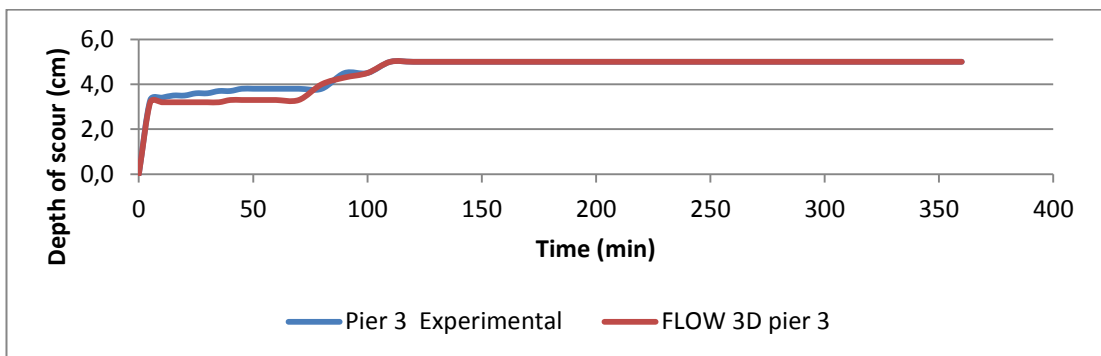


Figure 4.9 Comparison between Experimental and Flow-3D results of scour development with time in pier number (3) at a flow rate (0.038) m³/sec. and pier shape (4-10)

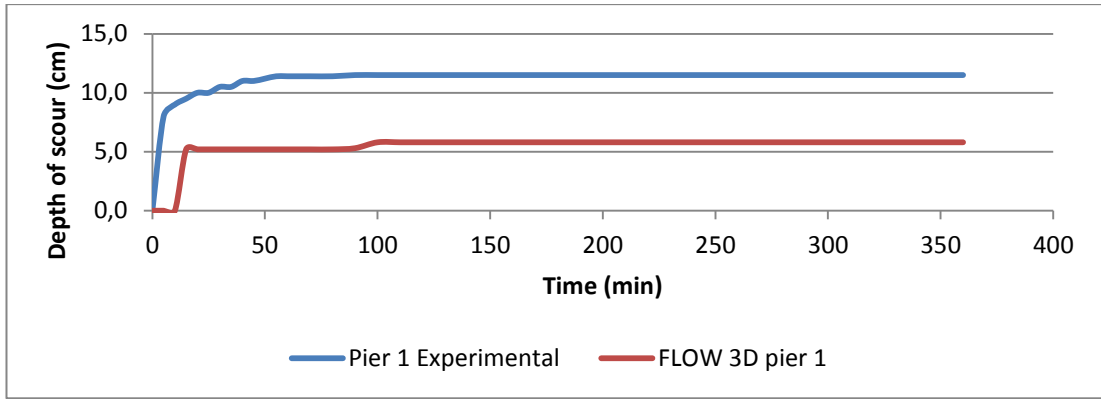


Figure 4.10 Comparison between Experimental and Flow-3D results of scour development with time in pier number (1) at a flow rate (0.038) m³/sec. and pier shape (10-10)

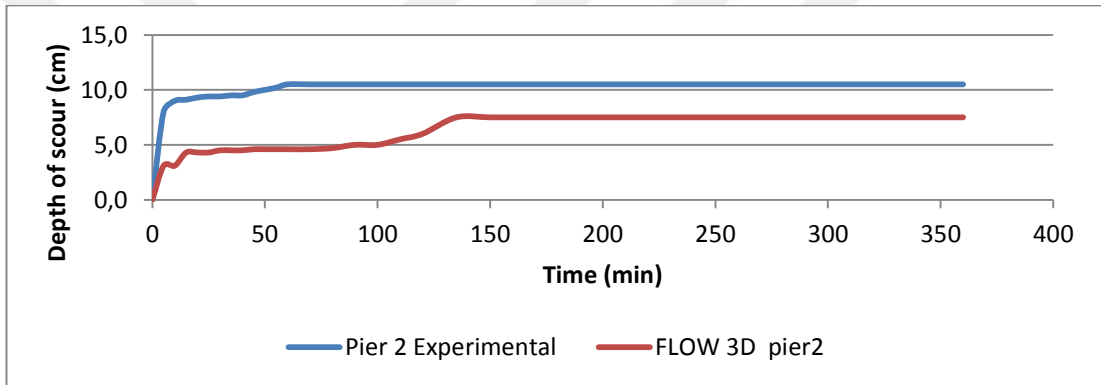


Figure 4.11 Comparison between Experimental and Flow-3D results of scour development with time in pier number (2) at a flow rate (0.038) m³/sec. and pier shape (10-10)

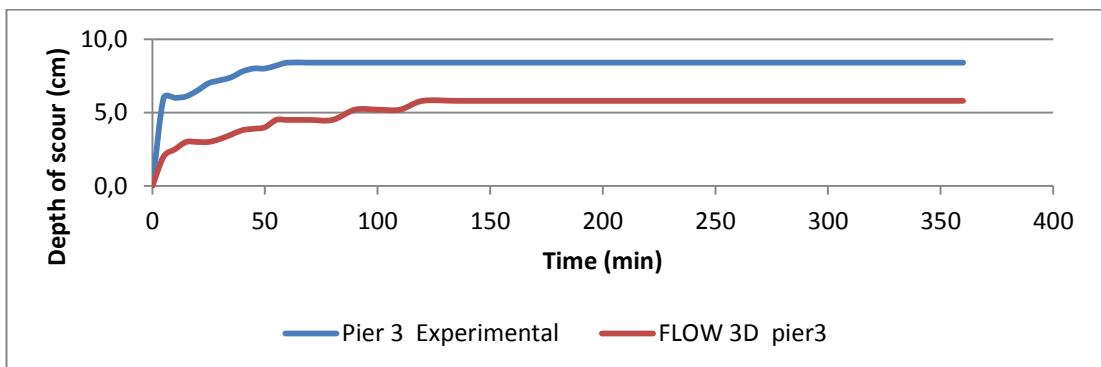


Figure 4.12 Comparison between Experimental and Flow-3D results of scour development with time in pier number (3) at a flow rate (0.038) m³/sec. and pier shape (10-10)

4.2.2 Longitudinal Bed Profile of Sand

In order to compare longitudinal bed profile of sand bed along the centerline of the flume, the results of computational fluid dynamic (CFD) and experimental data were plotted together for easy comparison, as shown in Figures 4.13 and 4.14. It can be seen in Figures the scour along the section of the Flume, the appearance of scouring in CFD and observed are identical in the aspect of form with difference in maximum scour at the same point and the same time, the scour in experimental was deeper than CFD.

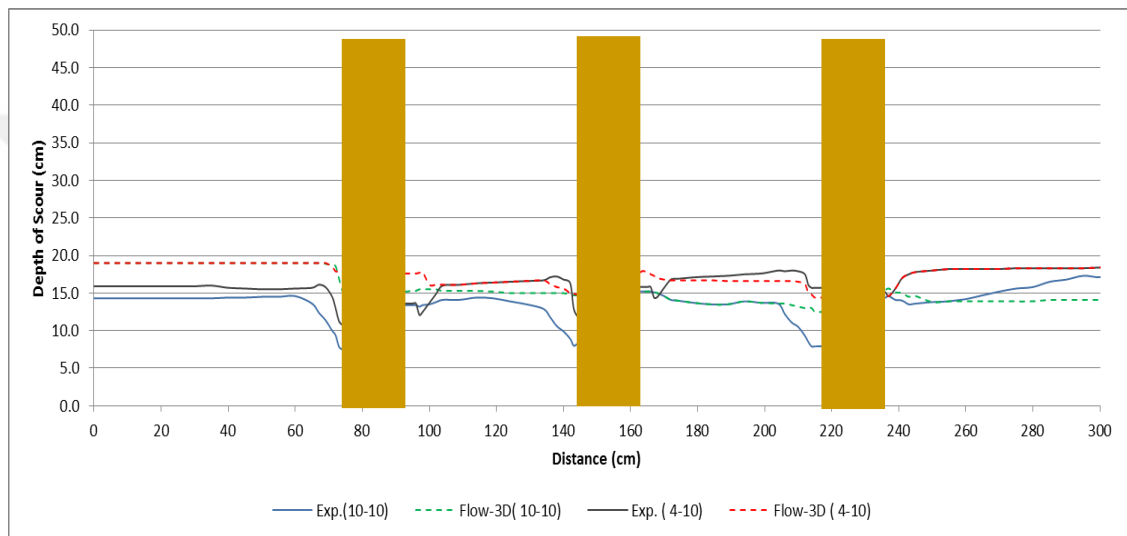


Figure 4.13 Comparison of the longitudinal profile of bed for bridge piers (10-10) and (4-10) for experimental and Flow-3D at flow rate $0.057 \text{ m}^3/\text{s}$.

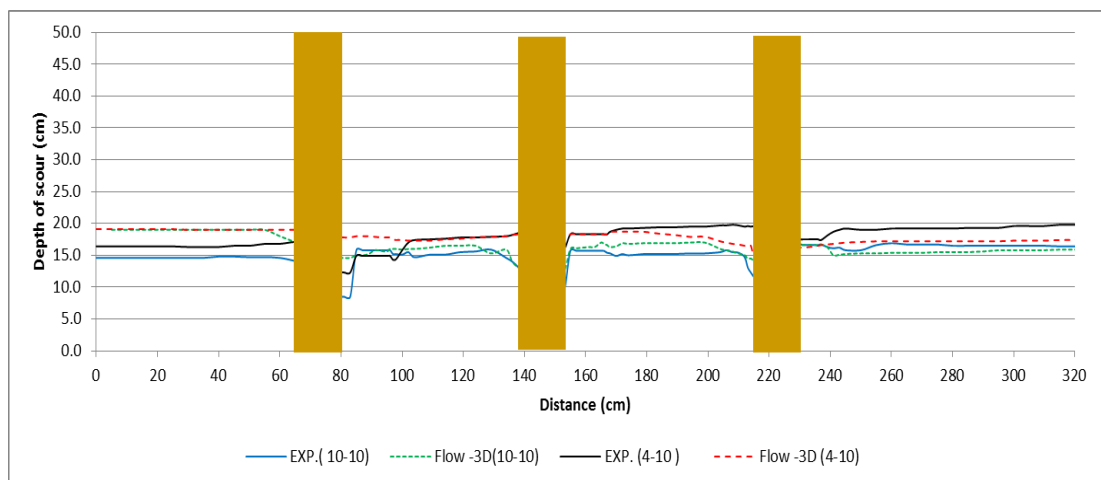


Figure 4.14 Comparison of the longitudinal profile of bed for bridge piers (10-10) and (4-10) for experimental and Flow-3D at flow rate $0.038 \text{ m}^3/\text{s}$.

In this work, for discharge of $0.057 \text{ m}^3/\text{sec}$ observed that scouring depth reduced in geometry shape (4-10) cm around (30.57) % in average if compared with shape geometry (10-10) cm, and it also for discharge $0.038 \text{ m}^3/\text{sec}$ the scour depth reduced by (42.75) % if we make a comparison between (10-10) shape and (4-10) shape.

In an experimental investigation for the discharge of $0.057 \text{ m}^3/\text{sec}$ it can be seen that the scour depth in upstream of pier reduced around (40.90) % if to comparing between (10-10) cm and (4-10) cm shape geometry and for discharge $0.038 \text{ m}^3/\text{s}$ it is reduced about (45.14) % for the same models. However, the CFD results are not exactly similar to experimental results; but it gives clear vision to know the best geometry shape.

The starting of scour is different between the models of the pier, it is depending on the pier shape and flow discharge. The shape of scouring begins started in form of mound and dispassion interspersed with deep points of scour holes. The scour hole development around the shape (10-10) cm is faster compared to the shape (4-10) cm for both discharges. It was noticed that almost change of scour depth occurred in the first third hours, see Figure 4.15 to Figure 4.18 show the comparing of scour in two models at each discharge, and it is very clear to notice that the most scouring quickly happened in the first hour of the test time.in order to compare the scour with other hours of the test time.

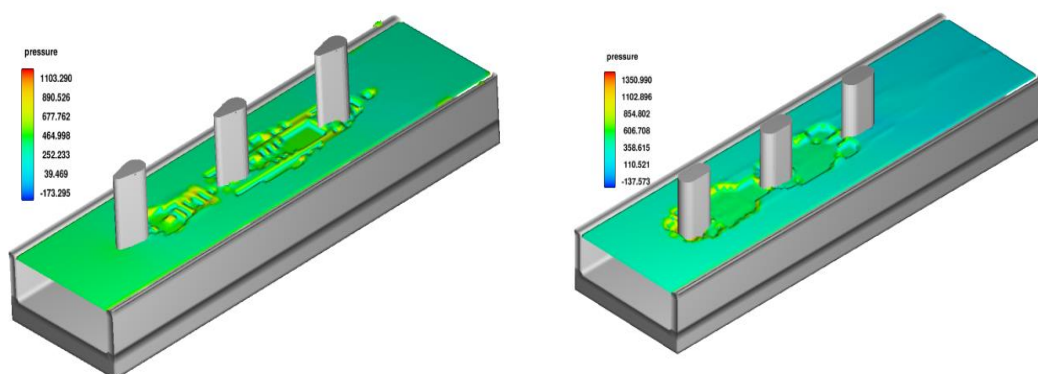


Figure 4.15 scour development at time = 5 min and discharge $0.057 \text{ m}^3/\text{sec}$

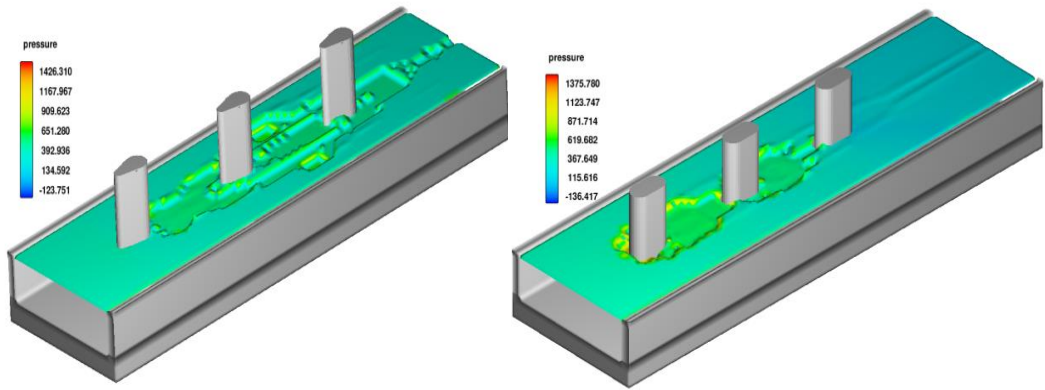


Figure 4.16 scour development at time = 15 min and discharge $0.057 \text{ m}^3/\text{sec}$

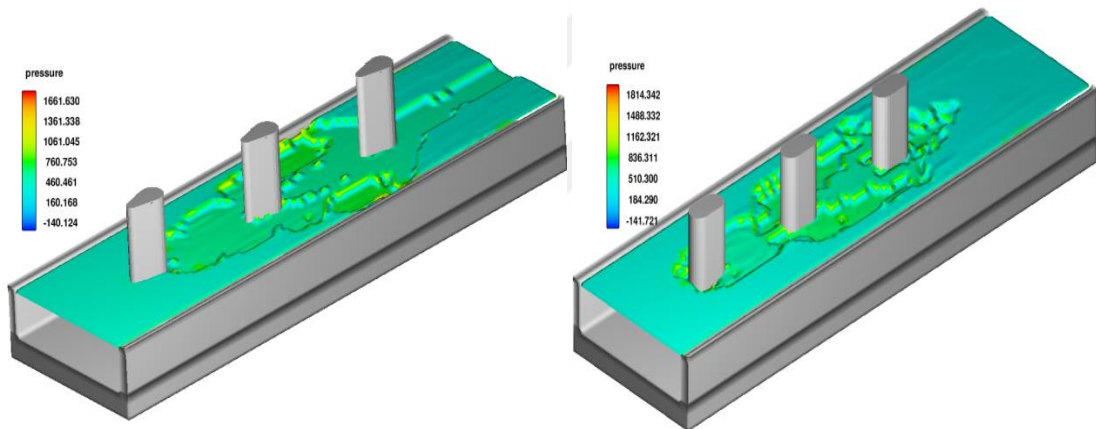


Figure 4.17 scour development at time = 60 min and discharge $0.057 \text{ m}^3/\text{sec}$

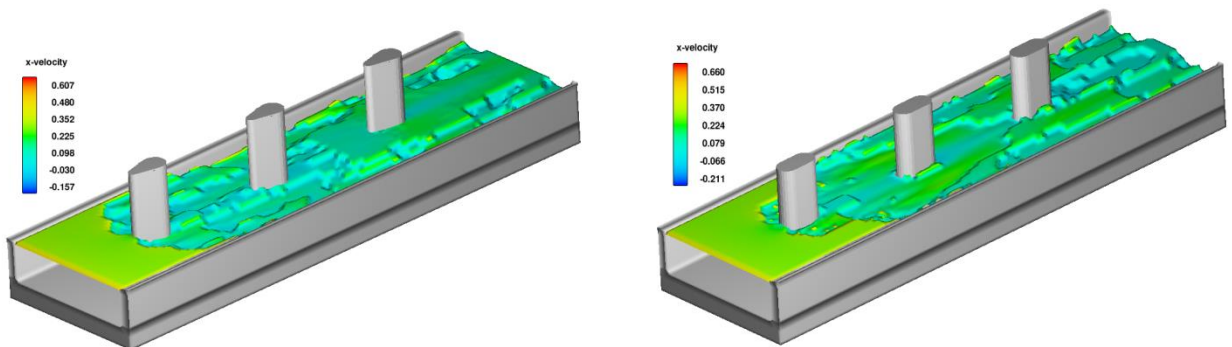


Figure 4.18 scour development at time = 360 min and discharge $0.057 \text{ m}^3/\text{sec}$

4.3 Velocity Field

Figures show the velocity vectors at vertical plan after 180 min. of running time through the centerline of the models. As is shown in Figure 4.19 to Figure 4.22 the vortices in flow field are deviated with the piers which indicates a complex behavior as it were expected, as a primary vortex, flow will be separated and turned backward. Figure 4.20 shows typical time-averaged velocity vectors for a cross-section of the model. It is clear that main vortices are formed behind the piers. The direction of this vortex rotation is count-clockwise. As it cleared Figure 4.22 that a strong horizontal vortex is formed in both upstream and downstream of piers.

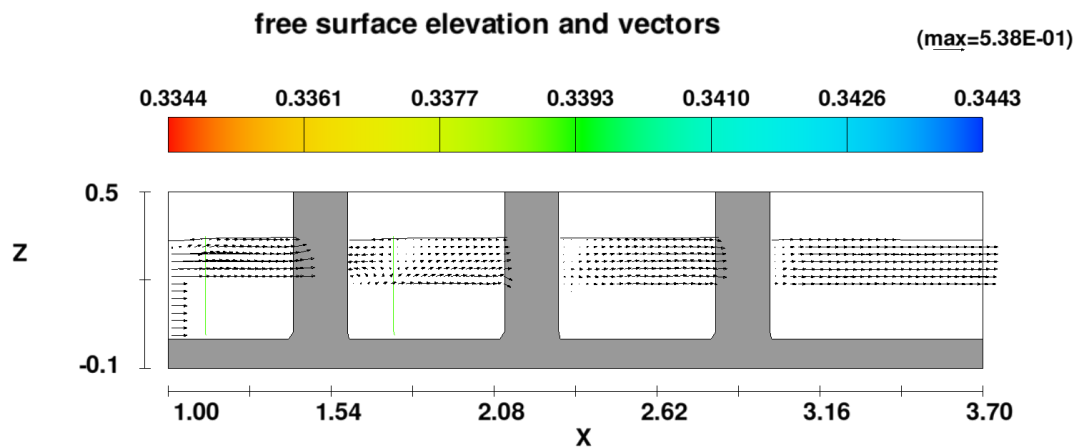


Figure 4.19 The velocity vectors in vertical plan for shape (4-10) at discharge $0.038 \text{ m}^3/\text{sec}$ and time 180 min

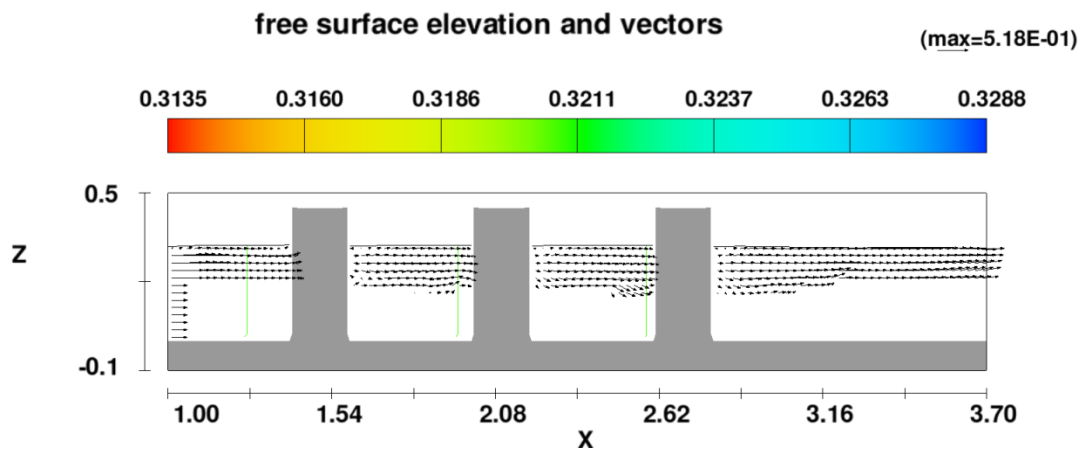


Figure 4.20 The velocity vectors in vertical plan for shape (10-10) at discharge $0.038 \text{ m}^3/\text{sec}$ and time 180 min

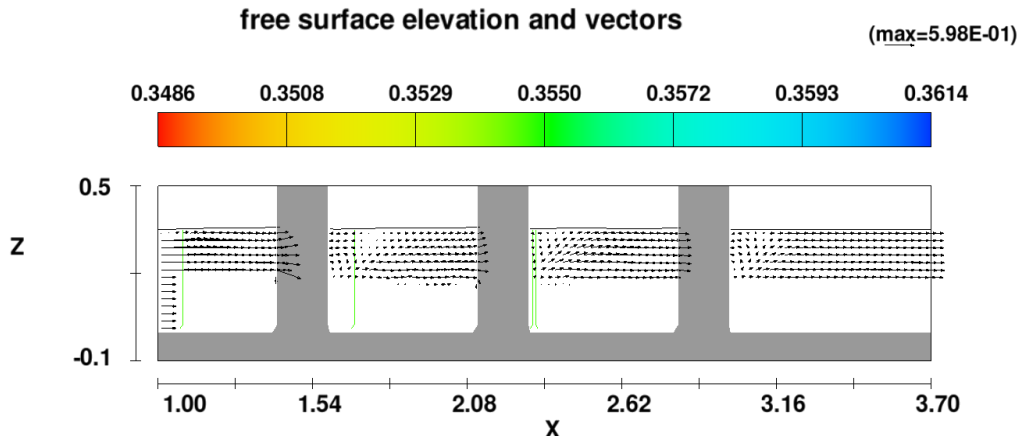


Figure 4.21 The velocity vectors in vertical plan for shape (4-10) at discharge $0.057 \text{ m}^3/\text{sec}$ and time 180 min

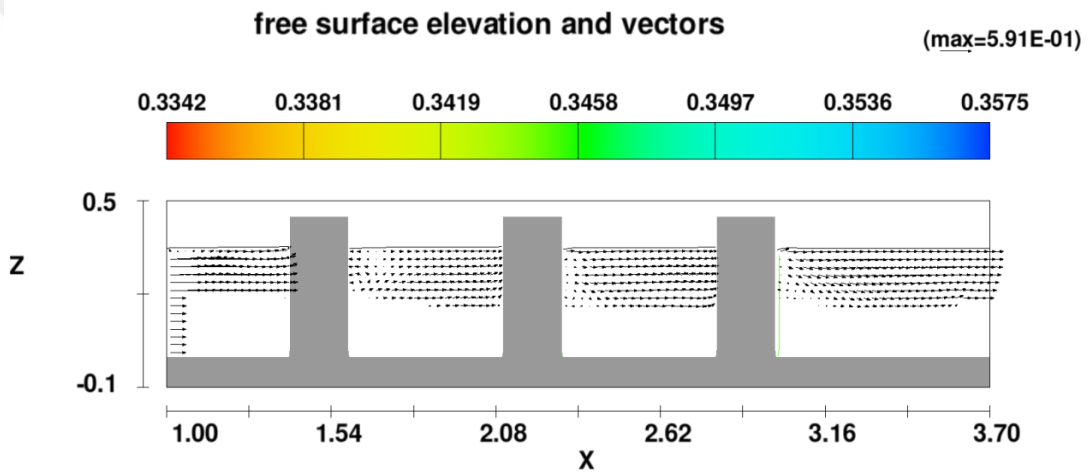


Figure 4.22 The velocity vectors in vertical plan for shape (10-10) at discharge $0.057 \text{ m}^3/\text{sec}$ and time 180 min

4.4 Rate of Scouring

The Figures below illustrated the velocity around each pier in same discharge after half of total running time which means after 180 min. of the test at commencement time, and the distribution of velocity in Figures 4.23 to 4.26 had illustrated, by color key bar, the red color donates to higher speed, as it is cleared in the figures, highest velocity magnitude distribution beside the piers and in front of the flume, the velocity about 0.50 m/s and 0.59 m/s for discharges (0.038 and 0.057) m^3/s respectively, while the blue color refers to the slow speed.

When the flow in upstream subjected to the front face of the piers, the velocity magnitude is increasing due to contraction of wide flow, which leads to create large

eddy and small eddy in the nose of the pier and the vicinity of the pier, this process is one of the most important causes of scour. The velocity gradually reduces after the pier. However, the velocity magnitude decrease in the downstream face of the pier, reduction of velocity magnitude is depending on geometry shape of the pier. Therefore, the rate of scouring, in this study will change from shape (4-10) shape to (10-10) shape according to this principle.

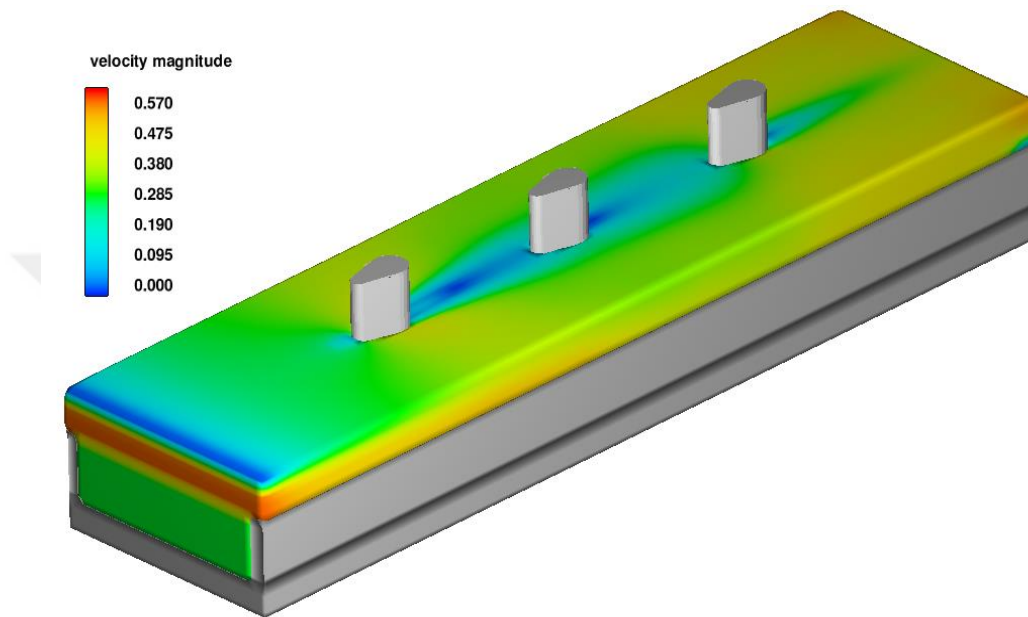


Figure 4.23 Flow around the shape (4-10) at $Q=0.038 \text{ m}^3/\text{s}$. and 180 min.

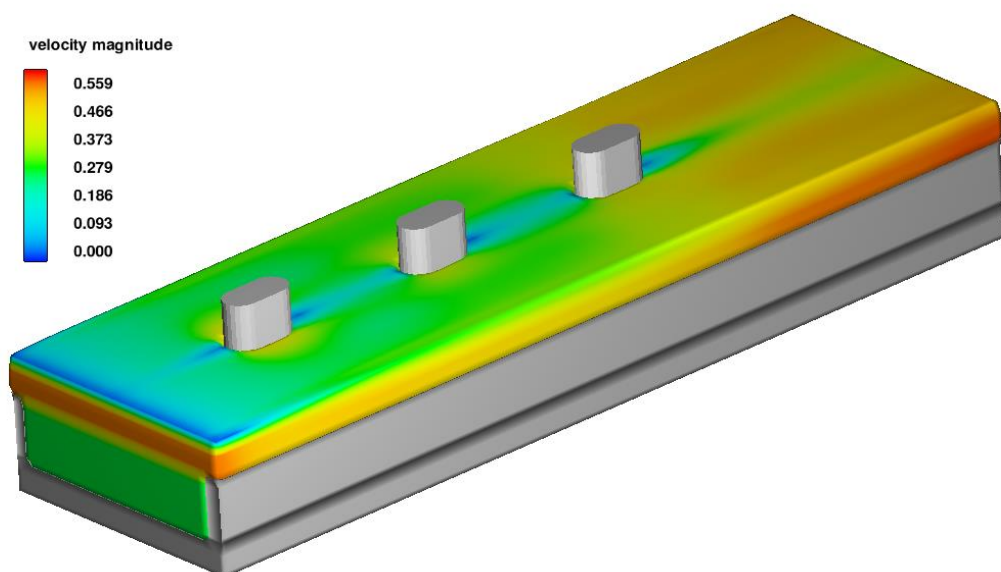


Figure 4.24 Flow around the shape (10-10) at $Q=0.038 \text{ m}^3/\text{s}$. and 180 min.

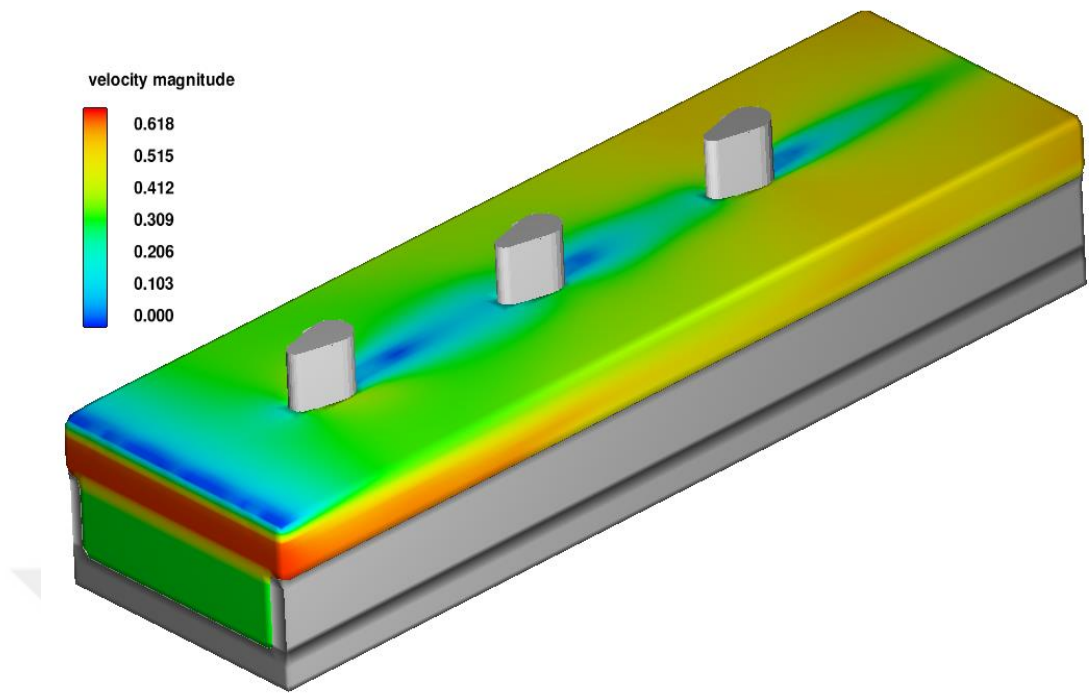


Figure 4.25 Flow around the shape (4-10) at $Q=0.057 \text{ m}^3/\text{s}$. and 180 min.

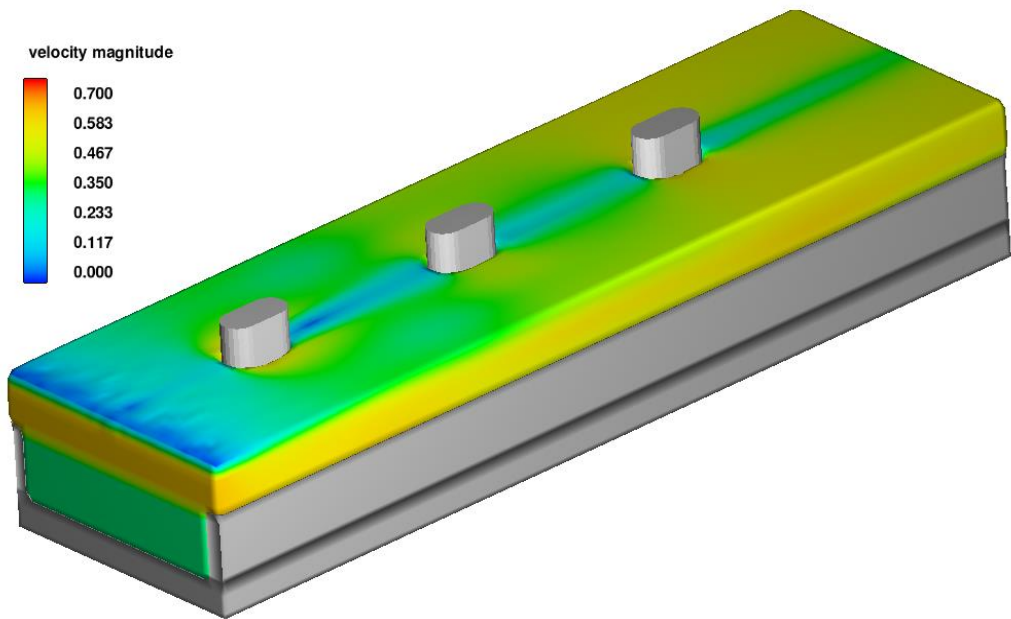


Figure 4.26 Flow around the shape (10-10) at $Q=0.057 \text{ m}^3/\text{s}$. and 180 min.

CHAPTER FIVE

CONCLUSIONS AND RECOMMENDATIONS

5.1 Conclusions

The present work was an attempt to investigate hydraulic characteristics and parameters due to the change of geometry of group of the bridge pier using CFD method compared with a physical model from an experimental study. The prediction of local scour around a group of the pier is complex because of the wide range of variable parameters which involve local scour, also the high three-dimensionality of flow. In this study, the effect of bridge pier diameter and shape for reduction of local scour and temporal development of scouring has been studied, the running was conducted using two different pier shapes to get the best geometry of piers which decrease the scour or prevent it. This research strongly based on the comparison of the numerical models (CFD) with obtained experimental results. Eventually, the results of models indicated that the range of scour is highly dependent on temporal development, also, the depth of local scour around a group pier increase with developing of time. This investigation has an important practical application in the real life and it gives the designer, clear vision to design the best shape of the pier which reduces the scour, thus rendering the risk of bridge pier failure and loss live insignificantly. Due to the current results, the aim of this study was successfully achieved.

The important points and conclusions from this study became evident as it showing in following:

- Flow-3D software is a respectable program for simulating, by comparing the Flow-3D results with observed consequence.

- The outcomes show that an agreement of the best model between the experimental and the numerical results are there for velocity distribution; with considering that the position of maximum depth scour does not occur exactly at the same location.
- The results at both studies shows that shape (4-10) is better at discharge (0.038 and 0.057) m³/sec. for reduction of scouring if comparing with bridge shape (10-10).
- The Flow-3D software is a perfect program and has low cost in simulation, but it needs high experience and perfecting in data inserting with the high performance of the computer.
- The position of maximum depth scour is changing according to the shape of the pier for both studies the only difference is that the location of the maximum scour does not take place at the same location when comparing the experimental result with the Flow-3D results
- Scour at the downstream of the piers are higher than upstream side of the piers according to the Flow-3D results, this is because of the weak horseshoe vortex that forms at the upstream and the strong ones that forms at the downstream which lead to the transportation of sediments to the sides of the bridge pier toward the downstream side and lead to the excessive scour at those locations.

5.2 Recommendation

Broadly, study the phenomenon of local scour was and still interesting subject for more of researcher and field monitoring in approaches of experimental and numerical. More of the previous study about changing of pier geometry to reduce the local scour around bridge pier was carried out in the laboratory and using physical hydraulic model, and under laboratory conditions (i.e. temperature, clear-water flow, cohesion-less material), therefore, the regarding possible future investigation are as following:

- The river is generally carrying debris especially in flood condition, and the result which was obtained in the current study will be different. It would be great to study the effect of shape and debris together and the effect of debris in separate with constant of each parameter in the current study.

- It would be useful to apply the investigation in real life and not stay like study in order to learn more about the effect of shape.
- In the most literature, the flow mechanism was described on local scour. Since no investigation has been done to define the behavior of flow with changing the shape in order to advance the knowledge about this sector.



REFERENCES

- Abbott, M. B., & Basco, D. R. (1989). Computational fluid dynamics-an introduction for engineers. NASA STI/Recon Technical Report A, 90.
- Acharya, A. (2011). Experimental study and numerical simulation of flow and sediment transport around a series of spur dikes. The University of Arizona.
- Ahmad, M. (1953, August). Experiments on design and behavior of spur dikes. In Proc. Int. *Hydraul. Convention* (Vol. 145).
- Ahmad, N., Bihs, H., Kamath, A., & Arntsen, Ø. A. (2015). Three-dimensional CFD modeling of wave scour around side-by-side and triangular arrangement of piles with REEF3D. *Procedia Engineering*, **116**, 683-690.
- Alabi, P. D. (2006). Time development of local scour at a bridge pier fitted with a collar (Doctoral dissertation).
- Al-Shukur, A. H. K., & Obeid, Z. H. (2016). Experimental Study of Bridge Pier Shape to Minimize Local Scour. *International Journal of Civil Engineering and Technology*, **7**(1), 162-171.
- Ataie-Ashtiani, B., & Beheshti, A. A. (2006). Experimental investigation of clear-water local scour at pile groups. *Journal of Hydraulic Engineering*, **132**(10), 1100-1104.
- Ballio, F., & Orsi, E. (2001). Time evolution of scour around bridge abutments. *Water Engineering Research*, **2**(4), 243-259.
- Beheshti, A. A., & Ataie-Ashtiani, B. (2008). Analysis of threshold and incipient conditions for sediment movement. *Coastal Engineering*, **55**(5), 423-430.

Bozkus, Z., & Yildiz, O. (2004). Effects of inclination of bridge piers on scouring depth. *Journal of Hydraulic Engineering*, **130**(8), 827-832.

Brethour, J. (2003). Modeling sediment scour. Flow Science, Santa Fe, NM. FloSci-TN62.

Breusers, H. N. C., Nicollet, G., & Shen, H. W. (1977). Local scour around cylindrical piers. *Journal of Hydraulic Research*, **15**(3), 211-252.

Cardoso, A. H., & Bettess, R. (1999). Effects of time and channel geometry on scour at bridge abutments. *Journal of Hydraulic Engineering*, **125**(4), 388-399.

Carstens, M. R. (1966). Similarity laws for localized scour. Proc. *ASCE Journal of the Hydraulic Division*, **92**(3), 13-36.

Cheremisinoff, P.N., Cheremisinoff, N.P. and Cheng, S.L. 1987. Hydraulic mechanics Civil Engineering Practice, Technomic Publishing Company, Inc., Lancaster, Pennsylvania, U.S.A. 780 p.

Chiew, Y. M., & Melville, B. W. (1987). Local scour around bridge piers. *Journal of Hydraulic Research*, **25**(1), 15-26.

Dey, S. (1997). Local scour at piers, Part I: A review of developments of research. *Int. J. Sediment Res., Beijing, China*, **12**(2), 23-46.

Dey, S., & Barbhuiya, A. K. (2004). Clear-water scour at abutments in thinly armored beds. *Journal of Hydraulic Engineering*, **130**(7), 622-634

EL-Ghorab, E. A. (2013). Reduction of scour around bridge piers using a modified method for vortex reduction. *Alexandria Engineering Journal*, **52**(3), 467-478.

Elsabaie, I. H. (2013). An Experimental Study of Local Scour around Circular Bridge Pier in Sand Soil. *International Journal of Civil & Environmental Engineering IJCEE-IJENS*, **13**(01).

Ettema, R., Arndt, R., Roberts, P., & Wahl, T. (2000). Hydraulic modeling: Concepts and practice.

Froehlich, D. C. (1989). Local scour at bridge abutments. In Proceedings of the 1989 National Conference on Hydraulic Engineering (pp. 13-18).

Froehlich, D.C. (1988). Analysis of onsite measurements of scour at piers, *American Society of Civil Engineers National Conference on Hydraulic Engineering*: Colorado Springs, CO, American Society of Civil Engineers, 534-539.

Garde, R., Subramanya, K. S., & Nambudripad, K. D. (1961). Study of scour around spur-dikes. *Journal of the Hydraulics Division*, **87**(6), 23-37.

Hager, W. H., & Oliveto, G. (2002). Shields' entrainment criterion in bridge hydraulics. *Journal of Hydraulic Engineering*, **128**(5), 538-542.

Heidarpour, M., Afzalimehr, H., & Izadinia, E. (2010). Reduction of local scour around bridge pier groups using collars. *International Journal of Sediment Research*, **25**(4), 411-422.

Hoffmans, G. J., & Verheij, H. J. (1997). *Scour manual* (Vol. 96). CRC press.

Huang, W., Yang, Q., & Xiao, H. (2009). CFD modeling of scale effects on turbulence flow and scour around bridge piers. *Computers & Fluids*, **38**(5), 1050-1058.

Ismael, A., Gunal, M., & Hussein, H. (2015). Effect of Bridge Pier Position on Scour Reduction According to Flow Direction. *Arabian Journal for Science and Engineering*, **40**(6), 1579-1590.

Johnson, P. A., & Niezgoda, S. L. (2004). Risk-based method for selecting bridge scour countermeasures. *Journal of hydraulic engineering*, **130**(2), 121-128.

Kandasamy, J. K. (1989). Abutment scour. UNIVERSITY OF AUCKLAND, SCHOOL OF ENGINEERING REPORT, (458).

Kohli, A., & Hager, W. H. (2001, June). Building scour in floodplains. In Proceedings of the Institution of Civil Engineers-Water and Maritime Engineering (Vol. 148, No. 2, pp. 61-80). Thomas Telford Ltd.

Lagasse, P. F., & Richardson, E. V. (2001). ASCE compendium of stream stability and bridge scour papers. *Journal of Hydraulic Engineering*, **127**(7), 531-533.

Lagasse, P. F., Clopper, P. E., Pagan-Ortiz, J. E., Zevenbergen, L. W., Arneson, L. A., Schall, J. D., & Girard, L. G. (2009). Bridge Scour and Stream Instability Countermeasures: Experience, Selection and Design Guidance. Volume **1** (No. FHWA-NHI-09-111).

Laursen, E. M. (1952, June). Observations on the nature of scour. In Proceedings of the Fifth Hydraulics Conference, State University of Iowa, Iowa City, Iowa (pp. 179-197).

Laursen, E. M., & Toch, A. (1956). Scour around bridge piers and abutments (Vol. 4). Ames, IA: Iowa Highway Research Board.

Liu, X., & Garcia, M. H. (2008). Three-dimensional numerical model with free water surface and mesh deformation for local sediment scour. *Journal of waterway, port, coastal, and ocean engineering*, **134**(4), 203-217.

Lu, A. L., & Chang, D. Y. (1988). A novel nucleotide excision repair for the conversion of an A/G mismatch to C/G base pair in *E. coli*. *Cell*, **54**(6), 805-812.

Mashahir, M. B., Zarrati, A. R., & Rezayi, M. J. (2004). Time development of scouring around a bridge pier protected by collar. In Proceedings 2nd International Conference on Scour and Erosion (ICSE-2). November 14.-17., 2004, Singapore.

May, R. W. P., & Escarameia, M. (2002). Local scour around structures in tidal flows. In First International Conference on Scour of Foundations.

Melville, B. W. (1995). Bridge abutment scour in compound channels. *Journal of Hydraulic Engineering*, **121**(12), 863-868.

Melville, B. W., & Chiew, Y. M. (1999). Time scale for local scour at bridge piers. *Journal of Hydraulic Engineering*, **125**(1), 59-65.

Melville, B. W., & Coleman, S. E. (2000). Bridge scour. Water Resources Publication.

Melville, B. W., & Sutherland, A. J. (1988). Design method for local scour at bridge piers. *Journal of Hydraulic Engineering*, **114**(10), 1210-1226.

Mostafa, E. A. (1994). Scour around skewed bridge piers. PhD diss., Alexandria University.

Olsen, N. R. B. (2003). Three-dimensional CFD modeling of self-forming meandering channel. *Journal of Hydraulic Engineering*, **129**(5), 366-372.

Olsen, N. R., & Kjellesvig, H. M. (1998). Three-dimensional numerical flow modeling for estimation of maximum local scour depth. *Journal of Hydraulic Research*, **36**(4), 579-590.

Olsen, N. R., & Melaaen, M. C. (1993). Three-dimensional calculation of scour around cylinders. *Journal of Hydraulic Engineering*, **119**(9), 1048-1054.

Paintal, A. S., & Garde, R. J. (1965). Effect of inclination and shape of obstruction on local scour. *Res. Journal*, 8.

Pitt, R., Clark, S. E., & Lake, D. W. (2007). Construction Site Erosion and Sediment Controls: Planning, Design and Performance. DEStech Publications, Inc.

Posey, C. J. (1974). Tests of scour protection for bridge piers. *Journal of the Hydraulics Division*, 100(Proc. Paper 11017).

Ramu, K. L. V. (1964). Effect of sediment size on scour.

Raudkivi, A. J., & Ettema, R. (1983). Clear-water scour at cylindrical piers. *Journal of Hydraulic Engineering*, **109**(3), 338-350.

Raudkivi, A.J. (1986). Functional trends of scour at bridge piers, *Journal of Hydr. Engrg. ASCE*, **112**(1), 1-13.

Richardson, E. V., Harrison, L. J., Richardson, J. R., & Davis, S. R. (1993). Evaluating scour at bridges (No. HEC 18 (2nd edition)).

Richardson, J. E., & Panchang, V. G. (1998). Three-dimensional simulation of scour-inducing flow at bridge piers. *Journal of Hydraulic Engineering*, **124**(5), 530-540.

Roulund, A., Sumer, B. M., Fredsøe, J., & Michelsen, J. (2005). Numerical and experimental investigation of flow and scour around a circular pile. *Journal of Fluid Mechanics*, **534**, 351-401.

Salaheldin, T. M., Imran, J., & Chaudhry, M. H. (2004). Numerical modeling of three-dimensional flow field around circular piers. *Journal of Hydraulic Engineering*, **130**(2), 91-100.

Schneible, D. E. (1951). An investigation of the effect of bridge-pier shape on the relative depth of scour (Doctoral dissertation, University of Iowa).

Shen, H.W. and Schneider, V.R. 1969. Local scour around bridge piers. *Journal of the Hydraulics Division, Proceedings of the American Society of Civil Engineers*, **95**(6):1919-1941.

Singh, S. M., & Maiti, P. R. (2012). Local Scouring around a Circular Pier in Open Channel.

Sumer, B. M., & Fredsoe, J. (2001). Scour around pile in combined waves and current. *Journal of Hydraulic Engineering*, **127**(5), 403-411.

Tison, L. J. (1961). Local scour in rivers. *Journal of Geophysical Research*, **66**(12), 4227-4232.

Tulimilli, B. R., Majumdar, P., Kostic, M., & LOTTES, S. (1792). Development of CFD Simulation for 3-D Flooding Flow and Scouring Around a Bridge Structure. ISSN, 4286, 129-135.

Wardhana, K., & Hadipriono, F. C. (2003). Analysis of recent bridge failures in the United States. *Journal of performance of constructed facilities*, **17**(3), 144-150.

Whitehouse, R. (1998). Scour at marine structures: A manual for practical applications. Thomas Telford.

Wong, W. H. (1982). Scour at bridge abutments (No. Monograph).

Wu, S., & Rajaratnam, N. (1996). Submerged flow regimes of rectangular sharp-crested weirs. *Journal of Hydraulic Engineering*, **122**(7), 412-414.

Yanmaz, A. M. (2002). Dynamic reliability in bridge pier scouring. *Turkish Journal of Engineering and Environmental Sciences*, **26**(4), 367-376.

Yanmaz, A. M., & Altinbilek, H. D. G. √. A. (1991). Study of time-dependent local scour around bridge piers. *Journal of Hydraulic Engineering*, **117**(10), 1247-1268.

Zaghloul, N. A. (1983). Local scour around spur-dikes. *Journal of Hydrology*, **60**(1-4), 123-140.



APPENDICES

APPENDIX A

Scour Hole

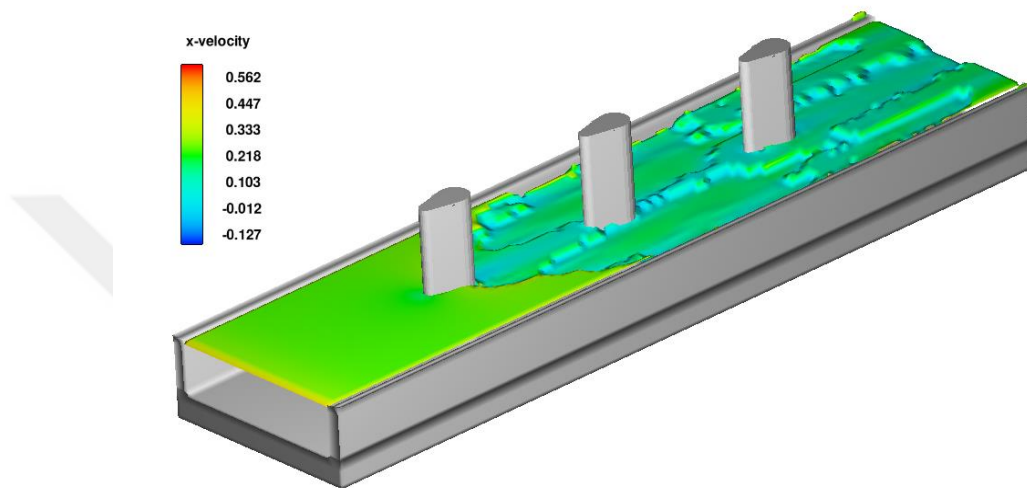


Figure A.1 Scour holes at time=180 min. corresponding to $Q=0.038 \text{ m}^3/\text{sec}$ and shape pier (4-10)

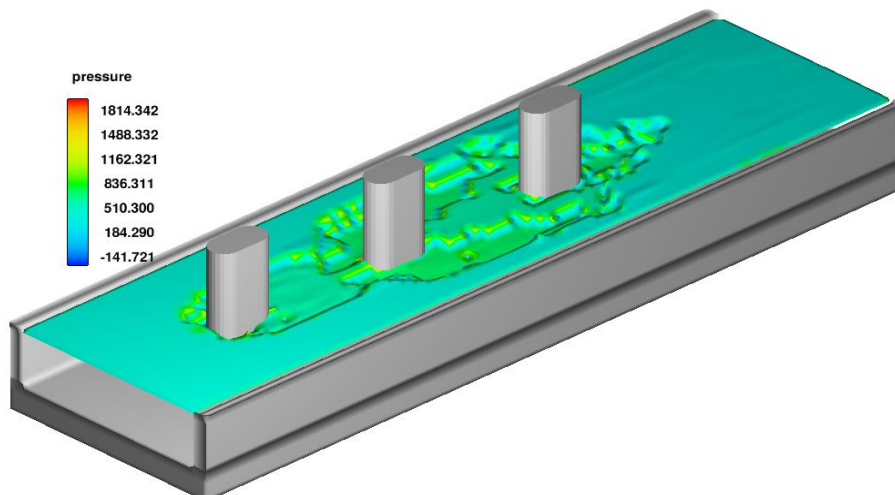


Figure A.2 Scour holes at time=180 min. corresponding to $Q=0.038 \text{ m}^3/\text{sec}$ and shape pier (10-10)

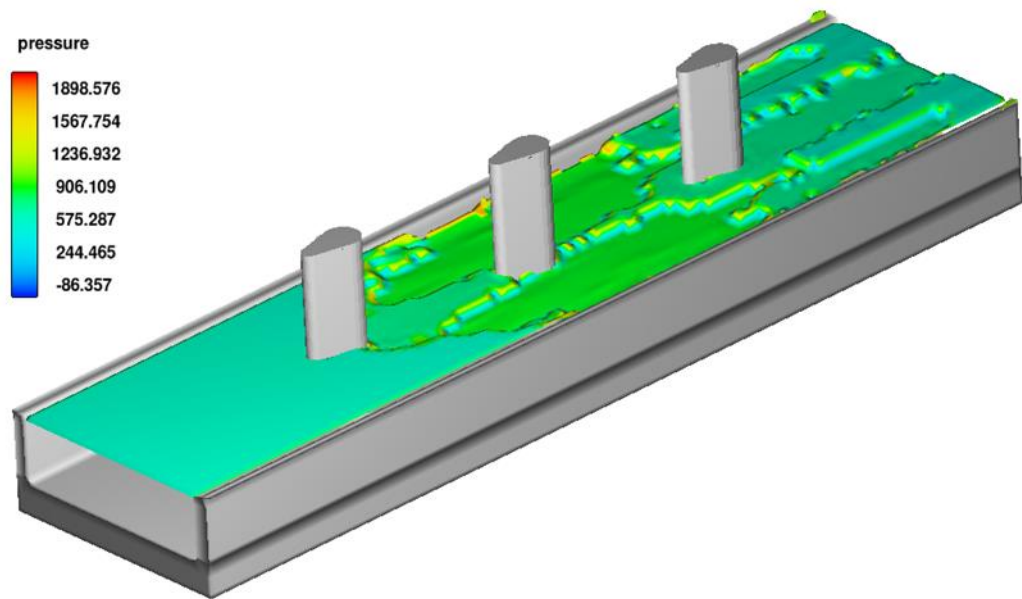


Figure A.3 Scour holes at time=180 min. corresponding to $Q=0.057 \text{ m}^3/\text{sec}$ and shape pier (4-10)

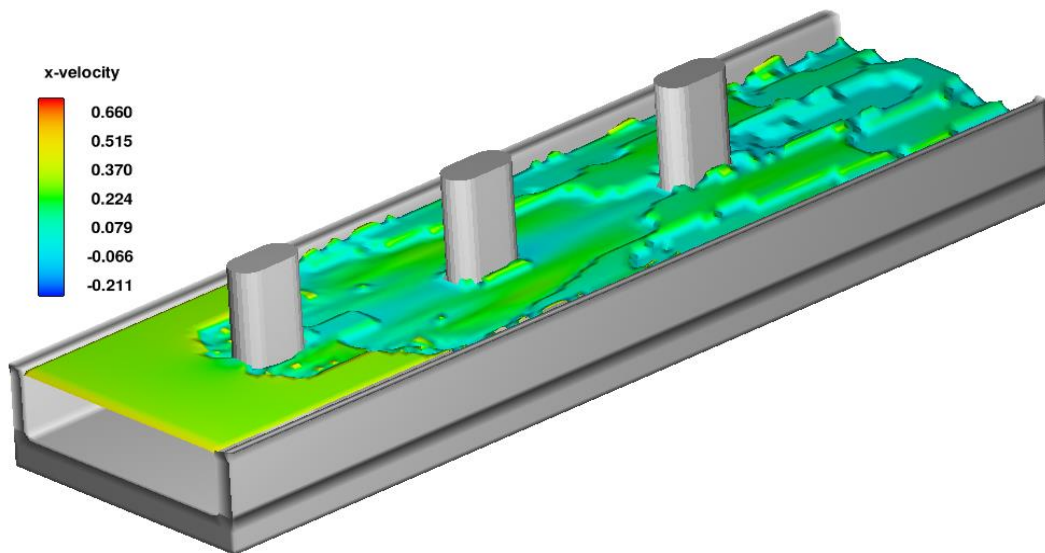
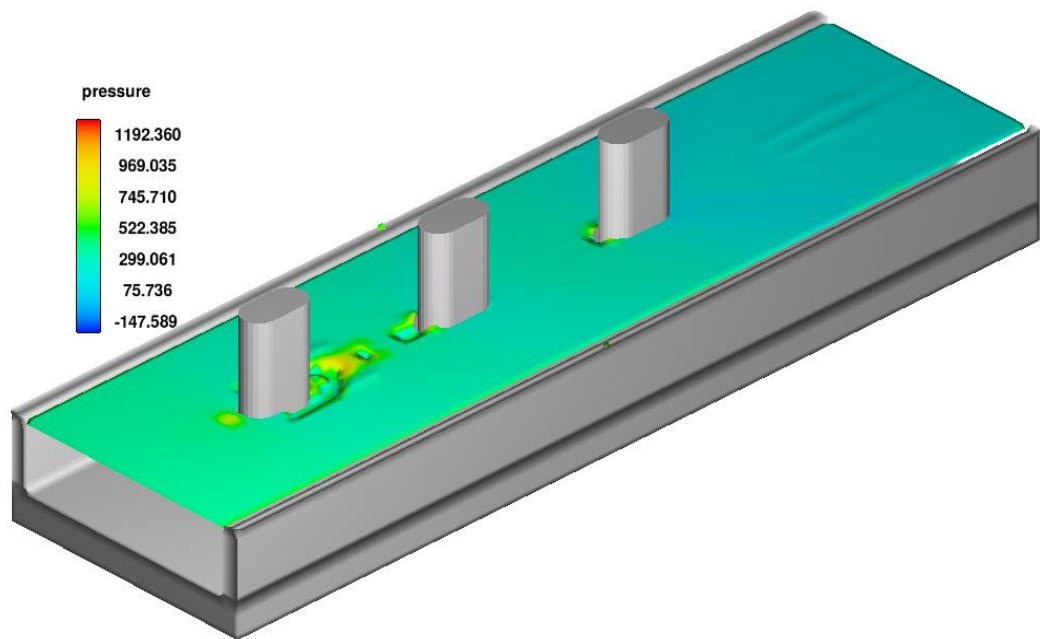
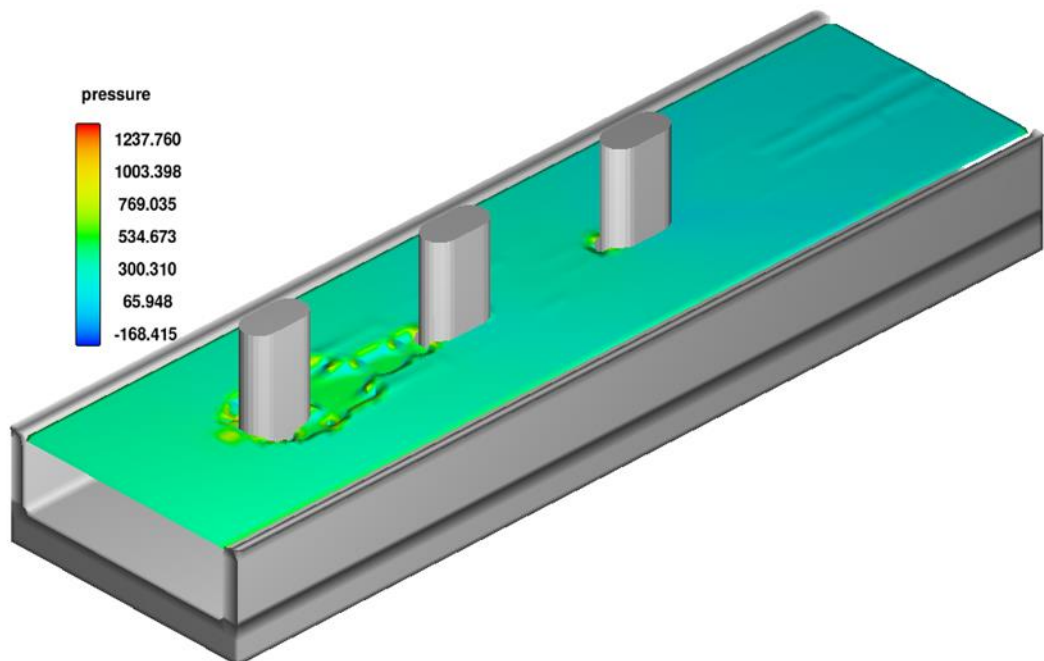


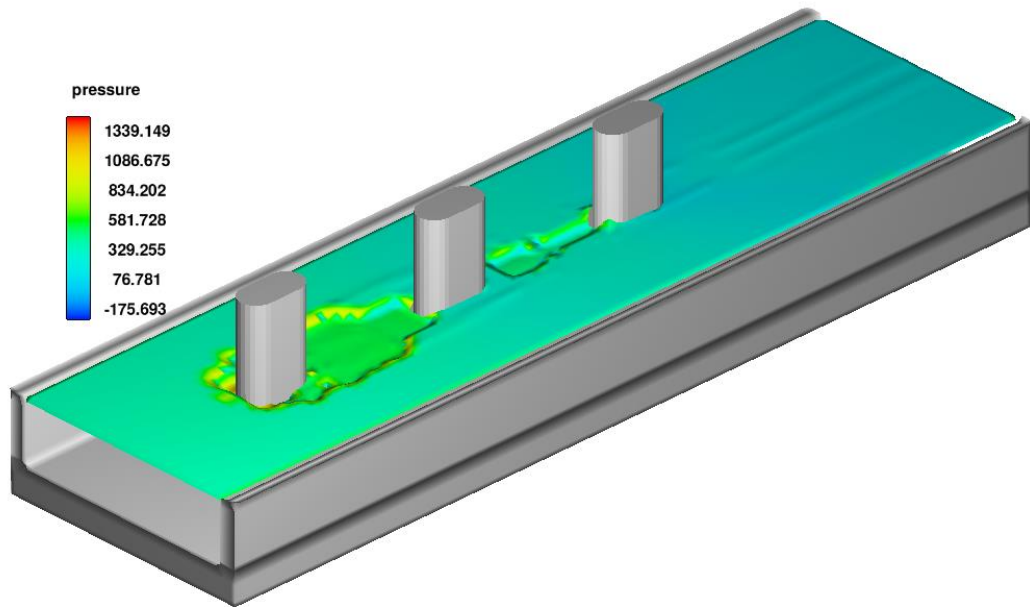
Figure A.4 Scour holes at time=180 min. corresponding to $Q=0.057 \text{ m}^3/\text{sec}$ and shape pier (10-10)



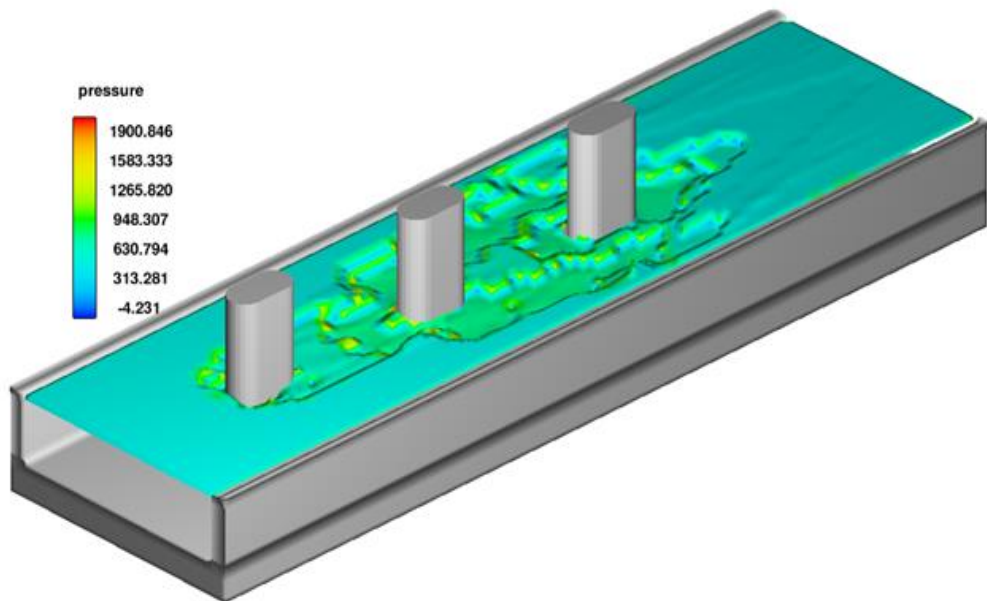
T= 5 min.



T= 15 min.

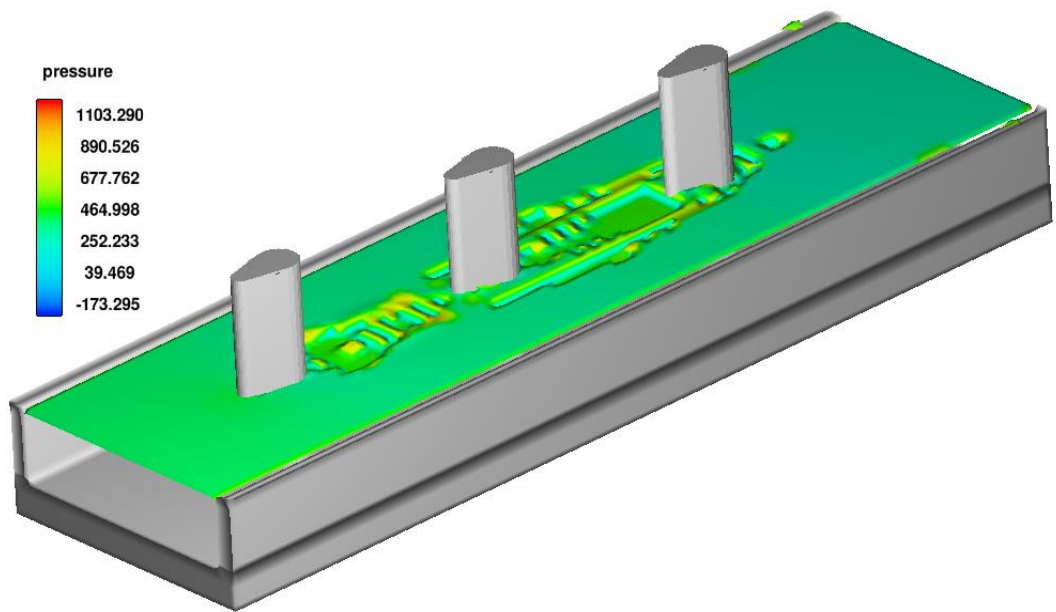


T= 60 min.

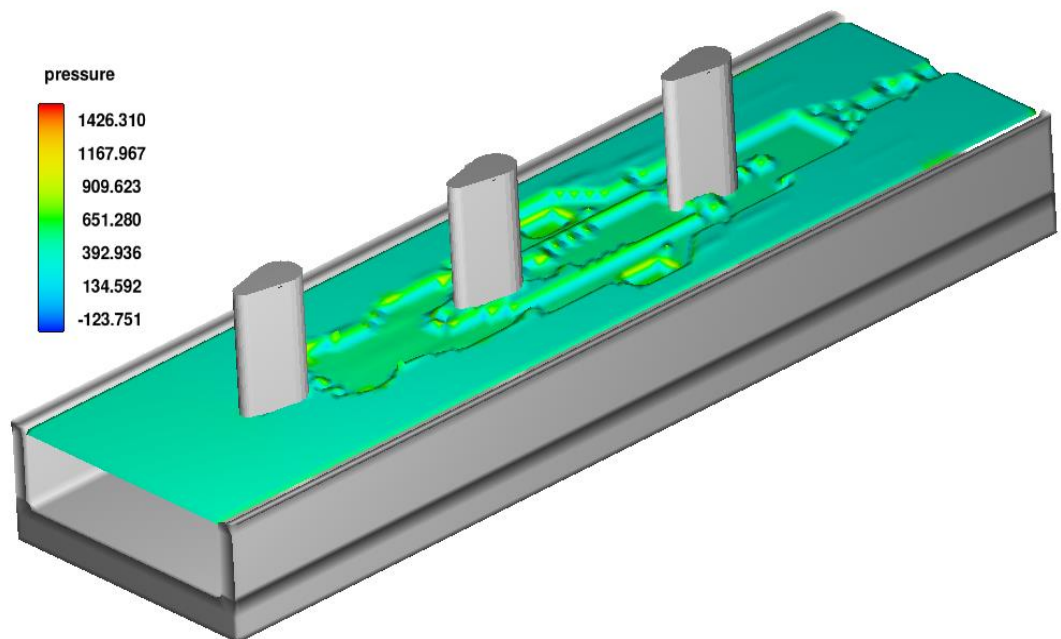


T= 360 min.

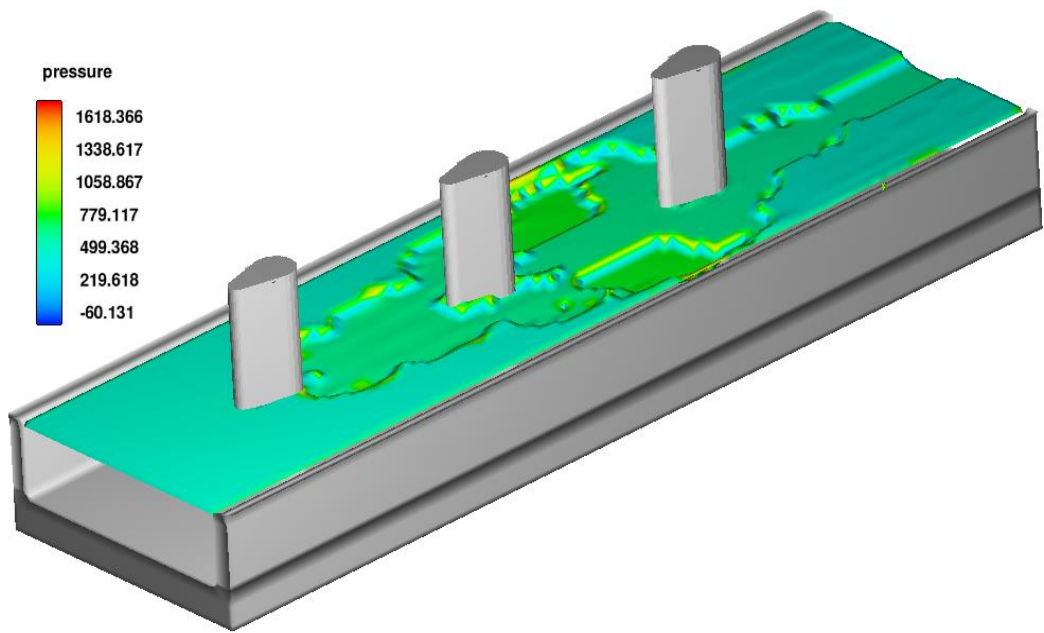
Figure A.5 Scour holes development with time for $Q= 0.038 \text{ m}^3/\text{sec}$ and shape pier (10-10)



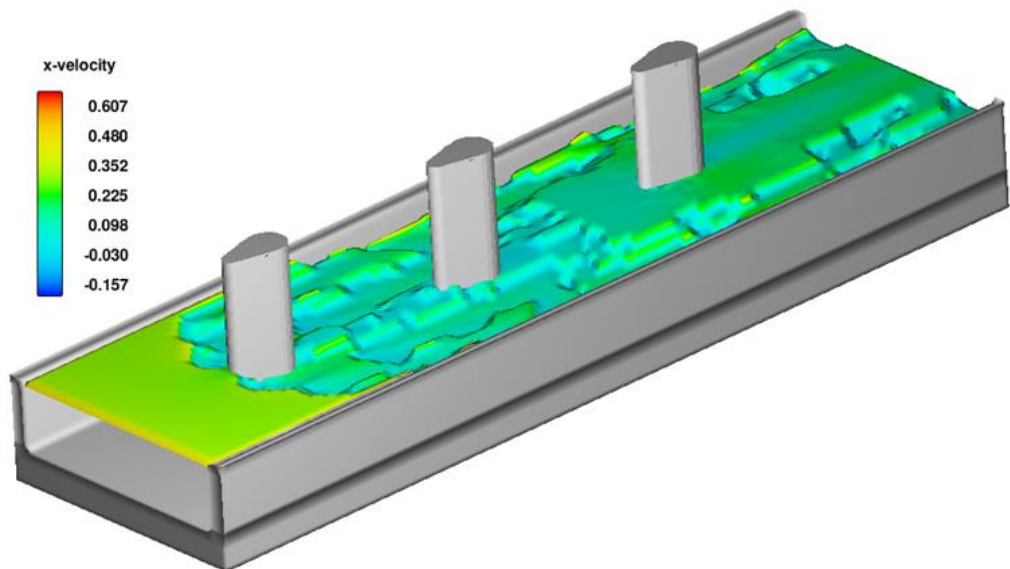
T=5 min.



T= 15 min.



T= 60 min.



T= 360 min.

Figure A.6 Scour holes development with time for $Q= 0.057 \text{ m}^3/\text{sec}$ and shape pier (4-10)

APPINDIX B

Water Surface and Vectors

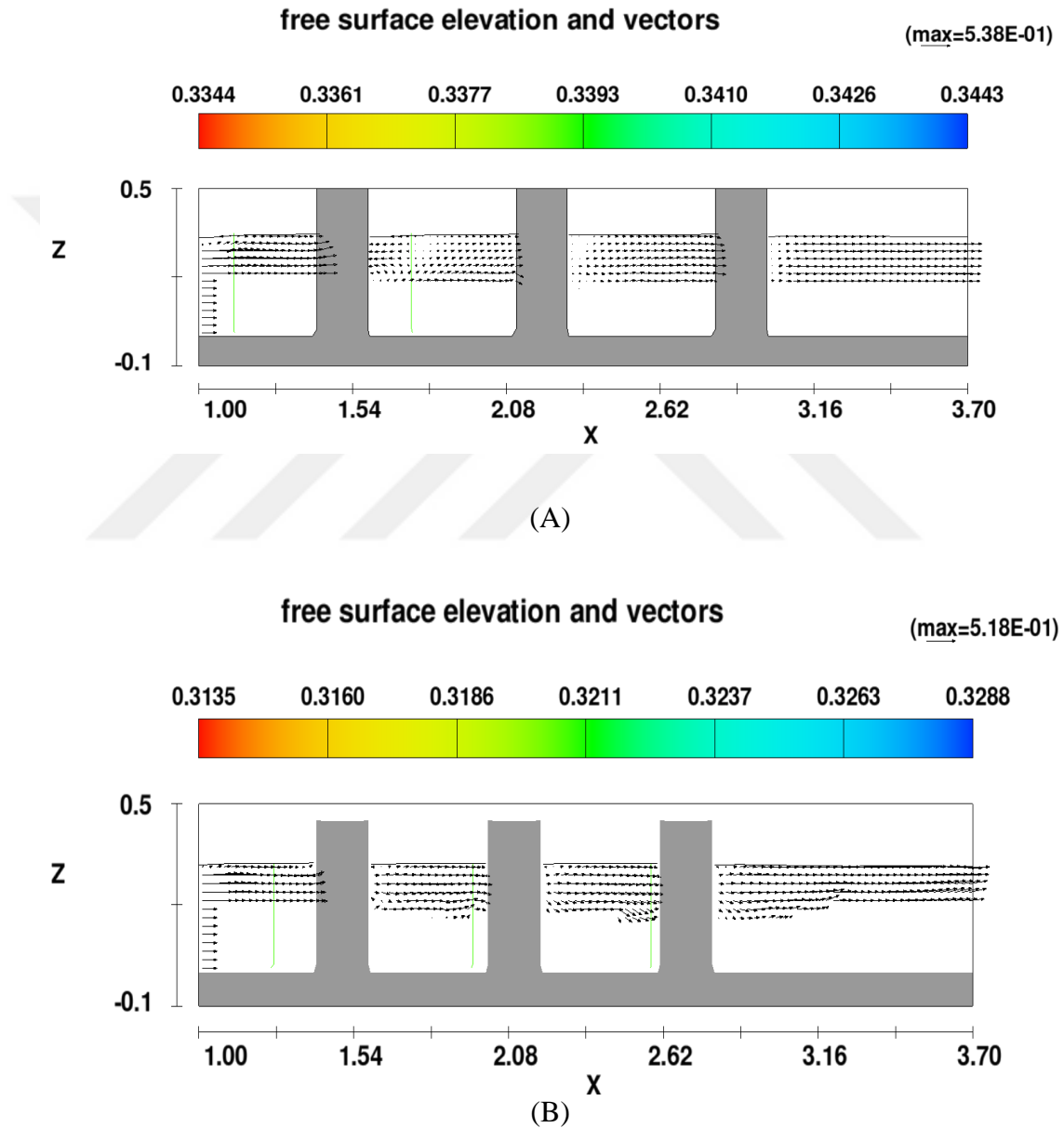


Figure B.1 water surface and vectors at $Q=0.038 \text{ m}^3/\text{sec}$ and time =180 min :

(A) Pier shape (4-10)

(B) Pier shape (10-10)

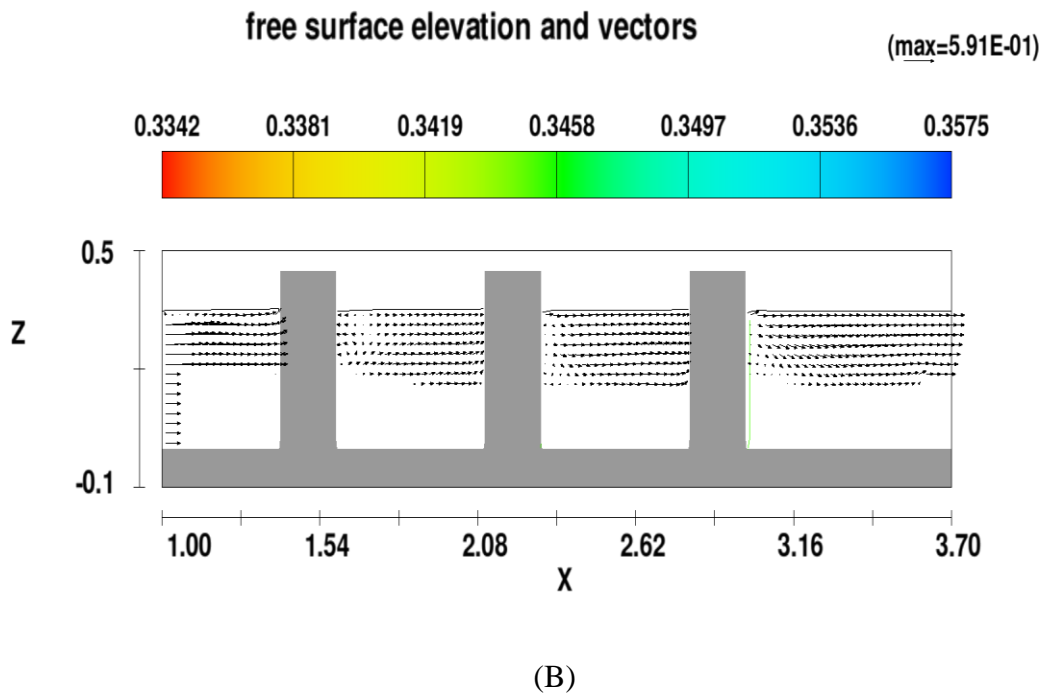
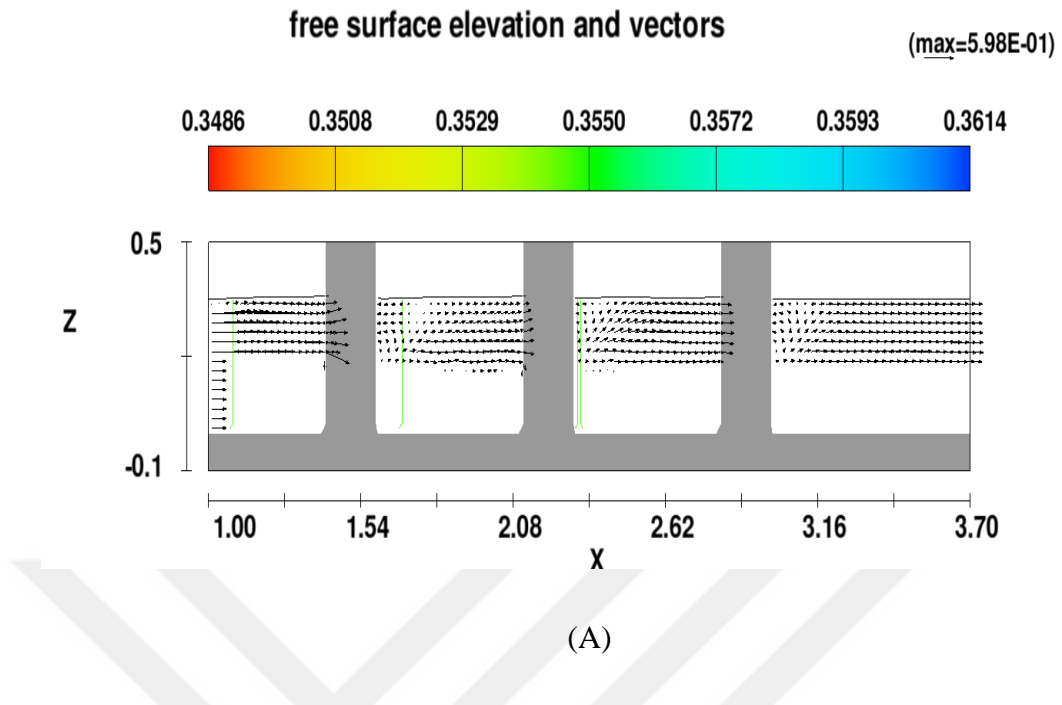


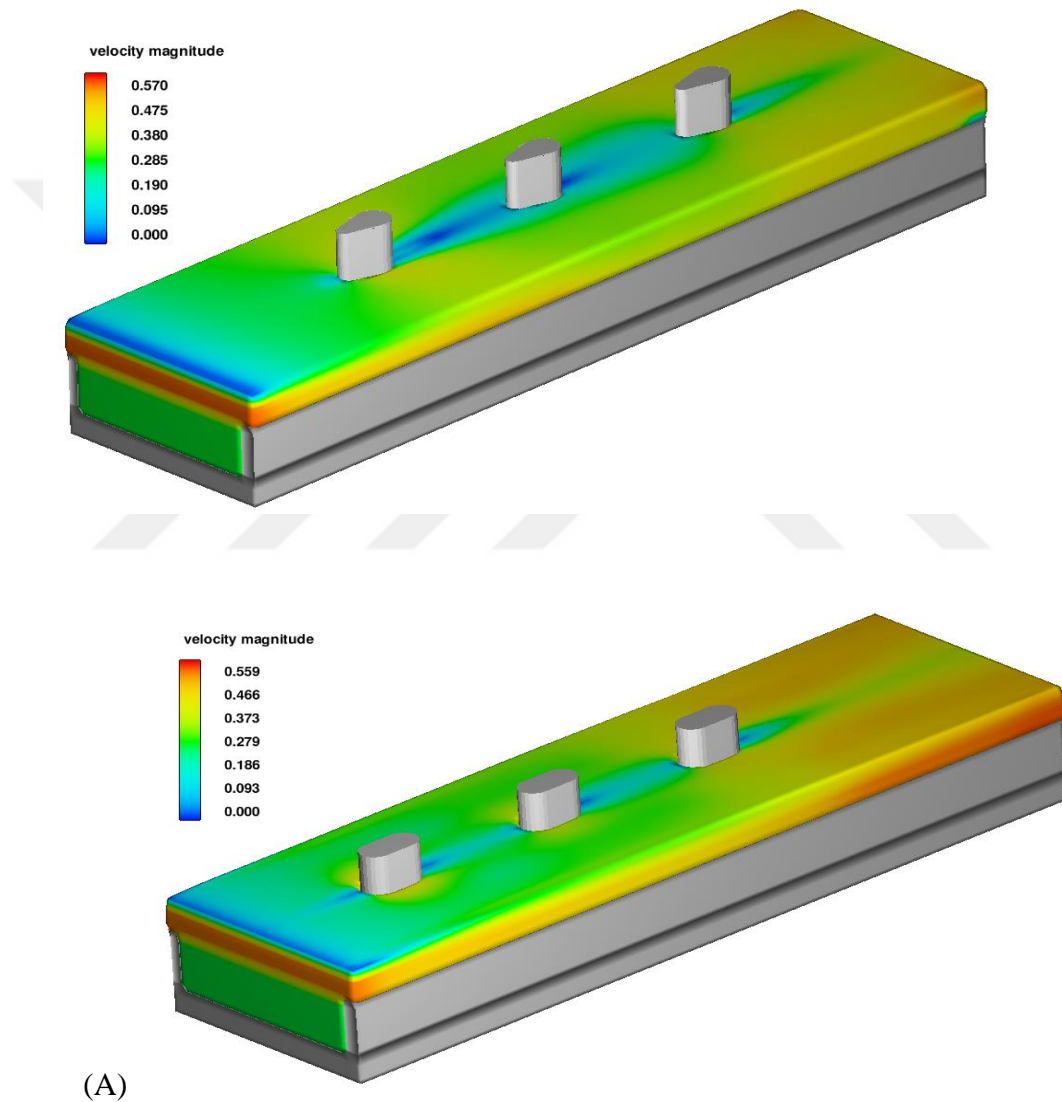
Figure B.1 water surface and vectors at $Q=0.057 \text{ m}^3/\text{sec}$ and time =180 min :

(A) Pier shape (4-10)

(B) Pier shape (10-10)

APPENDIX C

Velocity magnitude at different shapes



(A)

(B)

Figure C.1 Flow and velocity magnitude at $Q=0.038 \text{ m}^3/\text{sec}$ and time =180 min :

(A) Pier shape (4-10)

(B) Pier shape (10-10)

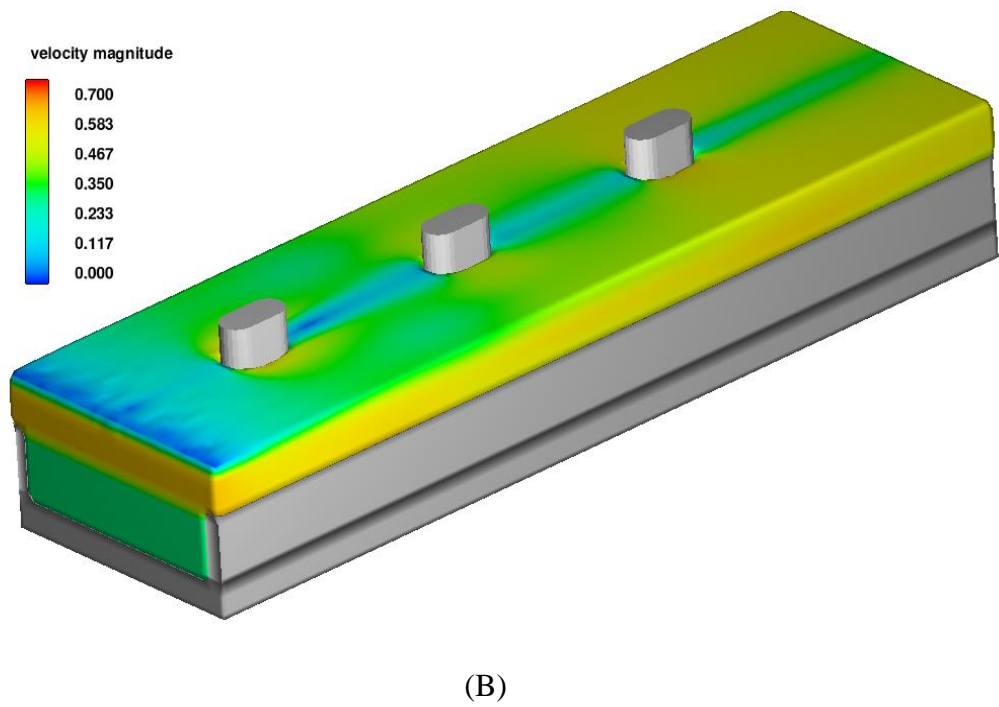
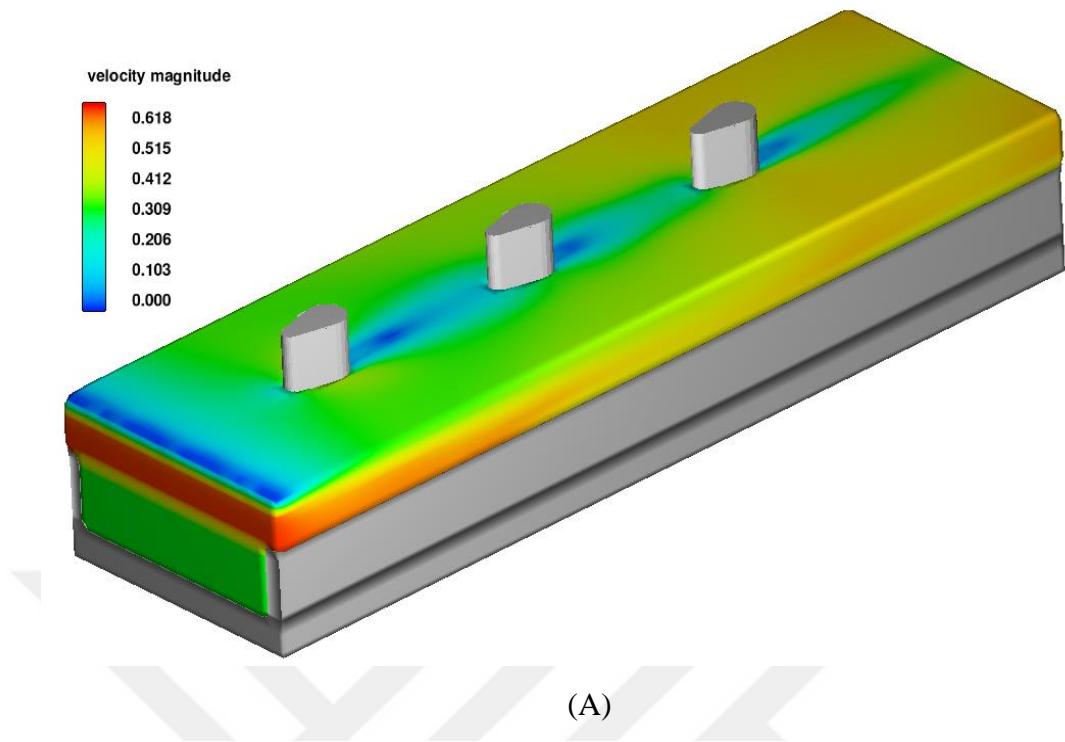


Figure C.2 Flow and velocity magnitude at $Q=0.057 \text{ m}^3/\text{sec}$ and time =180 min :

(A) Pier shape (4-10)

(B) Pier shape (10-10)

APPINDIX D

2D Pressure contours at different shape.

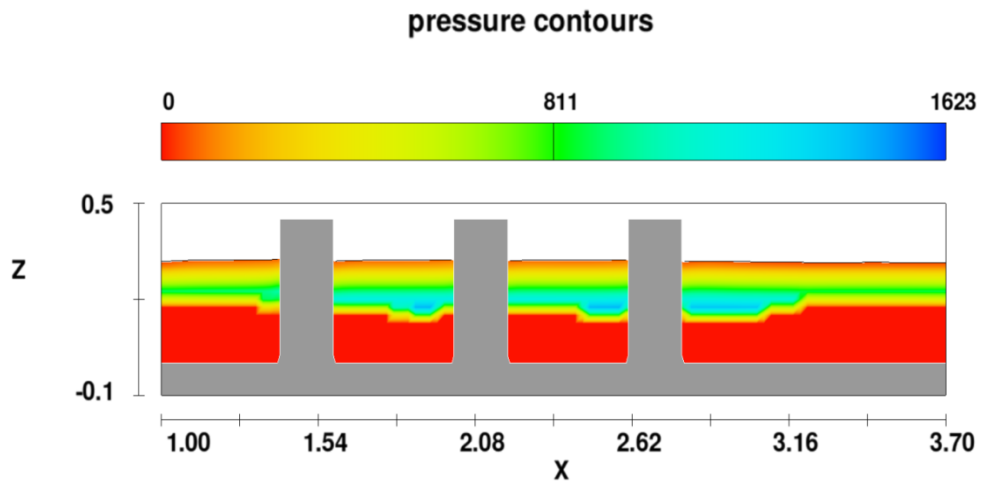
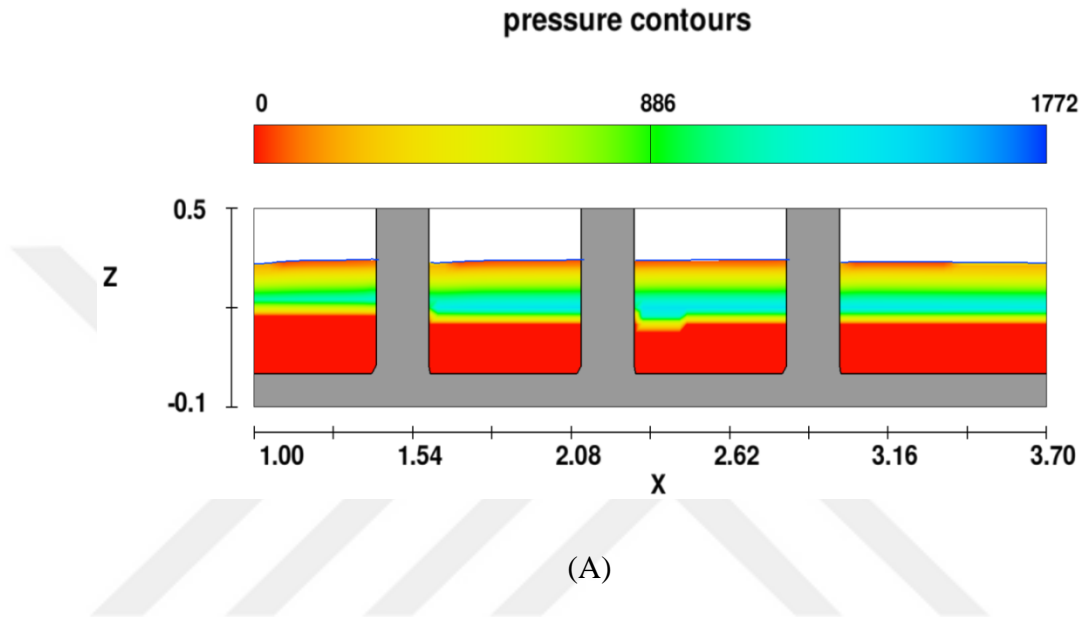


Figure D.1 2D Pressure contours at $Q=0.038 \text{ m}^3/\text{sec}$ and time =360 min:

(A) Pier shape (4-10)

(B) Pier shape (10-10)

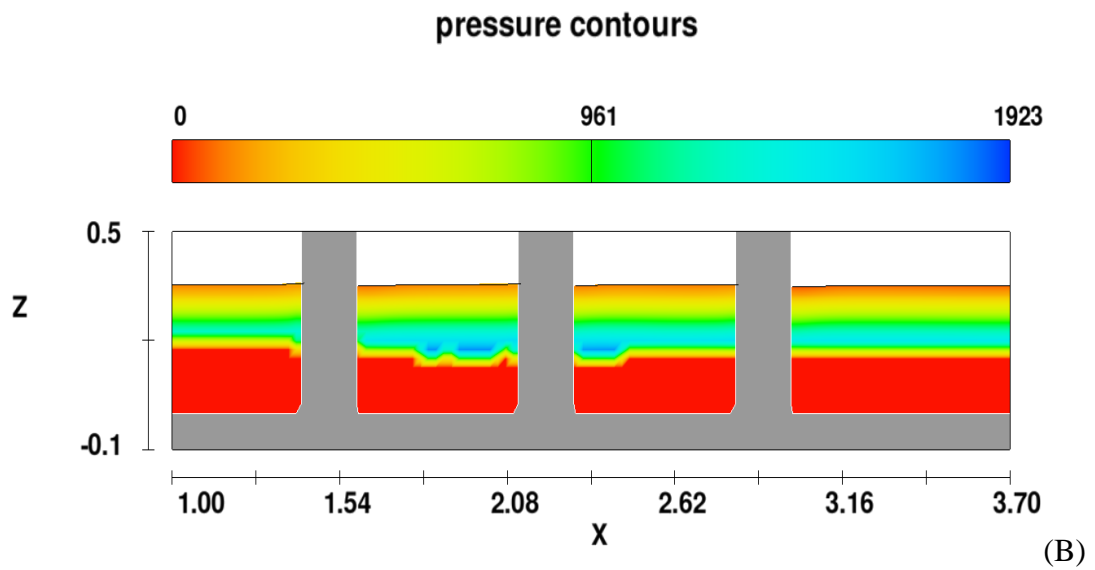
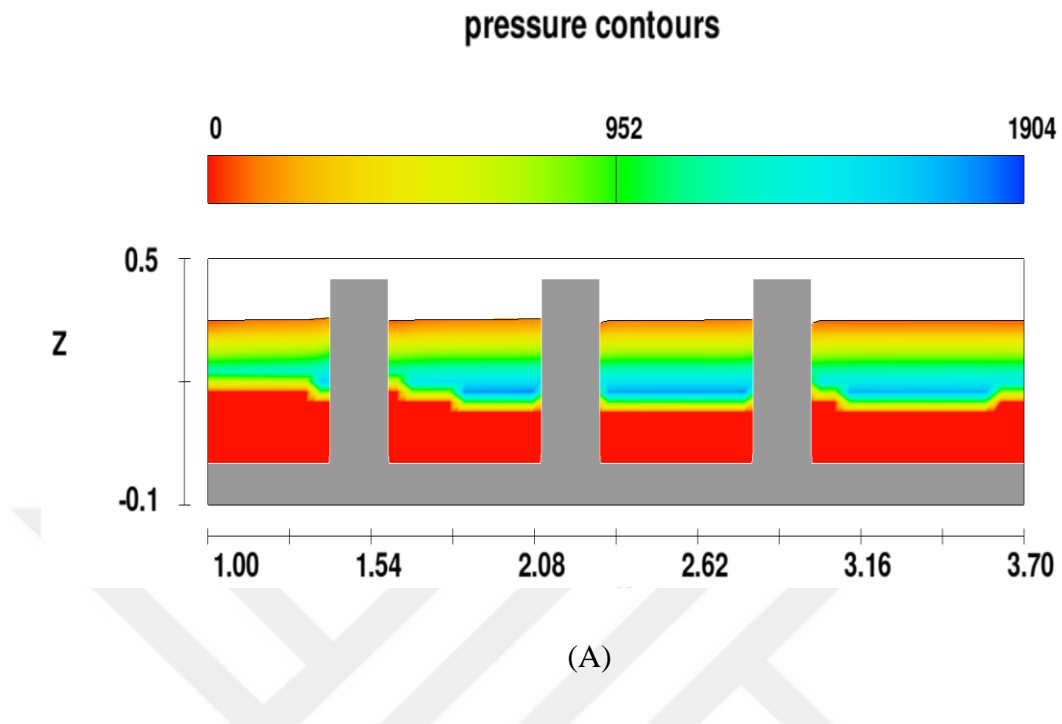


Figure C.1 2D Pressure contours at $Q=0.057 \text{ m}^3/\text{sec}$ and time =360 min:

(A) Pier shape (4-10)

(B) Pier shape (10-10)

RESULTS APPENDIX E

The data for the Scour hole contour

Table E- 1 The data are plotted and analyzed in chapter 4

Depth Scour - Time						
shape (10 - 10) cm						
Q= 0.038 m ³ /s. S= 50 cm						
Time (min)	Pier 1 Experimental (cm)	pier 1 FLOW 3D (cm)	Pier 2 Experimental (cm)	pier2 FLOW 3D (cm)	Pier 3 Experimental (cm)	pier3 FLOW 3D (cm)
0	0.0	0.0	0.0	0.0	0.0	0.0
5	8.0	0.0	8.0	3.1	6.0	2.0
10	9.0	0.0	9.0	3.1	6.0	2.5
15	9.5	5.2	9.1	4.3	6.1	3.0
20	10.0	5.2	9.3	4.3	6.5	3.0
25	10.0	5.2	9.4	4.3	7.0	3.0
30	10.5	5.2	9.4	4.5	7.2	3.2
35	10.5	5.2	9.5	4.5	7.4	3.5
40	11.0	5.2	9.5	4.5	7.8	3.8
45	11.0	5.2	9.8	4.6	8.0	3.9
50	11.2	5.2	10.0	4.6	8.0	4.0
55	11.4	5.2	10.2	4.6	8.2	4.5
60	11.4	5.2	10.5	4.6	8.4	4.5
70	11.4	5.2	10.5	4.6	8.4	4.5
80	11.4	5.2	10.5	4.7	8.4	4.5
90	11.5	5.3	10.5	5.0	8.4	5.2
100	11.5	5.8	10.5	5.0	8.4	5.2
110	11.5	5.8	10.5	5.5	8.4	5.2
120	11.5	5.8	10.5	6.0	8.4	5.8
135	11.5	5.8	10.5	7.5	8.4	5.8
150	11.5	5.8	10.5	7.5	8.4	5.8
165	11.5	5.8	10.5	7.5	8.4	5.8
180	11.5	5.8	10.5	7.5	8.4	5.8
210	11.5	5.8	10.5	7.5	8.4	5.8
240	11.5	5.8	10.5	7.5	8.4	5.8
270	11.5	5.8	10.5	7.5	8.4	5.8
300	11.5	5.8	10.5	7.5	8.4	5.8
360	11.5	5.8	10.5	7.5	8.4	5.8

Table E- 2 The data are plotted and analyzed in chapter 4

Depth Scour - Time						
Shape (4- 10) cm						
Q= 0.038 m ³ /s. S= 50 cm						
Time (min)	Pier 1 Experimental (cm)	pier 1 FLOW 3D (cm)	Pier 2 Experimental (cm)	pier2 FLOW 3D (cm)	Pier 3 Experimental (cm)	pier3 FLOW 3D (cm)
0	0.0	0.0	0.0	0.0	0.0	0.0
5	5.0	1.5	3.2	3.1	3.3	3.2
10	6.0	1.8	3.3	3.2	3.4	3.2
15	6.1	1.8	3.3	3.2	3.5	3.2
20	6.2	1.8	3.3	3.2	3.5	3.2
25	6.4	2.0	3.4	3.3	3.6	3.2
30	6.4	2.0	3.4	3.3	3.6	3.2
35	6.8	2.0	3.4	3.3	3.7	3.2
40	6.8	2.1	3.4	3.4	3.7	3.3
45	6.8	2.1	3.4	3.4	3.8	3.3
50	7.0	2.1	3.5	3.4	3.8	3.3
55	7.2	2.1	3.6	3.4	3.8	3.3
60	7.4	2.1	3.6	3.4	3.8	3.3
70	7.4	2.1	4.0	3.4	3.8	3.3
80	7.5	2.1	4.0	3.5	3.8	4.0
90	7.5	2.1	4.0	3.5	4.5	4.3
100	7.7	2.1	4.0	3.5	4.5	4.5
110	7.7	2.1	4.0	3.5	5.0	5.0
120	7.7	2.1	4.0	3.5	5.0	5.0
135	7.7	2.1	4.0	3.5	5.0	5.0
150	7.7	2.1	4.0	3.5	5.0	5.0
165	7.7	2.1	4.0	3.5	5.0	5.0
180	7.7	2.1	4.0	3.5	5.0	5.0
210	7.7	2.1	4.0	3.5	5.0	5.0
240	7.7	2.1	4.0	3.5	5.0	5.0
270	7.7	2.1	4.0	3.5	5.0	5.0
300	7.7	2.1	4.0	3.5	5.0	5.0
360	7.7	2.1	4.0	3.5	5.0	5.0

Table E- 3 The data are plotted and analyzed in chapter 4

Depth Scour - Time						
Shape (4- 10) cm						
Q= 0.038 m ³ /s. S= 50 cm						
Time (min)	Pier 1 Experimental (cm)	pier 1 FLOW 3D (cm)	Pier 2 Experimental (cm)	pier2 FLOW 3D (cm)	Pier 3 Experimental (cm)	pier3 FLOW 3D (cm)
0	0.0	0.0	0.0	0.0	0.0	0.0
5	5.5	0.5	3.2	3.0	3.0	3.1
10	5.5	0.6	5.4	3.0	3.0	3.1
15	5.5	0.7	6.1	3.1	3.0	3.1
20	5.6	0.8	6.7	5.0	3.2	5.0
25	5.8	1.0	7.2	5.0	3.2	5.0
30	6.2	1.0	7.4	5.2	3.4	5.0
35	6.8	1.0	7.7	5.2	3.6	5.0
40	7.0	1.5	7.8	5.3	3.6	5.0
45	8.5	1.6	7.8	5.3	3.8	5.0
50	8.5	1.6	7.8	5.3	4.0	5.1
55	9.0	1.8	8.0	5.3	4.3	5.1
60	9.2	2.0	8.0	5.3	4.3	5.1
70	9.2	2.0	8.0	5.3	4.3	5.2
80	9.2	2.2	8.0	5.3	4.3	5.2
90	9.2	2.2	8.0	5.3	4.3	5.2
100	9.2	2.2	8.0	5.3	4.3	5.3
110	9.2	2.2	8.0	5.3	4.3	5.3
120	9.2	2.2	8.0	5.3	4.3	5.5
135	9.2	2.2	8.0	5.3	4.3	5.5
150	9.2	2.2	8.0	5.3	4.3	5.5
165	9.2	2.2	8.0	5.3	4.3	5.5
180	9.2	2.2	8.0	5.3	4.3	5.5
210	9.2	2.2	8.0	5.3	4.3	5.6
240	9.2	2.2	8.0	5.3	4.3	5.6
270	9.2	2.2	8.0	5.3	4.3	5.6
300	9.2	2.2	8.0	5.3	4.3	5.6
360	9.2	2.2	8.0	5.3	4.3	5.6

Table E- 4 The data are plotted and analyzed in chapter 4

Depth Scour - Time						
SHAPE (10 - 10) cm						
Q=0.057 m³/s. S=50						
Time (min)	Pier 1 Experimental (cm)	pier 1 FLOW 3D (cm)	Pier 2 Experimental (cm)	pier2 FLOW 3D (cm)	Pier 3 Experimental (cm)	pier3 FLOW 3D (cm)
0	0.0	0.0	0.0	0.0	0.0	0.0
5	8.8	3.1	7.0	3.4	6.8	3.5
10	8.9	3.2	9.5	3.4	8.9	3.6
15	10.0	3.2	9.5	3.4	10.2	5.0
20	10.0	3.2	9.5	3.4	10.9	5.0
25	10.0	4.5	10.2	3.5	11.1	5.3
30	10.5	4.8	10.5	3.8	11.1	5.3
35	11.0	5.1	11.2	4.5	11.1	5.3
40	11.2	5.1	11.2	5.0	11.1	5.3
45	11.2	5.1	11.5	5.0	11.1	5.3
50	12.0	5.2	11.5	5.0	11.6	5.3
55	12.1	5.6	11.5	5.0	11.6	5.8
60	12.1	5.6	11.6	5.0	11.6	5.8
70	12.1	5.6	11.6	5.0	11.6	5.8
80	12.1	5.6	11.6	5.0	11.6	6.0
90	12.5	6.0	11.8	5.0	11.6	6.0
100	12.5	6.2	11.8	5.4	11.8	6.0
110	12.5	6.2	11.8	5.4	12.0	6.5
120	12.5	6.2	11.8	5.4	12.0	6.5
135	12.5	6.2	11.8	5.4	12.0	7.0
150	12.5	6.2	11.8	5.4	12.0	7.0
165	12.5	6.2	11.8	5.4	12.0	7.0
180	12.5	6.2	11.8	5.4	12.0	7.5
210	12.5	6.2	11.8	5.4	12.0	7.5
240	12.5	6.2	11.8	5.4	12.0	7.5
270	12.5	6.2	11.8	5.4	12.0	7.5
300	12.5	6.2	11.8	5.4	12.0	7.5
360	12.5	6.2	11.8	5.4	12.0	7.5